Radio-Based Satellite Tracking Systems for the DelfiSpace Program

Phase Interferometry and Time Difference of Arrival

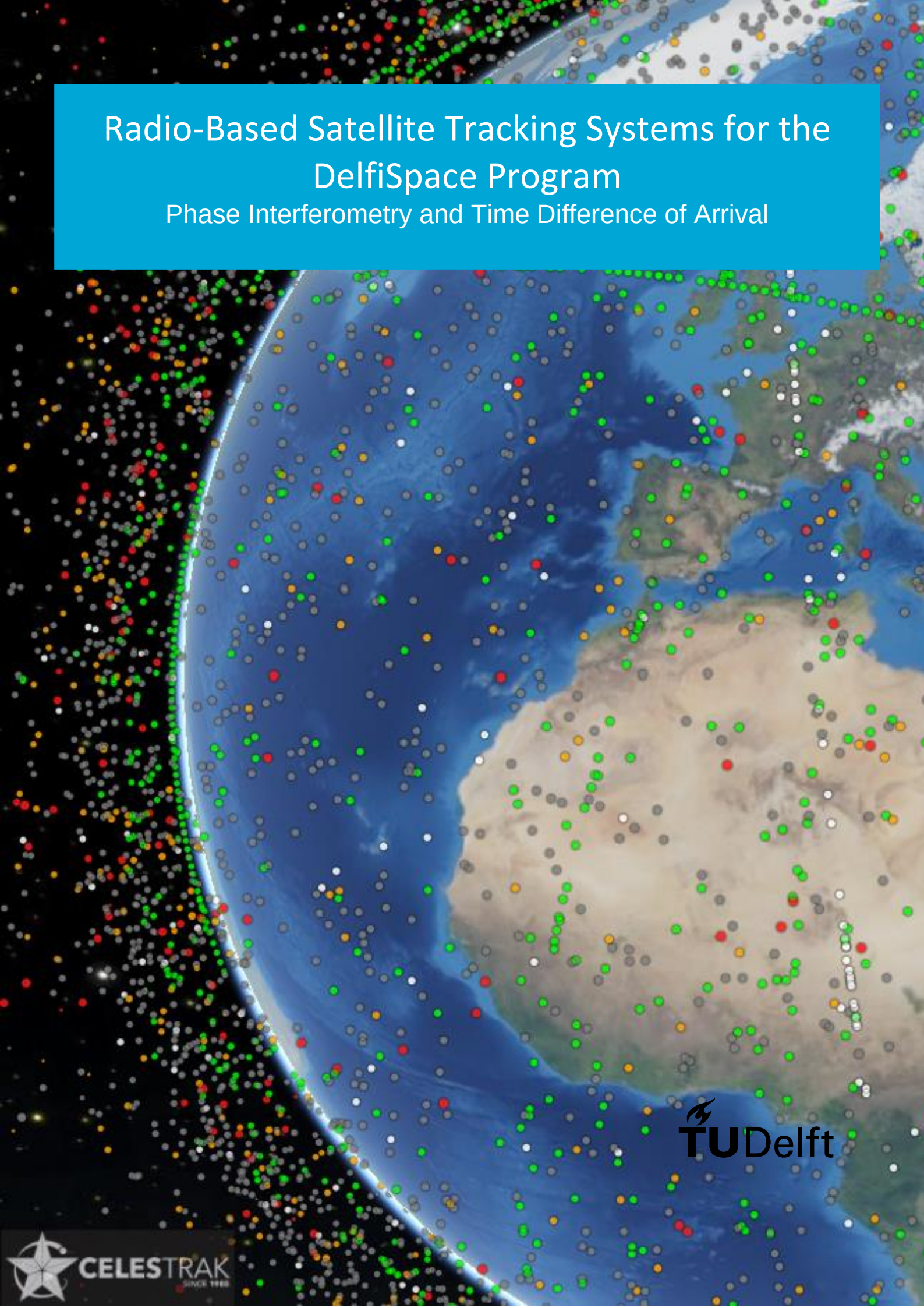

This page intentionally left blank

TUDelft

Radio-Based Satellite Tracking Systems for the DelfiSpace Program

By

Tim André John Patrick Nachtergaele

in partial fulfilment of the requirements for the degree of

Master of Science
in Aerospace Engineering

At the Faculty of Aerospace Engineering of Delft University of Technology, 2022

Supervisor:	Dr. Stefano Speretta	
Thesis committee:	Dr. J. Guo,	TU Delft
	Dr. Stefano Speretta,	TU Delft
	Dr.ir. B.C. Root,	TU Delft

Cover picture by: Celestrak orbit visualizer, taken on 31/03/2021 at 2021-03-31-10:08:51Z
URL: https://celestrak.com/cesium/orbit-viz.php?tle=/pub/TLE/catalog.txt&satcat=/pub/satcat.txt&referenceFrame=1

TU Delft

An electronic version of this thesis is available at http://repository.tudelft.nl/.

Preface

Completing my thesis is the crowning achievement to my degree as an aerospace engineer. I am very happy and proud to have completed my degree at TU Delft. It is my sincere hope you find this thesis useful and informative and that it contributes to humanities' presence in space.

First, I would like to thank my supervisor, Stefano Speretta. I would like to thank you for all the advice and support you gave me during the thesis. I am going to miss our weekly chats and I wish you and your family all the best.
Erdem Turan, your advice was very helpful and informative. I wish you best of luck with your satellite tracking research.
Paulien van den Berg, you are the light of my life, thank you for your love and support.
True Ravelengée and Patrick Nachtergaele, thank you for supporting me for all these years, and for listening to me talk about my thesis for hours on end.

Turning my eyes to the future I am confident that the skills, knowledge and experience I have accumulated in my years at TU Delft will be instrumental in starting my career at the European space agency. TU Delft was the best educational experience I could have wished for.

Tim Nachtergaele
Huldenberg, January 2022

Contents

List of Figures

List of Tables

List of Abbreviations

Abbreviation	Meaning
bps	Bits per second
deg	Degrees
DORIS	Doppler Orbitography and Radiopositioning Integrated by Satellite
ECEF	Earth-Centered Earth Fixed
ESA	European Space Agency
GHz	Giga hertz (10^9 hertz)
GNSS	Global Navigation Satellite System
GPS	Global Positioning System
GRAVES	Grand Réseau Adapté à la Veille Spatiale
grnd(s)	Ground station(s)
kbit	kilo bit
km	Kilometer
Kph	Kilometer Per Hour
LEO	Low Earth Orbit
LLS	Linearized Least Squares
LOFAR	LOw-Fequency ARray
m	Meter
MHz	Megahertz (10^9 hertz)
NEO	Near-Earth Objects
NOAA	National Oceanic and Atmospheric Administration
ns	Nano seconds
RSO	Resident Space Object
RSOs	Resident Space Objects
sat	Satellite
SD	Standard Deviation
sec	Seconds
SGP4	Simplified General Perturbations 4
SNR	Signal to Noise Ratio
SSA	Space Situational Awareness
SST	Space Surveillance and Tracking
STM	State Transition Matrix
SWE	Space Weather
TDOA	Time Difference Of Arrival, also know as DTOA (Differential Time Of Arrival)
TEC	Total Electron Content
TECU	Total Electron Content Unit (1 TECU = 10^16 electrons/m^2)
TLE	Two Line Elements
TNO	Nederlandse Organisatie voor Toegepast Natuurwetenschappelijk Onderzoek, (Netherlands Organisation for Applied Scientific Research)
UHF	Ultra High Frequency (300-1000 MHz)
UNOOSA	United Nation Office for Outer Space Affairs
USD	United States Dollars
VHF	Very High Frequency (30 to 300 MHz)

Abstract

Satellite tracking is used to predict a satellite's orbit to communicate and perform other key functions. It is commonly performed using large ground-based radars with an accuracy of 1 to 10 km or specialized onboard satellite systems. Ground optical systems are a proliferating technology for satellite tracking, identification, and communications. Such optical systems have a narrow field of view, and to ensure smooth and quick satellite acquisition, the satellite must be tracked with higher accuracy (in the order of 100 m). Hence, to allow for optical ground systems to function smoothly they require satellite tracking systems providing sufficient accuracy which is not common for small satellites.

This work analyses two radio-based methods to provide sufficiently accurate satellite tracking for the next TU Delft satellite to be acquired optically. These methods utilize the innate satellite radio communications subsystem of the satellite without modifications. To optimize the analysis work, the model complexity was gradually built up. The first method analysed is phase interferometry, which based on a first-order model, turned out to be non-viable. The second method investigated is time difference of arrival. Increasingly more sophisticated models were developed to understand its performance and limitations. For example, for Delfi-PQ, by utilizing 25 ground stations in a square configuration with 1000 km baseline and a noise level of 236 ns (71 m), the target satellite in a 500 km circular orbit can be acquired, with at least the required accuracy, for 18% of the area where the satellite can be received by a minimum of 4 ground stations. It is expected that this performance can be improved through future work. Specifically, by utilizing multiple measurements taken at different times, the satellite orbital parameters can be estimated directly.

We conclude time difference of arrival to be a promising method for further research, development, and eventual implementation by TU Delft. The approach and structure of an even more sophisticated model is detailed for future work.

1) Introduction

There are tens of thousands of objects in space, and they are currently tracked daily by radars with a tracking accuracy in the order of 1 to 10 km [1]. Tracking is determining the current and future position and velocity of the target satellite under consideration. The time to acquire and identify space objects can be several weeks, complicating operations. For satellite tracking, identification, and communications an emerging technology is optical systems, which utilizes lasers, telescopes, reflectors, etc. The narrow field of view of telescopes necessitates accurate satellite tracking information prior to acquisition by the optical system. Hence the need for more performant tracking systems bridging the gap between the existing radar and future optical systems. This thesis analyses two such radio-based methods for more accurate satellite tracking.
Dozens of techniques exist and have been proposed for (improved) satellite tracking, such as various radars, new sensors, etc. An overview of satellite tracking techniques is given in the literature study which preceded this thesis [2]. A summary of the most salient techniques is given as background in chapter 2).
The literature study was used to select the most promising techniques to be implemented on the next TU Delft satellite.
The two considered radio tracking techniques piggy-back on the innate radio communications system present on the vast majority of satellites in order to improve satellite tracking. These techniques would be used to improve the satellite tracking accuracy to the point where ground based optical systems can quickly and easily "lock onto" or acquire the satellite. Optical systems typically have a narrow field of view meaning acquiring the satellite is challenging without an accurate satellite tracking information prior to acquisition.
Once the optical system has acquired the target satellite it can be used to transmit data much faster than via radio [3], and/or to identify the satellite [4] and/or to improve the satellite tracking by orders of magnitude [5].
TNO (Netherlands Organisation for Applied Scientific Research) is working on such an optical system to be tested by tracking and identifying the next TU Delft Satellite. Hence the interest in a tracking technique to bridge the precision gap of the publicly available satellite tracking information [1] to the level required for an optical system.
The first tracking technique investigated is phase interferometry in chapter 4). However, this option is dismissed as it is not feasible to implement a space interferometry solution that meets our requirements, as set forth in chapter 4).
The next tracking technique considered is TDOA (Time Difference Of Arrival), which is analysed in chapter 5) as a simplified 2D system and, after promising results, as a 3D system in chapter 7). In chapter 6) error sources which affect TDOA performance are analysed. In chapter 8) recommendations for future work on a more advanced TDOA simulation tool are given.

1.1 Problem Statement and Approach

This thesis is an exploration of radio-based techniques to improve satellite tracking from the publicly available radar tracking data (which have an accuracy of about 1-10 kilometres for 1-day propagation [1]). The objective of this thesis is to explore and investigate radio-based options to track the target satellite with a lateral error of 83 meters or less. This is the requirement set for sufficiently quick and reliable acquisition of the target satellite by means of the optical system. The optical system will then be able to identify and communicate with the target satellite. If a laser ranging system is available at the optical ground station the satellite tracking could be done up to centimeter level accuracy [5].
The optical ground station is being developed by TNO and a collaboration with TU Delft is underway to utilize the next TU Delft satellite as a test platform for satellite tracking techniques and optical identification.
As such, this thesis is a study of radio-based techniques with the objective to improve satellite tracking to the point where the TNO optical system can acquire the satellite. In addition, the future TU Delft satellite may also carry a GNSS system to be able to verify the tracking performance.

In addition, the proposed system must be compatible with available TU Delft resources and expertise and have a minimal impact on the satellite design.

The approach taken in this thesis is to gradually build up complexity, or in other words the doctrine of "start simple" was followed. This was done to ensure the available resources were committed optimally and effort was not wasted on an option that could quickly be proven to be unsuitable for application by TU Delft. For instance, in phase interferometry (chapter 3) a relatively simple model was first used to explore the design space.

1.2 Research Question I

Below the first research question is given, note that the colour marked terms are explained in detail in the next section.

1) Is **phase interferometry**, a **radio**-based **tracking** technology, applied to a **cooperating** **spacecraft** in **low-earth orbit,** a suitable technique to be used by TU Delft for the **DelfiSpace program** to improve the tracking accuracy?

- 1A) What are the consequences with respect to the target satellite?
- 1B) What are the consequences with respect to the ground station(s)?
- 1C) What are the consequences with respect to the entire tracking system?

1.3 Research Question II

Below the second research question is given.

2) Is **Time Difference Of Arrival (TDOA)**, a **radio**-based **tracking** technologies applied to **cooperating** **spacecraft** in **low-earth orbit** a suitable technique to be used by TU Delft for the **DelfiSpace program**?

- 2A) What are the consequences with respect to the target satellite?
- 2B) What are the consequences with respect to the ground station(s)?
- 2C) What are the consequences with respect to the entire tracking system?

In the text below some of the terms and definitions mentioned in the research questions are elaborated.

radio
This thesis focuses on radio-spectrum techniques.

tracking
The objective is tracking, determining the current and future position and velocity of the target satellite under consideration.

cooperating
The target satellite is assumed to be cooperating, meaning the transmission frequency, modulation scheme, etc. are known and no active or passive measures are taken to obscure the target or hinder tracking.

spacecraft
This thesis deals with tracking satellites and/or spacecraft. The techniques presented here can also be used to track non-satellite objects such as ships, planes, automobile, stationary transmitters, etc. These alternate applications are not considered in this thesis.

low-earth orbit
The target is assumed to be in low earth orbit (160-1000 km above the surface of the earth), with a practical demonstration at 500 km during this thesis [6].

DelfiSpace program
Label for a future TU Delft satellite project, assumed to have one or more space situational awareness and/or space surveillance and tracking payloads onboard.

1.4 Requirements

In this section the requirements are given as applied to the radio tracking systems being investigated in this thesis. The requirements are split into 3 sections covering: accuracy, satellite, and ground station requirements.

1.4.1 Accuracy Requirement

As explained above one of the applications of the radio tracking system is to provide trajectory information for communications (or observation) by means of an optical telescope/laser. Since the optical segment is not the focus of this thesis the required accuracy of the radio tracking system is set at a radius of 83 meters for one sample standard deviation at an altitude of 500 km. This is then converted to a tracking area by taking 83 meters as the radius of a circle, yielding an area of 21642 square meters. This "tracking area" is the area located at the satellite and orthogonal to a vector connecting the satellite and the optical telescope. This is the area the telescope must search through to acquire the target satellite optically. This requirement is based on conversations with Dr. Stefano Speretta and several TNO experts on optical communications and does not reflect the full complexity of the combined optical and radio system. However, it is a useful measure to establish if the proposed system is viable.

Requirement ACC.1
The tracking system shall have a one sample standard deviation tracking area equivalent to a circle with a radius of 83 m (21642 m^2). Tracking area is the plane located at the target satellite and orthogonal to the vector connecting the target satellite and the optical ground station, representing the area the optical system has to search to acquire the target satellite. As such, there is no requirement placed on range accuracy (the length of the vector connecting the target satellite with the optical ground station).

Note that no requirement is placed on range accuracy, or how far away the satellite is from the radio ground station. This is because both the radio and optical tracking system operate close to the speed of light in vacuum, so range accuracy is not a driving requirement. Or in other words if the satellite is 1 km more to the left or right from where we think it is, we will not find it with the optical telescope. But if it is 1 km closer or further

away, we will still be able to acquire the satellite, since the apparent lateral shift due to the range error will be on the order of centimetres.

1.4.2 Satellite Requirements

An important aspect of the system is the space segment. Our concept is to rely on the inherent radio communications capabilities of the target satellite. Note that this satellite is expected to be cooperative as per the research question. Hence information on the frequency, modulation scheme etc. are assumed to be known, but no modifications have been made to the satellite, either in software or hardware, to facilitate radio ranging and tracking.

Requirement SAT.1
The radio tracking system shall rely on the inherent radio communications hardware of the target satellite.

The satellite orbit is an important aspect of the design since it affects the visibility of the satellite, positioning accuracy, etc.

Requirement SAT.2
The target satellite shall be in a circular reference orbit of 500 km altitude.

1.4.3 Ground Station Requirements

The ground station(s) is (are) a critical aspect of the tracking system design. Theoretically a tracking ground station could be anything from a simple antenna and a computer to a state-of-the-art space radar array such as the French GRAVES [7] or the American space fence [8]. Clearly it is unrealistic for TU Delft to have the budget, time, or permission to develop such a system.
Hence the requirements in this section were established to ensure that the ground station(s) can be implemented by TU Delft. The requirement GRND.1 was established to ensure use of commercially available components in the ground station(s). Whereas GRND.2 and GRND.3 were established to ensure that the size, cost, weight, and performance are in line with prevailing ground station(s).

Requirement GRND.1
The ground station or ground stations shall consist of commercial of the self-components.

Requirement GRND.2
The ground station or ground stations shall be of a form factor, cost, and weight range of a typical communications ground station.

Requirement GRND.3
The ground station or ground stations shall have a performance of a typical communications ground station in use by TU Delft [9].

Note that TU Delft already has one radio ground station for communications with its satellites [9].

1.5 Thesis Outline

In this section the structure of the thesis will be explained, in Figure 1 a schematic outline of the thesis is given. In chapter **2) Background** (page 18) the literature study preceding this thesis is recapitulated to give the reader an overview of potential tracking technologies available.
Chapter **3) Methodology** (page 21) discusses the tools, methods and approach taken to answer the research questions given in chapter **1) Introduction** (page 12). Note that the Introduction and Methodology chapters are not shown in Figure 1 for clarity.
In chapter **4) Phase Interferometry (**page 22) from the information gathered during the literature study the first option to be considered was phase interferometry. A first order analysis was performed, evaluating the expected performance of a phase interferometry system with respect to the requirements presented above. Based on this analysis the decision was made to not continue development of the phase interferometry system. At this point the next technique to investigate was selected based on the literature study.
In chapter **5) 2D Time Difference of Arrival** (page 30) the first order analysis of the TDOA system is performed, restricted to 2D and the minimum number of ground stations. The results were promising, hence development continued in chapters 6) and 7).
Chapter **6) Sources of Noise and Measurement Errors in TDOA** (page 43) analyses the sources of error and noise which are critical to be able to more accurately assess the performance of the TDOA techniques with respect to the accuracy requirement ACC.1.
In chapter **7) 3D Time Difference of Arrival** (page 48) a more detailed, and intricate simulation of the performance of a TDOA system is performed and used to analyse the TDOA system. Here multiple ground stations can be used simultaneously, the errors are simulated stochastically, etc.
Chapter **8) Future Work: 4D TDOA Simulation Tool** (page 93) continues on the previous chapter and contains information, suggestions and plans for future work on a 4D TDOA simulation tool. This tool would be able to estimate target satellite orbital elements directly and would enable the assessment of the requirements pertinent to the implementation of an operational TDOA system. It could also serve as a coding basis for the operational TDOA system itself.
Finally in chapter **9) Conclusions** (page 100) the conclusions are presented. It is not shown in Figure 1 for clarity as it relates to all other chapters.

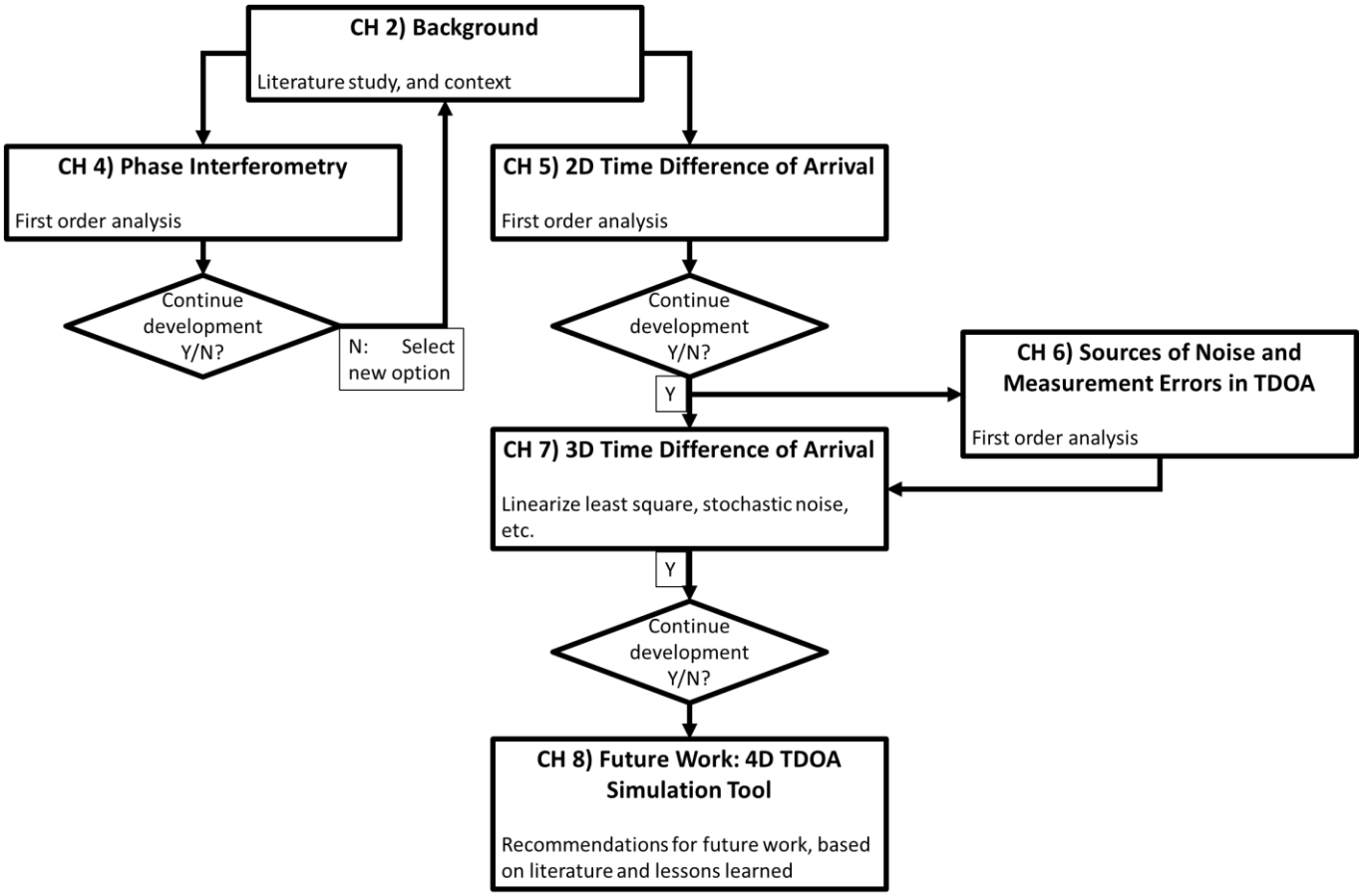

Figure 1: diagram showing the outline of the thesis

2) Background

In this section background information will be given on the topics of satellite tracking. It is based on the literature study preceding this thesis [2], unless mentioned otherwise.

2.1 Space Situational Awareness

Space situational awareness (SSA) is the umbrella term under which this thesis falls. SSA is defined by the European union satellite centre [10] as consisting of 3 elements:

- Space WEather (SWE) deals with space weather such as solar wind, coronal mass ejections, sun cycle, etc.
- Near-Earth Objects (NEO) keeps tabs on naturally occurring space objects, such as comets and asteroids.
- Space Surveillance and Tracking (SST) detect, tracks, and monitors artificial objects (called RSOs, short for Resident Space Objects)

As this thesis deals with tracking artificial satellite in earth orbit it falls under Space Surveillance and Tracking.

SST is a broad topic with many different aspects and intricacies, below some of these aspects are briefly introduced and defined.

- **Detection**: knowing an object is in orbit, but having no, or only a very rough idea of its orbit and position.
- **Tracking**: the ability to determine the orbit of an object with some accuracy. Note that the orbital positions can determined at millimeter level for some high-performance tracking systems or up to kilometers for others.
- **Prediction**: the capability to predict where a given RSO is going to be at some future date. This also includes prediction of (potential) collisions.
- **Identification**: knowing what a given RSO is and who it belongs to if anyone. This matters greatly when collisions are to be avoided.

To further clarify the difference between detection, tracking, prediction, and identification it is useful to consider an analogy. Detection is hearing the noise of a car, but not knowing where it is. Tracking is seeing the car and thus knowing its position, velocity, and direction. Prediction is being able to predict where the car will be some seconds in the future. Identification is being able to read the license plate. Note that the literature study focused on detection, tracking and identification of RSOs. But the thesis pertains to tracking by radio means.

2.2 Importance of Space Surveillance and Tracking

In this section the growing importance of SST will be clarified.

The orbital space around earth is host to 2700 working satellites and 8800 tonnes of debris according to ESA (European Space Agency) and the UNOOSA (United Nation Office for Outer Space Affairs) [11]. This debris varies in size from sub millimeter fragments to defunct satellites and discarded rocket stages. At impact velocities up to 14 km/sec the effects of collisions can be extremely destructive. Such as in 2009 when Iridium 33 and Cosmos 2251 collided. Both satellites (one of which was still active) were utterly destroyed [12] and created more than a thousand pieces of debris. In fact, even small objects can have very destructive effects when they collide with satellites, a collision with a 5 cm piece of space debris has approximately the same kinetic energy [13] as a mass of 20 tonnes traveling at 100 Kp/h [14] and can cause major damage to a satellite [13].
Collisions can be avoided by slightly changing the orbit of the satellite, but this requires fuel, time and usually interferes with the ongoing mission [15]. Not all satellites have a propulsion system, and even the ones that do can be nonoperational or unable to perform the required maneuver in time. Another complication is position

uncertainty: the satellite in the collision mentioned above were predicted to pass 1.2 km from each other [12]. This is an excellent example of a lack of reliable SST data leading to the loss of a space asset.
Accurate SST becomes even more pressing when one realizes that the number of objects in earth orbit has been increasing for the past 30 years [16]. And is expected to increase even more rapidly in the future with the introduction of big constellations such as Starlink [17], Kuiper [18] and many others.

For some satellite operators SST is essential, because for some missions (very) accurate satellite positional data must be known (e.g. earth observation). In such a context, the mission specifics will determine the required accuracy, which can then be achieved in many ways. SST is also useful to determine the communications windows between ground station(s) and the satellite and to be able to predict the Doppler shift due to satellite motion. The third aspect is to prevent collision between the satellite and RSOs. As explained previously these can be catastrophic.
The need for better satellite tracking is also emerging from the development of optical communications. Optical communications or laser communications operates by transmitting information through (modulated) laser pulses. It can be used to communicate between satellites or between a satellite and ground stations [3]. This has several advantages such as much higher transmission rates [3], harder to intercept, etc. Optical systems can also be used to identify the target satellite [4] and/or to improve the satellite tracking by orders of magnitude [5].

One might think that the aspects mentioned above are trivial since satellite operators know in which orbit their satellite will be inserted. However, satellites often ride-share with potentially a hundred or more satellites in close orbital proximity [19], making unique identification difficult. Furthermore, many different disturbances (solar pressure, earth gravity, solar radiation pressure, drag etc. [20]) act on satellites, constantly changing their orbits. This means that even if the satellite is launched into a unique, well-known orbit it can deviate quickly (tens of kilometers per day [1]), which can interfere with the satellite mission and operations.

The total contribution to the world economy from the space sector and space derived activities are estimated at 280-300 billion USD per year [21]. Making SST an important aspect to many nation's economies. In addition, many governments operate and own satellites and as such have an interest in keeping them safe and operational.

2.3 Space Surveillance and Tracking Options

In this section a brief overview of the tracking technologies considered in the literature study is given, please see [2] for a more in-depth discussion of each. Figure 2 gives a schematic overview of the considered SST options, split into 4 domains: radar, optical, radio and maverick options. The maverick options are more "exotic" and/or rely on techniques and principle that do not fit well in the other domains.
The 46 SST systems are analysed and rated on 15 different criteria. All the results are combined in an Excel table to facilitated future trade-offs and analysis. The criteria include aspects such as the impact on the satellite and ground segment, but also the expected accuracy, capability for tracking, identification, and detection, etc. In this way a list has been compiled of possible SST technologies applicable to satellite in LEO and their advantages and disadvantages.
One of the conclusions of the literature study was the lack of a currently available "One-size fits all solution" A satellite using, for example, DORIS (Doppler Orbitography and Radiopositioning Integrated by Satellite) [22] has round-the-clock positional accuracies in the cm-range [23], more than accurate enough for precise collision prediction and (optical) communications. But this system has a big impact on the space segment and can break down. Other systems such as ground based radar are broadly applicable but not very accurate and do not allow for satellite identification.
Perhaps the most promising maverick is event-based sensors. These have been used to successfully detected satellites in orbit, even during daytime [24] with possibly meter level accuracy. But it is still in the prototype phase and as deemed not ready for application.

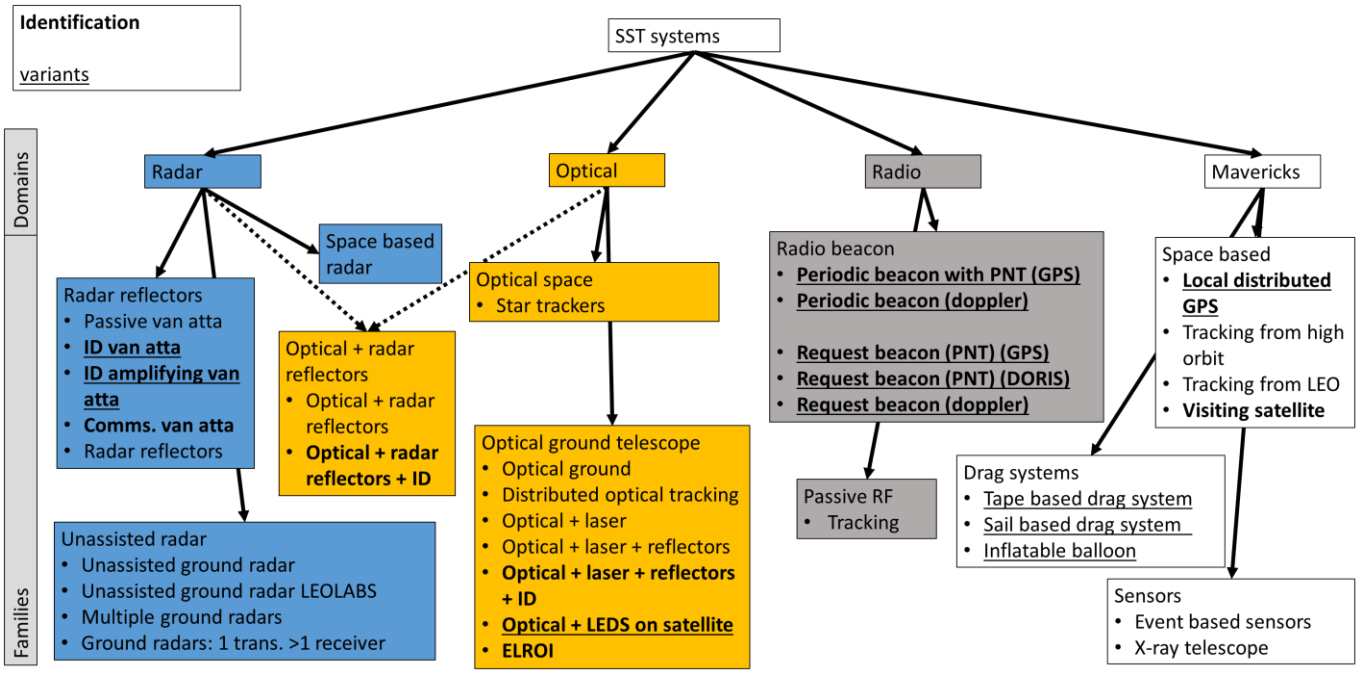

Figure 2: tree diagram of the SST options, at the highest level the domains are listed, which are split into the families, each consisting of one or more options. Note that options in bold allow for identification of the satellite.

One of the options of interest selected for possible research was the use of ground-based radio tracking techniques to track the target satellite, which was first assumed to carry a specialized radio beacon for this purpose. However, during the thesis, it quickly became apparent that this system could piggyback of the radio communications system aboard the satellite. This is considered advantageous since it reduces the demands placed on the satellite.
Another promising option is the use of optical systems, as it turns out TNO is working on an optical satellite communications and identification system. Where a combination of a ground-based laser and telescope can be used to find the satellite and it can be identified by laser reflectors. However, this system has a narrow field of view and as such requires the satellite orbit to be known with a certain minimum accuracy to ensure successful operations (see section 1.4.1).
The decision was made to focus on a radio-based tracking system to support the TNO optical system.

2.4 Proposed System Architecture

The high-level system architecture consists of 3 chronological steps, the second step is the focus of this thesis.

1) Publicly available tracking information is used as a rough initial guess of the satellite orbit (around 1-10 km accuracy). Alternatively simulated pre-launch elements could also be used to estimate the initial satellite orbit.
2) A radio-based tracking technique is used to refine the accuracy of the satellite track to the required level (83-m accuracy, see section 1.4.1).
3) Tracking/communications/identification by the TNO optical ground station once the satellite track has been sufficiently refined.

3) Methodology

In this chapter the methodology followed throughout the thesis will be elaborated in addition to the tools used.

The primary programming tool used in this thesis was Matlab. Some processing, analysis and generation of diagrams were done in Microsoft Excel and PowerPoint.
Given the exploratory nature of this thesis the complexity was gradually built up. This was done to ensure engineering resources were not wasted. In the case of phase interferometry, the simulation tool was developed quickly, this tool has a limited simulation scope, but still allows for a first order assessment of the performance of a phase interferometry system. This then guided the strategic decision on whether to proceed or select an alternative tracking technique.
Another advantage of this gradual complexity build-up is that it facilitates verification and validation, since there are multiple models available, simulating the same tracking technique with different assumptions, conditions, and approaches.
In the context of this thesis, we have developed simulation tools to be able to predict how a given tracking technique will perform with respect to accuracy, impact on ground stations, etc. Then we can analyse if the tracking technique can meet the requirements set forth in section 1.4. Specifically, if the required accuracy can be achieved without imposing on the satellite and with a realistic number and complexity of ground stations. Note that these tools can be reused to assess the viability of the tracking techniques for a different set of initial requirements. The developed simulation tools may also serve as the basis for simulation of other tracking techniques and/or the operational code of the tracking system.

4) Phase Interferometry

In this chapter the radio-based satellite tracking technique called phase interferometry is analyzed. First the technique is explained, and a model of the technique is explained and implemented. Subsequently the verification and validation are elaborated. Finally, the results are covered by reviewing the numerical results and practical considerations.
This chapter focuses on answering the first research question, see section 1.3.

4.1 Implementation of Phase Interferometry

In this section the radio location method of phase interferometry is explained. In this method two radio receivers (antennae) are located some distance away from each other. The operating procedure can best be described chronologically, see also Figure 3.

1) Two antennae are located some distance apart called the baseline indicated by the symbol B.
2) The radio signal from the satellite must travel slightly farther to one of the antennae, due to the angle with respect to the baseline θ.
3) The phase difference between the two signals can be measured.
4) From the phase difference the arrival time difference of the two signals can be found.
5) From this time difference and knowledge of the baseline B the angle θ can be calculated.
6) This angle gives information on the direction of the satellite with respect to the baseline at the time of transmission. Note that to determine the satellite position two or more such angles are needed.

Note that the signal being detected and compared is the carrier frequency of the satellite radio communications system. Hence the correlation is being performed in the radio frequency domain necessitating high frequency measurements and consequently high-volume data transfers from the antenna to the processing location.
In chapter 5) the TDOA technique is elaborate, which relies on comparing the message being sent rather than the carrier frequency itself.

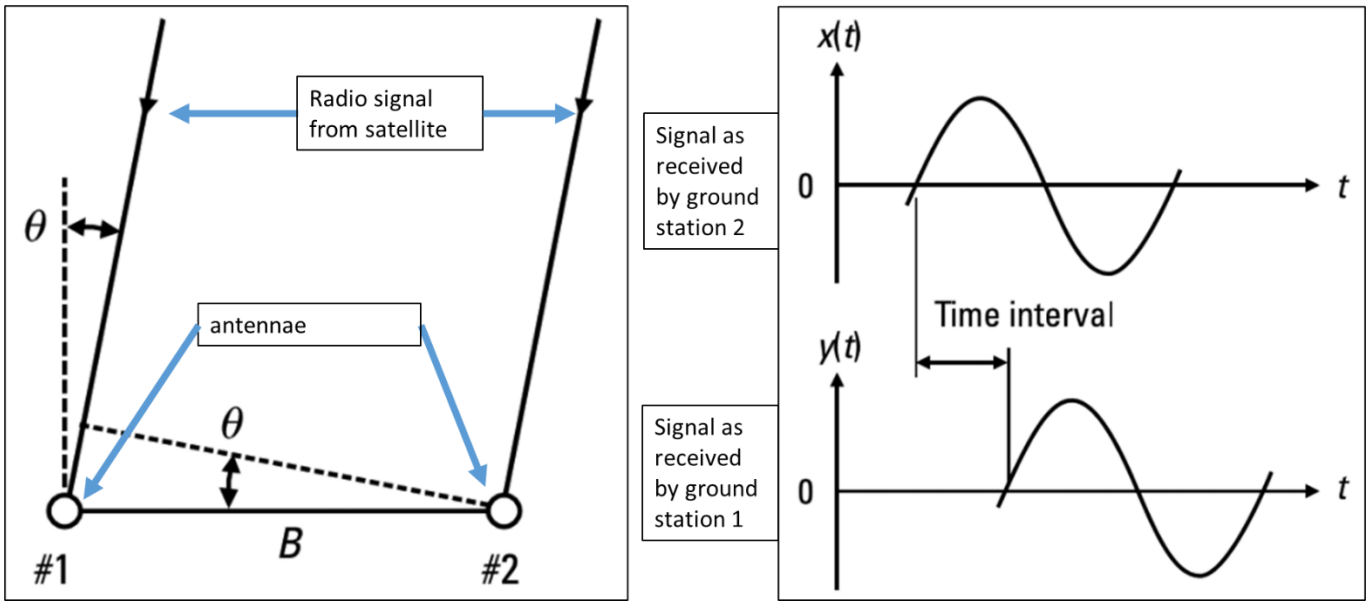

Figure 3: diagram of the antenna baseline, $\delta\theta$ and δl, modified from [25]

In [25] formulae are presented allowing for a first order assessment of a phase interferometry system:

$$k * \frac{S}{N} = \left(\frac{1}{RMS\{\delta\phi\}}\right)^2 \quad 4\text{-}1$$

$$\delta\phi = \frac{2\pi\delta l}{\lambda} \quad 4\text{-}2$$

$$\delta l = sin(\delta\theta) * B \quad 4\text{-}3$$

Where:

k	integration gain, the number of samples (measurements) used to come to a result [-]
$\frac{S}{N}$	signal to noise ratio [dB]
$RMS\{\delta\phi\}$	interferometric phase root-mean-square-error [-]
δl	relative path length change caused by angular accuracy (difference in path between the two antennae) [m]
λ	wavelength [m]
$\delta\theta$	angular accuracy [deg]
B	Baseline [m]

Using simple geometry, the lateral accuracy can be derived, see the equation below. Which is used to convert the angular accuracy to the lateral accuracy.

$$sin(\delta\theta) * r_{sat} = lateral\ accuracy \quad 4\text{-}4$$

Where:

r_{sat}	distance between the ground station containing the antennae and the target satellite [,]
$lateral\ accuracy$	signifies the positioning uncertainty derived from the angular accuracy expressed in meters in a plane perpendicular to a line connecting the ground station to the target satellite, placed at the satellite.

The equations listed above were implemented in a Matlab live script with several plots to allow for quick iteration with results presented in a clear manner, see section 4.3.1 for (some of) the plots. First **equation 4-4** is used to relate the lateral and angular accuracies. With **equations 4-1, 4-2, and 4-3** the relationship between the various inputs can be written as:

$$k * \frac{S}{N} = \left(\frac{1}{RMS\left\{\frac{2\pi * sin(\delta\theta) * B}{\lambda}\right\}}\right)^2 \quad 4\text{-}5$$

With this equation one can calculate the required $\frac{S}{N}$ for a certain angular accuracy based on various combinations of the wavelength (or frequency) and baseline. The code also allows for the calculation and plotting of the required SNR with respect baseline and angular accuracy or with respect angular accuracy and frequency. All these plots give insight into the design space.
The user can define a required lateral accuracy and calculate the associated angular accuracy. Then the impact of a range baseline and frequency combinations on the required SNR is calculated and plotted. Figure 5 is an example of such a plot. From this plot one can quickly assess if the system is viable and what combinations of SNR, baseline, and frequency are viable. One may need to iterate this process if no viable options are present such as increase the integration gain or lower the accuracy requirements.

The Matlab model assumes a 2D system, this implies the phase interferometry system is only conferring a single angle (for example azimuth), see also section 4.3.2.
The baseline is assumed to be perpendicular to the satellite signal.

Many of the error sources present in a phase interferometry system are not quantified in the model such as atmospheric reflection/diffraction, baseline errors, etc. as they are considered to be beyond the scope of this first order evaluation of viability.

4.2 Verification & Validation

The validation of the Matlab script was performed through comparison with examples in [25]. The results of which are listed in Table 1 below. These results were also checked visually on the plots.

Frequency [GHz]	Book result [dB]	Matlab code [dB]	Percentual difference [%]	Absolute difference [dB]
4	36.4	36.69	0.81%	-0.29
12	26.9	27.15	0.94%	-0.25

Table 1: Verification and Validation of phase interferometry. Input values: k=1, baseline 10m, angular accuracy 0.001 degrees.

In addition, the impact of the integration gain parameter (k) was also validated by using examples listed in the book specifically [25] on page 47. The results of which are listed in Table 2.

Integration gain (k) [-]	Book result, gain [dB]	Matlab code, gain [dB]	Percentual difference [%]	Absolute difference [dB]
512	27	27.09	0.34%	-0.09
20000	43	43.01	0.02%	-0.01

Table 2: Verification and Validation of phase interferometry. Gain with Input values: baseline 10m, angular accuracy 0.001 degrees.

The validation results presented in Table 1 and Table 2 show percentual errors of less than 1%. This is a good indication that the Matlab code developed is giving similar results as he examples from the book.
The largest absolute difference between the book and the code is 0.29 dB. At the time of writing is Delfi-PQ, which has a downlink signal to noise of 13 to 23 dB depending on elevation. These pervious numbers are given as an indication that on a typical link budget, an error of 0.29 dB in SNR would not be significant.

With the results presented above the Matlab script is considered validated.

4.3 Results

The results of the phase interferometry chapter can be split into two parts: the simulation results and feasibility consideration.

4.3.1 Numerical Results

In this section the tool developed in Matlab (see section 4.1) will be used to perform a first order sizing of a phase interferometry satellite tracking system.

A phase interferometry system gives angular information. For clarity we express the system accuracy in meters from the true satellite position in a plane normal to a vector connecting the satellite and the ground station. The relation between angular accuracy, satellite distance and lateral accuracy is represented visually in Figure 4.

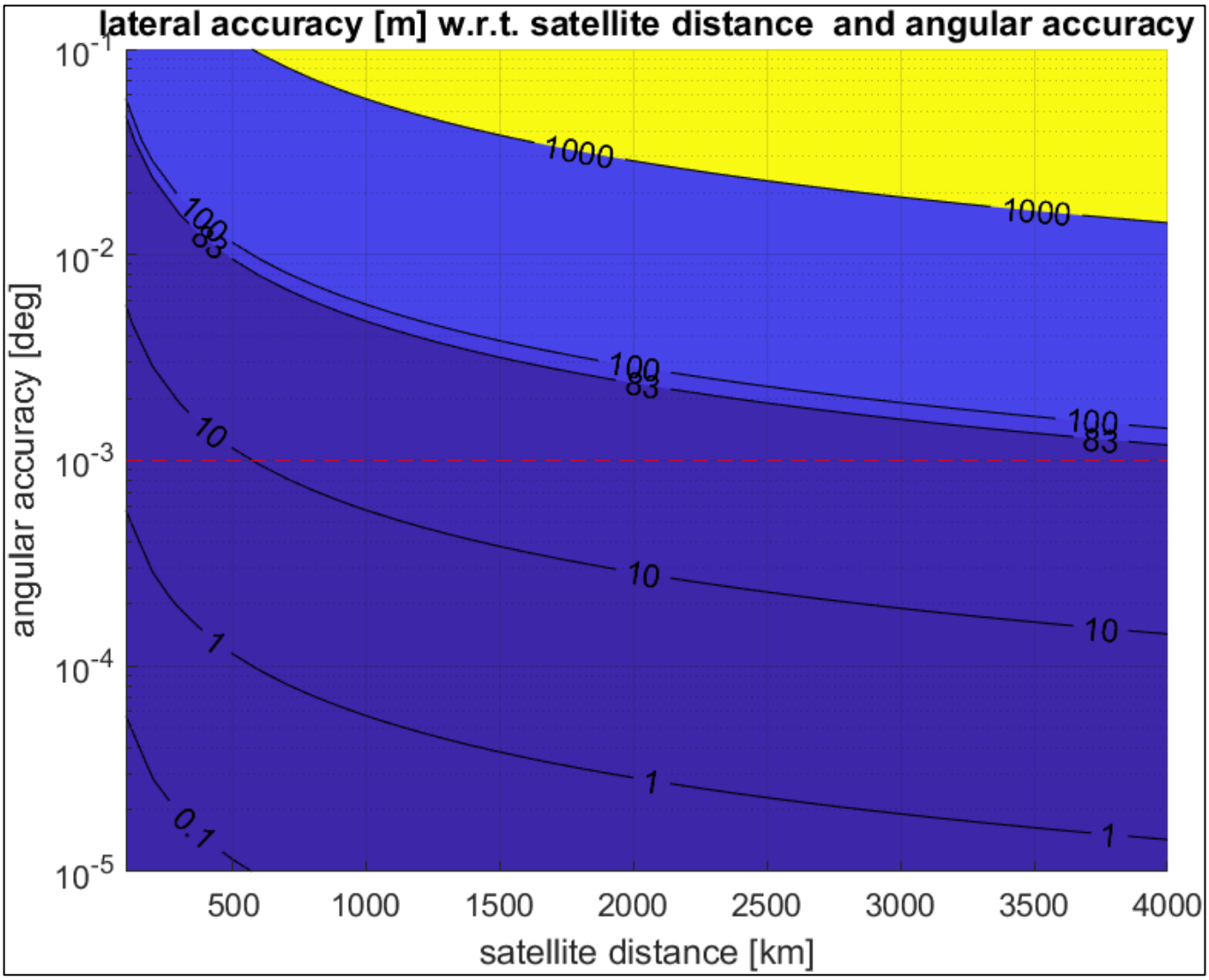

Figure 4: contour lines of the lateral accuracy in meter, with respect to the angular accuracy and satellite distance, with red dotted line at an angular accuracy of 0.001 deg.

Note that the satellite range is the distance between the phase interferometry ground station and the satellite at the time of the measurement. For a satellite at an orbital altitude of 100 to 1000 km this will vary between approximately 1133 to 3700 km at maximum to respectively 100 to 1000 km at closest possible approach.
In this example the angular accuracy of 10^{-3} deg is taken as a result from this plot giving an accuracy of at least 83 m across the ranges considered. The 83 m lateral accuracy requirement was derived from requirement ACC.1, stipulating a tracking error area less than 21642 m^2, which corresponds to a circle with radius 83 m.

In Figure 5 the contour indicates the required SNR in decibels to achieve an angular accuracy of 0.001 deg with respect to the baseline size and transmission frequency.
Two continuous vertical red lines indicate the frequency range from 30 MHz to 1 GHz (VHF and UHF bands), which are the most technologically mature bands for cube satellites [26].

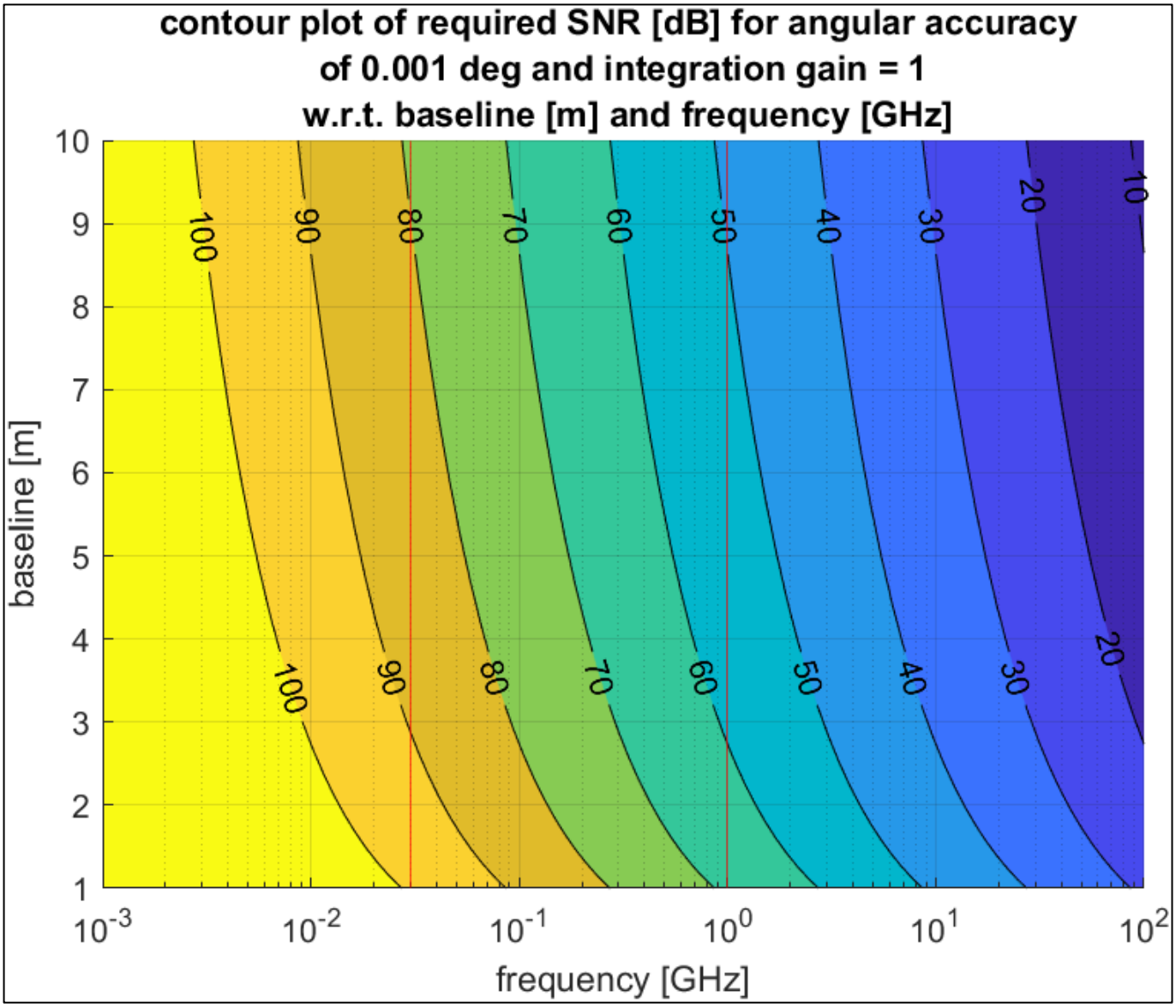

Figure 5: contour lines of the required SNR, with respect to the transmission frequency and baseline with integration gain set at 1.

From the Figure 5 one can conclude that phase interferometry benefits from higher frequencies and longer baselines. For reasons that will be covered in the next section extremely large baselines are not realistically for phase interferometry in our application. This means very high signal to noise ratios are required to achieve the desired accuracy, which is not realistic. For example, the Signal to noise ratio for Delfi-PQ is 14.53 dB for a direct overhead pass and a 2.02 dB when at 5 deg elevation [27].

One factor that can dramatically reduce the required signal to noise ratio is the integration gain. A high integration gains means we take multiple phase measurements and "average" the results. Note: one cannot directly do this for a moving satellite, in reality a procedure such as linearized least squares with transition matrices (see chapter 8) would be applied. This procedure will introduce its own errors, which are not accounted for in this model.
The equations presented in section 4.1 allow for a first order consideration of the impact of the integration gain. For example, Figure 6 has identical input values as Figure 5, except the integration gain is set to 500000 samples. This leads to a noticeable shift in the required SNR.

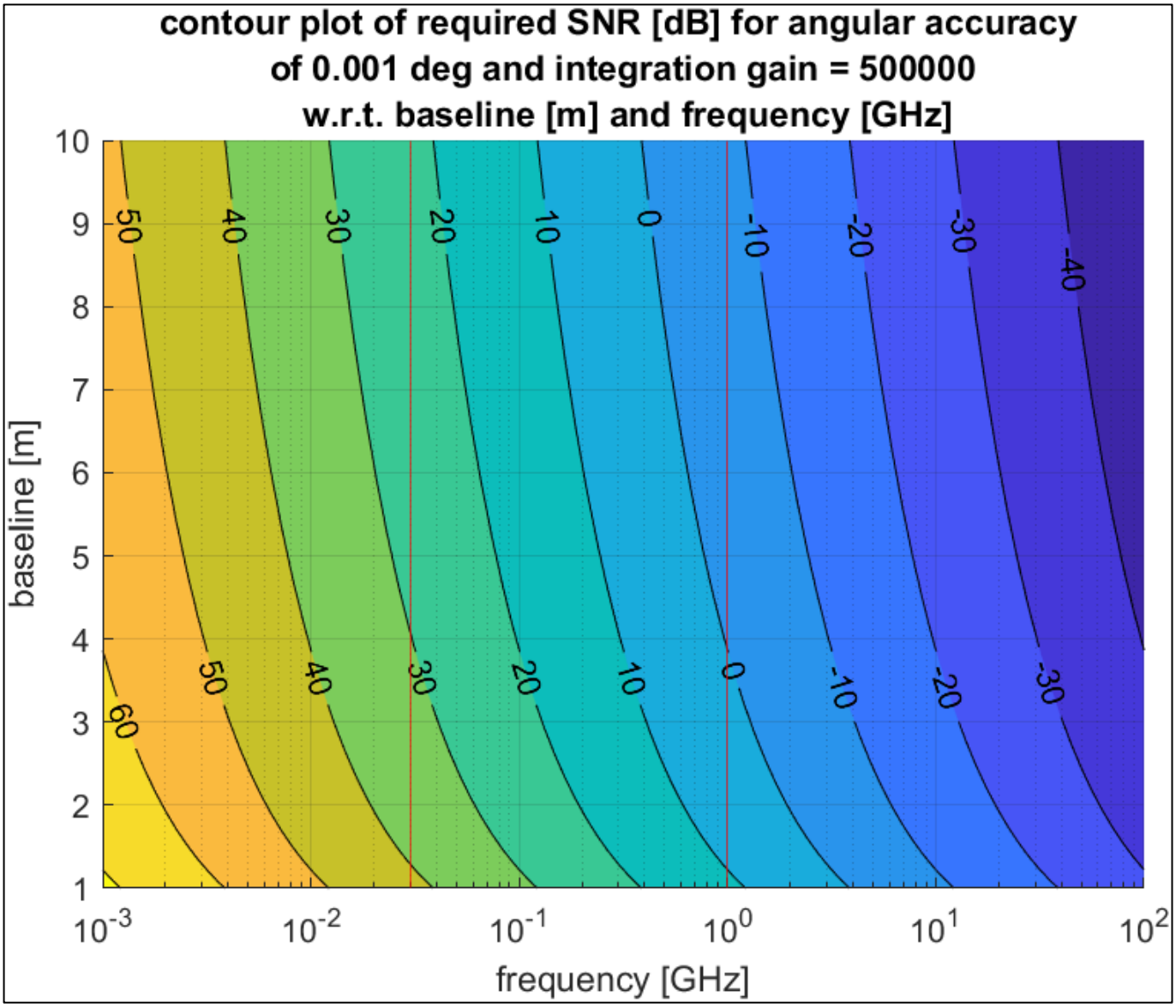

Figure 6: contour lines of the required SNR, with respect to the transmission frequency and baseline with integration gain set at 500000.

4.3.2 Feasibility Consideration

In the previous section the numerical results were presented, here some practical considerations are given with respect to the construction of a phase interferometry ground station. In addition, some limitation of the system discussed. Unless mentioned otherwise this section is based on [25].

Even though theoretically the two antennae of the system can be at any distance; in practice the analogue signal from each antenna must be brought to the same location to compare the phase. Furthermore, since the phase interferometry system compares the phase difference between the two antennae to find a difference in arrival time, the analogue signals must be transmitted through cables of the same length, and even at the same temperature according to [25]. Since the cable temperature will affect the electric signal propagation speed and different propagation speeds will lead to an apparent phase shift. This imposes limits on the maximum baseline that can realistically be achieved and increases the implementation cost due to the tolerances required. In addition the baseline is assumed to be perpendicular to the incoming signal, which implies at least one antenna to be movable (increasing cost and complexity), to ensure the optimal baseline at all times as the satellite moves through the sky. Or that the effective baseline will usually be lower than the physical distance between the antennae.
To counter the previous two problems a rotary baseline can be used, such as can be seen in Figure 7 below. In addition, the signal is reflected through the air reducing the cable lengths.

Figure 7: scale model of a rotary reflecting phase interferometry ground station, note human for scale [25]

Note that the signals could also be converted from analogue to digital and transmitted and compared digitally. For example, LOFAR [28], the largest radio telescope uses enormous baselines (e.g. Latvia to Ireland) and relies on analogue to digital signal conversion.

In [29], another challenge of phase interferometry is mentioned: phase cyclic ambiguity. See Figure 3 the incoming signal can be plotted as a sine wave; we measure the difference in phase of this since between the two antennae. However, since the incoming signal itself is sinusoidal and repeating at the transmission frequency one of the antennae could be any integer number of phase cycle behind the other. Or when the phase difference is measured as 23 degrees the phase difference could also be for example 383. In fact, the "true" phase difference could be: $23 + 360 * n$ where n in any whole number. This phase ambiguity can lead to tracking errors.

Note that for geostationary satellites where the satellite has a low apparent velocity, it would be feasible to use large integration times to improve accuracy. This is also the application for which phase interferometry is proposed by [25].

Another aspect of phase interferometry is that two antennae only generate a single satellite angle, whereas two such angles are needed to determine the satellite position in elevation and azimuth. Note that range cannot be directly measured by phase interferometry but can be calculated based on the change in elevation and azimuth in time of the satellite, or by using trilateration from multiple phase interferometry ground stations.

As part of the phase measurement process the incoming signals are multiplied with a local oscillator which must be tuned to the incoming signal frequency. A signal from a satellite in LEO will have a doppler shift changing the incoming signal frequency in time, further complicating matters.

When considering a full system consisting of an optical ground station for high-speed communications and/or identification of the satellite and the supporting phase interferometry system, then these two should ideally be collocated to ensure that tracking data in azimuth and elevation from the interferometry station can be used directly by the optical station. If this is not the case the phase interferometry tracking data will need to be converted to orbital elements and then these converted to tracking information for the optical ground station, introducing additional errors, not considered in this simplified model.

To conclude, though phase interferometry is likely to not by compliant with requirement ACC.1, by requiring higher signal to noise ratios then generated by the satellite communications subsystem and/or requiring higher operating frequencies.
In addition, it does not comply with the requirements GRND.2 and GRND.3 by necessitating large, complex and specialized ground station(s).

Hence there are several practical concerns with the implementation of a phase interferometry satellite tracking system, in addition to the requirements imposed on the signal to noise ratio, baseline, etc. Hence the decision was made to peruse alternative techniques.

4.3.3 Answer to Research Question I

Research question I:

1) Is **phase interferometry**, a **radio**-based **tracking** technology, applied to a **cooperating** **spacecraft** in **low-earth orbit,** a suitable technique to be used by TU Delft for the **DelfiSpace program** to improve the tracking accuracy?
- 1A) What are the consequences with respect to the target satellite?
- 1B) What are the consequences with respect to the ground station(s)?
- 1C) What are the consequences with respect to the entire tracking system?

First the sub questions will be answered:
1A) What are the consequences with respect to the target satellite?
As elaborated in section 4.3.1 the design space is highly restricted and may require a high signal to noise ratio to be achieved by the satellite's communications system to meet the required tracking accuracy.

1B) What are the consequences with respect to the ground station(s)?
As covered in section 4.3.2 a phase interferometry ground station would fall outside the requirements placed on the ground station(s).

1C) What are the consequences with respect to the entire tracking system?
A phase interferometry system implementation will necessitate long baselines, high frequencies, and high signal to noise ratios. This is not a practical solution for implementation by TU Delft.

In summary, we conclude that a phase interferometry system is not a suitable technique for the TU Delft DELFI-X program.

5) 2D Time Difference of Arrival

In this section the basic concept of Time Difference Of Arrival or TDOA is explained, and a first order 2D model is constructed and used to substantiate continued effort into a more complex and accurate model.

5.1 Implementation of a 2D TDOA Model

In this section a brief overview of the functioning of a TDOA system will be given. Note that in this chapter the problem is simplified to two dimensions, effectively we are neglecting altitude and simplifying the problem to a plane parallel to the ground. For clarities sake we will begin with a conceptually simpler system: position finding through ranging, see also Figure 8:

1) The target satellite transmits a message containing the transmission time of the message.
2) The ground stations receive the message and compares the transmission time with the time of arrival. From these the time of flight of the message can be derived and hence the satellite range at time of transmission. This can be expressed as a circle of a certain radius centred on the receiving ground station. The satellite must be positioned at a point where the circles of the ground stations intersect.

By repeating this procedure for a number of ground stations the location of the satellite at the time of transmission can be found.

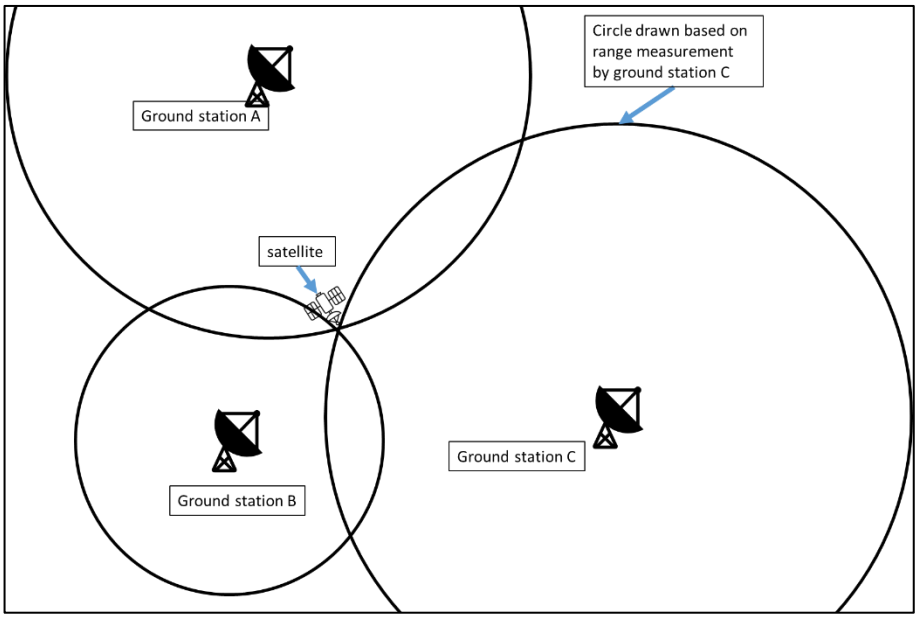

Figure 8: schematic representation of positioning finding based on range measurements.

Note in this case the diagrams and formula are given for the two-dimensional case, however this same technique can also be applied in three dimensions, in which case the circles become spheres.

The above procedure can be described mathematically in 2D as (adapted from [29]):

$$r_{sat\leftrightarrow grnd} = c * (t_{flight}) = \sqrt{(x_{sat} - x_{grnd})^2 + (y_{sat} - y_{grnd})^2} \qquad 5\text{-}1$$

The above equation assumes a two-dimensional problem in a vacuum for clarity, where:

$r_{sat\leftrightarrow grnd}$ distance between the ground station and the satellite at the moment of transmission
c speed of light in a vacuum
t_{flight} time of flight of the message/transmission

x_{sat}, y_{sat} satellite Cartesian coordinates
x_{grnd}, y_{grnd} ground station Cartesian coordinates

Note that the subscript "grnd" is used to identify variables related to the ground station(s) and the subscript "sat" is used for variables related to a satellite/spacecraft.

The TDOA system operates on similar lines with some key differences, see also Figure 9 below:

1) The satellite transmits an arbitrary message.
2) The ground stations (at least two) receive the message and record the time of arrival of the message. By combing the time difference of arrival of the two-ground station a hyperbolic curve can be defined mathematically.
3) The satellite is located at some point on the curve at the moment of transmission. By combining several such hyperbolic curves, the satellite position can be determined.

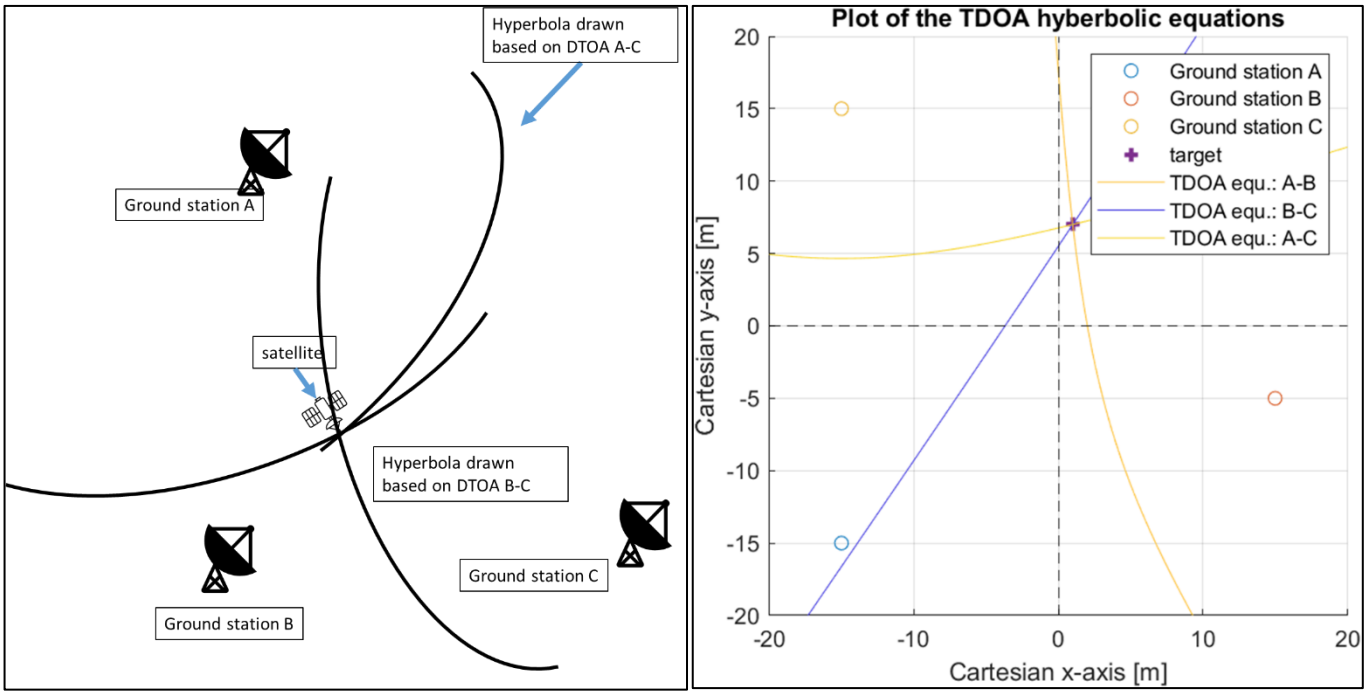

Figure 9: left: schematic representation of positioning finding based on TDOA, right: 2D plot of TDOA-based position finding, made in the qualitative Matlab script.

Note that the "message" being detected and compared by TDOA can be any radio transmission by the target satellite for example when the satellite is transmitting data back to earth. This means that the TDOA system can "piggy-back" on regular transmissions (as long as these transmissions are identifiable and not a repetition of the same bit). No changes to the message or format are needed to make it compatible with TDOA. Note the difference between TDOA and phase interferometry (see chapter 4). In TDOA we are detecting "messages" consisting of one or more bits. In phase interferometry we are detecting changes in the radio carrier frequency containing the message. The radio carrier frequency typically is in the 30 MHz to 1 GHz range (VHF and UHF bands) for cube satellites [26]. Whereas for example Delfi-PQ's data rate is 9.6 kbit/sec.

One may note that the conceptual procedure of TDOA has a lot of similarities with the phase interferometry technique described in chapter 4). One important distinction is that TDOA relies on detecting messages from the satellite, which can be done by any ordinary satellite ground station whereas phase interferometry requires more specialized equipment, see section 4.3.2. In addition, because TDOA relies on detecting the arrival time of "messages" there is less chance of ambiguity in the measurements, this facilitates measurements to be sent

across large geographic distances. Hence when discussing TDOA each receiver is referred to as a ground station, whereas with phase interferometry the word antenna is used.

Note in this chapter the diagrams and formula are given for the two-dimensional case, however this same technique can also be applied in three dimensions, in which case the hyperbolic curve becomes a hyperbolic surface, see section: 7.1.

The above procedure can be described mathematically as (adapted from [29]):

$$f(x,y) = \sqrt{(x-x_A)^2 + (y-y_A)^2} - \sqrt{(x-x_B)^2 + (y-y_B)^2} \quad 5\text{-}2$$

$$c * \left(t_{grnd\,A} - t_{grnd\,B}\right) = \sqrt{(x-x_A)^2 + (y-y_A)^2} - \sqrt{(x-x_B)^2 + (y-y_B)^2} \quad 5\text{-}3$$

The above equation assumes a two-dimensional problem (in vacuum for clarity), where:

$f(x,y)$	the hyperbolic function on which the satellite is located at the time of transmission
c	speed of light in a vacuum
$t_{grnd\,A}$	arrival time of the transmission at ground station A
$t_{grnd\,B}$	arrival time of the transmission at ground station B
x_{sat}, y_{sat}	Satellite position, in Cartesian coordinates
x_A, y_A	ground station A position, in Cartesian coordinates
x_B, y_B	ground station B position, in Cartesian coordinates

5.1.1 Qualitative Matlab Script

A Matlab script was written to plot the hyperbolic TDOA equations, the result of which can be observed in Figure 9 (right), this script is referred to as the "Qualitative Matlab script" since it can be used for a qualitative analysis, and especially to elucidate how TDOA functions. Using this script two aspects of TDOA are elucidated: multiple simultaneously correct solutions and the impact of the geometry with respect to the accuracy.

As can be seen in Figure 10, for certain geometries of the ground stations with respect to the target multiple mathematically correct solutions may exist. Mathematically the real and "alternate" solutions are both equally correct. In future work the assumption will usually be made that the system can distinguish between real and "alternate" solutions. Note that not all geometries have "alternate" solutions and that additional ground stations can also be used to distinguish between real and "alternate" solutions.

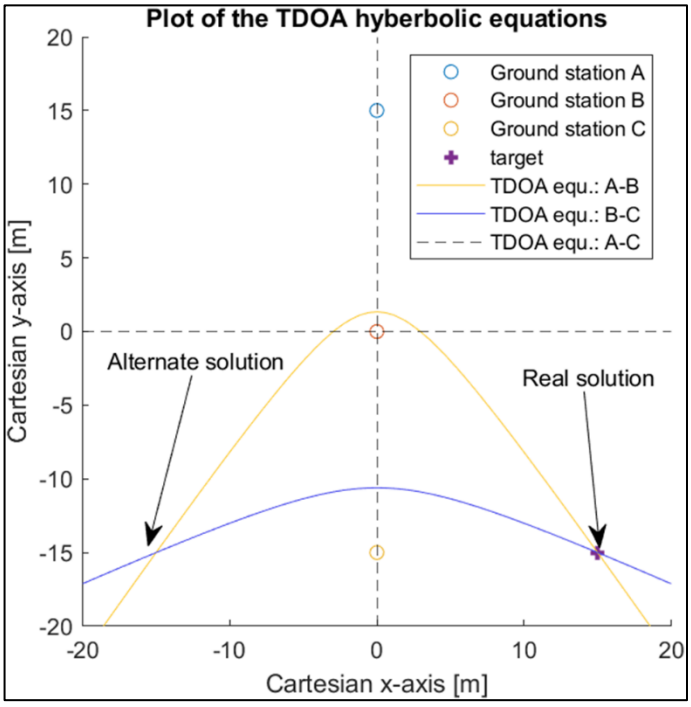

Figure 10: 2D plot illustrating how TDOA can lead to alternate solutions for certain geometries of target and ground stations, made in the Qualitative Matlab script. The inputs: noise: 0.5, 0, and -0.5-meter, ground stations A, B, C at respectively [0, 15], [0, 0], and [0, -15] and the target at [15, -15].

Note that the term $c * (t_{grnd\,A} - t_{grnd\,B})$ in equation 5-3 is a distance calculated based on the transmission propagation speed and the time difference of arrival between two ground stations and is used to make the function f in equation 5-2 implicit.

To account for errors/noise (see chapter 6) equation 5-3 is modified to:

$$c * (t_{grnd\,A} - t_{grnd\,B}) \pm noise_{meter} = \sqrt{(x - x_A)^2 + (y - y_A)^2} - \sqrt{(x - x_B)^2 + (y - y_B)^2} \qquad 5\text{-}4$$

Or

$$c * (t_{grnd\,A} - t_{grnd\,B} \pm noise_{time}) = \sqrt{(x - x_A)^2 + (y - y_A)^2} - \sqrt{(x - x_B)^2 + (y - y_B)^2} \qquad 5\text{-}5$$

By adding the $noise_{meter}$ or $noise_{time}$ term the response of the system to certain disturbances can be analyzed. Note that $noise_{meter} = c * noise_{time}$ (adapted from [30]). Also note that the noise can be either positive or negative (i.e., the time of arrival as measured by the ground station can be later or earlier than the correct time). Figure 11, the hyperbolic curve A-B is drawn for no noise, + noise and – noise. One can see that the hyperbolic curve is shifted towards one ground station or the other when noise is added. It can also be observed that due to the hyperbolic nature of the equations the equations "shift" more the farther they are away from the ground stations.

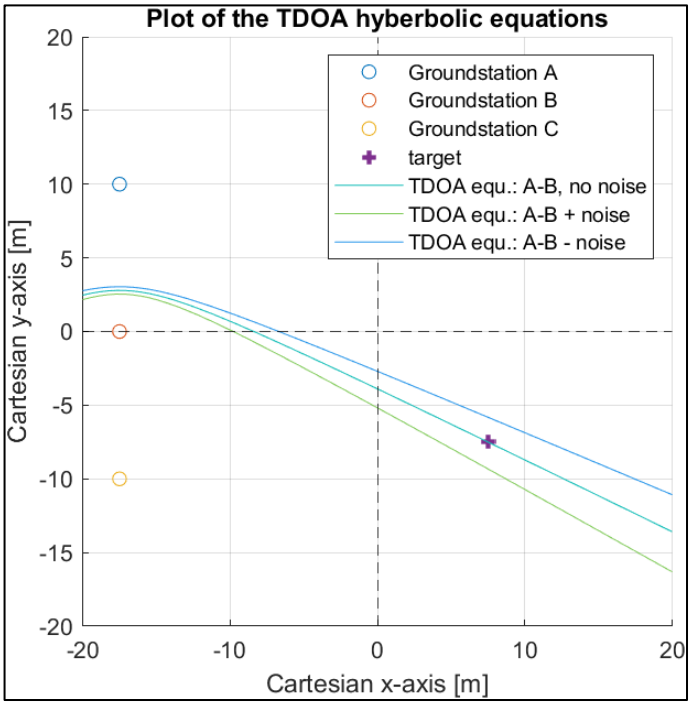

Figure 11: plot illustrating how noise in TDOA estimation leads to a different hyperbolic curve, made in the Qualitative Matlab script. The inputs: noise: 0.5, 0, and -0.5-meter, ground stations A, B, C at respectively [-17.5, 10], [-17.5, 0], and [-17.5, -10] and the target at [7.5, -7.5].

To assess the impact of noise on the accuracy qualitatively the problem is first simplified, namely: the assumption is made that only two hyperbolic equations are used to find a target, this is done to keep the complexity manageable.

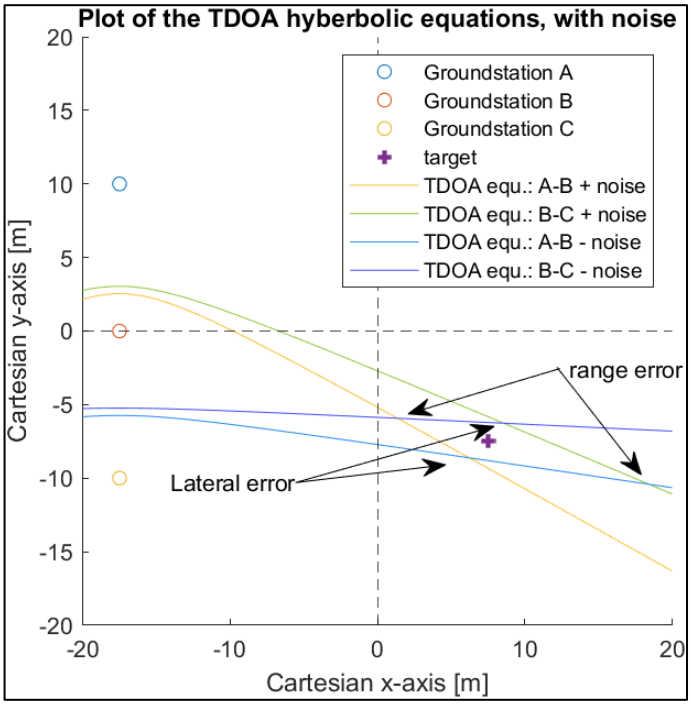

Figure 12: plot illustrating how noise in TDOA estimation leads to errors in the estimated position, made in the Qualitative Matlab script, noise=0.5m, ground stations A, B, C at respectively [-17.5, 10], [-17.5, 0], and [-17.5, -10] and the target at [7.5, -7.5]. Note that this is just an example, the noise level, ground station and target locations were chosen in function of the clarity of the plot.

In Figure 12, the results are plotted. The hyperbolic functions intersect at four points. Two of these correspond to lateral errors. Two others correspond to range errors, as indicted on the plot. Interestingly the range errors are much larger than the lateral errors, and one of the range errors is larger than the other. This points towards a fascinating aspect of TDOA: the errors and accuracies are not omni-directional, for instance the error in range may be several times larger than the lateral error. This is especially relevant with respect to the

combination of a radio TDOA system with one or more optical ground stations, see section 2.4 since there is a lateral accuracy requirement (ACC.1) but no range accuracy requirement (as seen from the optical ground station).

5.1.2 Quantitative Matlab Script

In order to facilitate a thorough investigation a quantitative Matlab script was written. The main objective was to allow for a first order quantification of the accuracy to assess if further resources should be committed.

The following assumptions were made:

- The problem is strictly two-dimensional.
- Distinguishing between real and "alternat" solutions is always possible, see Figure 10.
- The positioning errors are assumed to only come from uncertainties in the time of arrival measurement, or the $noise_{time}$ term from equation 5-5 is the only source of errors/noise.
- The $noise_{time}$ is the same for all ground stations.
- The assumption is made that there is no uncertainty in ground stations positioning. Since the uncertainty in position of the target satellite is orders of magnitude larger than the ground station positioning.
- The problem is assumed to take place in a vacuum.
- Three ground station are defined, but only 2 hyperbolic equations are used to find the estimated position (based on ground station pairs A-B and B-C).

The quantitative Matlab script allows the user to define a number of points at a specified range from the origin and spread over a partial or complete circular circumference at a certain angular interval. Each of these points is a target for which the performance of the TDOA system is assessed. In addition, 3 ground stations are specified.
Recall equation 5-5, which for the ground station pair A-B can be written as:

$$r_{grnd,A} - r_{grnd,B} \pm c * noise_{time} = \sqrt{(x - x_A)^2 + (y - y_A)^2} - \sqrt{(x - x_B)^2 + (y - y_B)^2} \qquad 5\text{-}6$$

And for the ground station pair B-C can be written as:

$$r_{grnd,B} - r_{grnd,C} \pm c * noise_{time} = \sqrt{(x - x_B)^2 + (y - y_B)^2} - \sqrt{(x - x_C)^2 + (y - y_C)^2} \qquad 5\text{-}7$$

Note: $r_{grnd,A}$ is the (true) range target-ground station A, etc. this can be easily calculated from the input values. We wish to find the intersections of equations 5-6 and 5-7 to find the estimated target position for a given $noise_{time}$, the only unknowns are x and y, or the coordinates where the two hyperbolic curves intersect or put another way the coordinates where the TDOA system thinks the target is for a certain noise level.
The intersection of these equations is found by plotting both equations with a certain user-defined mesh within a certain user-defined box around the target. Effectively each of the equations above is simplified to a number of straight-line segments, and subsequently the intersection is found by using the built in Matlab function polyxpoly(). In Figure 13 one can see a representation of this. The hyperbolic functions are effectively discretized into straight line segments which closely follow the hyperbolic curve. It is important to note that the hyperbolic curve closely resemble a straight line in the neighborhood of the target in all cases considered in this chapter.

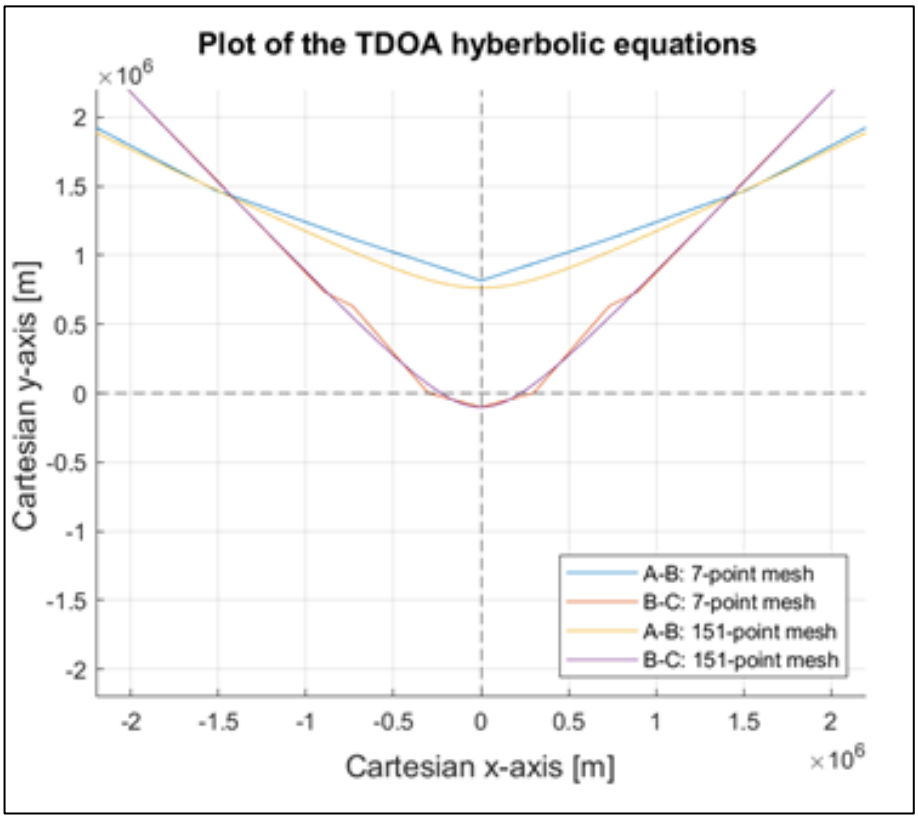

Figure 13: example of intersection finding of discretized hyperbolic functions for 7 and 151 mesh points, made in the Quantitative Matlab script. Note that both axis are in meters.

Since the TDOA solution relies on two equation and since the noise can be added or subtracted (early or late signal arrival detection), we actually have four intersection points:

1) A-B + noise & B-C + noise
2) A-B - noise & B-C + noise
3) A-B + noise & B-C - noise
4) A-B - noise & B-C - noise

These correspond with the points plotted in the qualitative Matlab script in Figure 12. Each of these cases is considered and the results are converted to angular error with respect to the origin, angular error expressed as a lateral distance at the target and range error as in 4.1.These results are then plotted for clarity, see section 5.3.1.

5.2 Verification & Validation

The verification and validation of the code was performed in multiple ways. The first and most straightforward can be seen in Figure 14. Here the time error is set to zero and as expect the predicted range, lateral and angular errors are calculated to be zero by the Matlab script, as can be seen in the bottom 4 subplots of Figure 14, which are empty since there is no error.

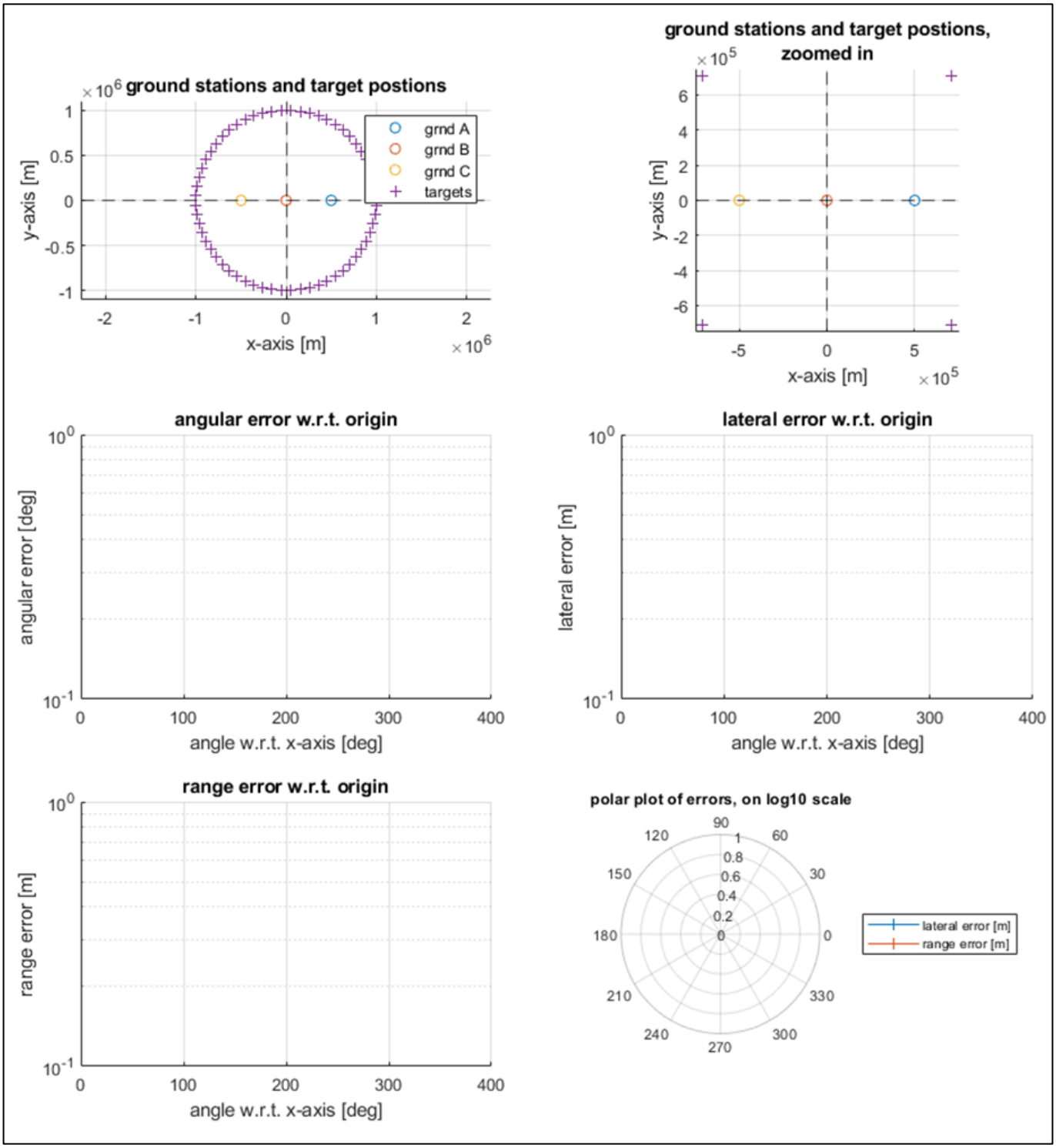

Figure 14: summary plots of the results of the quantitative Matlab script with time noise set to 0 inputs:: Ax=500000, Ay=0, Bx=0, By=0, Cx=0, Cy=-500000, target_range=1000000, time_noise=0, box=5000000, mesh=151, target_angle = 3:6:366;

Secondly, since the qualitative script was available this could also be used to validate the quantitative scripts. For example, from Figure 12 it can be expected that the range errors should be larger than the lateral errors when the ground stations are placed in a line, this could then easily be verified by looking at the results from the quantitative script.

Note that in section 7.3 the verification and validation of the 3D TDOA code is performed, in part using the 2D code. These two scrips have a fundamentally different approach to solve the problem. But can still be compared qualitatively and quantitatively.

5.3 Results

5.3.1 Numerical Results

In Figure 15 one can see the impact of variations in range, noise and baseline and the effect this has on lateral and range error. The lateral error is affected roughly equally by the three variations made to the inputs. Each one order of magnitude variation changes the lateral error with approximately one order of magnitude. However, the behaviour is different for the range errors. When the noise is increased by one order of magnitude, the range error increases by one order of magnitude. But a one order of magnitude variation to the range or baseline leads to approximately two orders of magnitude increase in the range error.

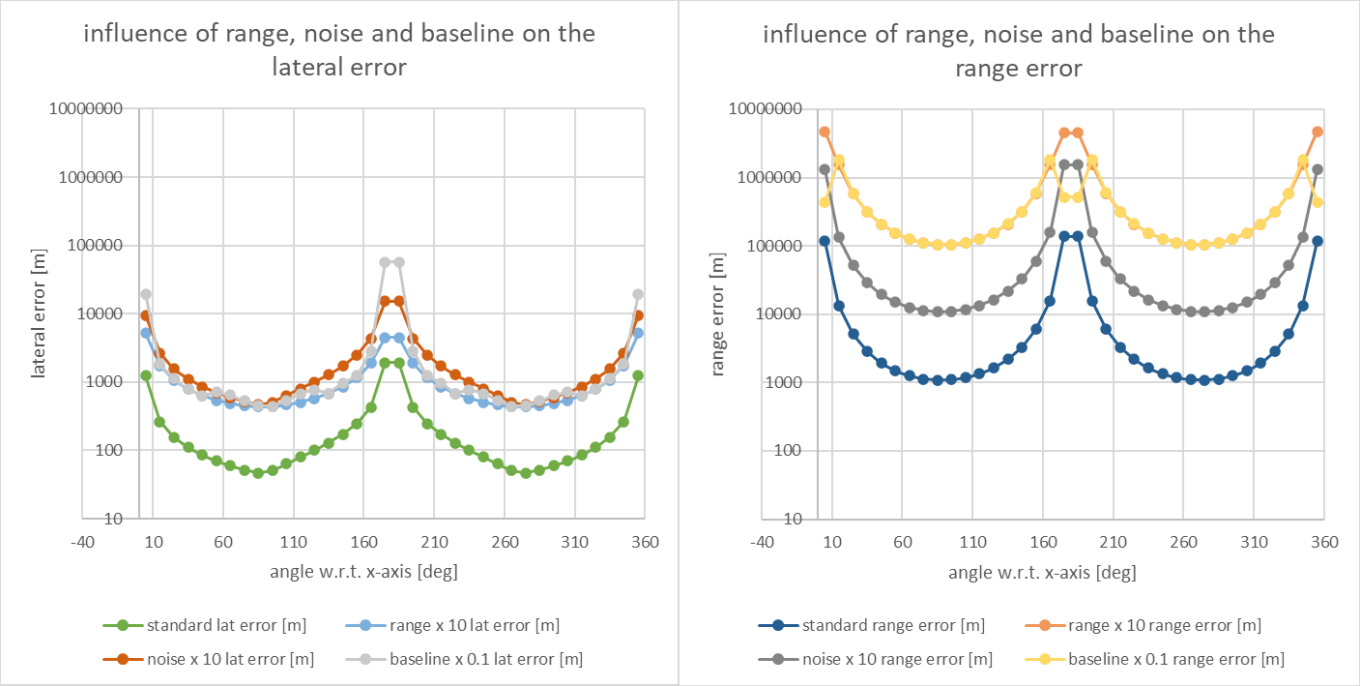

Figure 15: comparison of lateral error (left) and ranger error (right) for standard input data: Ax=500000, Ay=0, Bx=-500000, By=0, Cx=0, Cy=0, target_range=2000000, time_noise=0.000000036, box=5000000, mesh=151. With results from the standard cases and noise x10, target range x10 and baseline x 0.1 for comparative purposes.

The results presented in Figure 15 can be formulated as follows: the lateral error is proportional to the noise and the range between the ground stations and the target. It is inversely proportional to the baseline size. This is summarized in equation 5-8 below, where $C_{lat\ 2D}$ is the constant of proportionality.
The range error on the other hand is proportional to square of the range between the ground stations and the target and inversely proportional to the square of the baseline size. Note that it is still proportional to the noise. This relation is summarized in equation 5-9 below, where $C_{lat\ 2D}$ is the constant of proportionality for the two-dimensional range error.
Note that these relations are indicative only of the results presented above and do not constitute results from a derivation.

$$TDOA\ 2D\ lateral\ error\ \propto C_{lat\ 2D}\frac{range_{grnd\leftrightarrow target}\ \times\ noise}{baseline} \qquad 5\text{-}8$$

$$TDOA\ 2D\ range\ error\ \propto C_{lat\ 2D}\frac{\left(range_{grnd\leftrightarrow target}\right)^2\ \times\ noise}{(baseline)^2} \qquad 5\text{-}9$$

Figure 16 and Figure 17 are used to illustrate the effect of different geometries on the TDOA system performance.

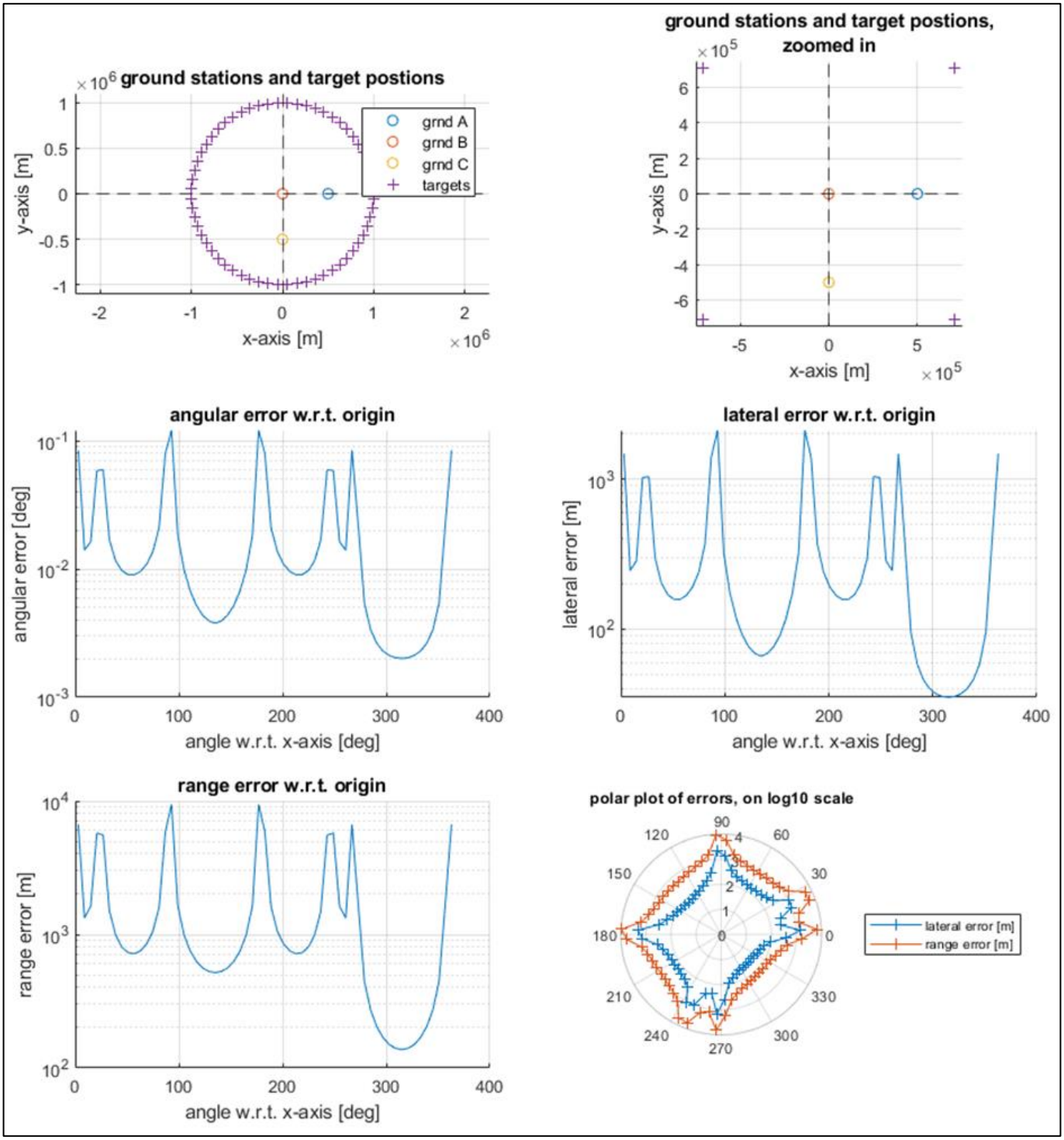

Figure 16: summary plots of the results of the quantitative Matlab script with inputs: Ax=500000, Ay=0, Bx=0, By=0, Cx=0, Cy=-500000, target_range=1000000, time_noise=0.000000028, box=5000000, mesh=151, target_angle = 3:6:366;

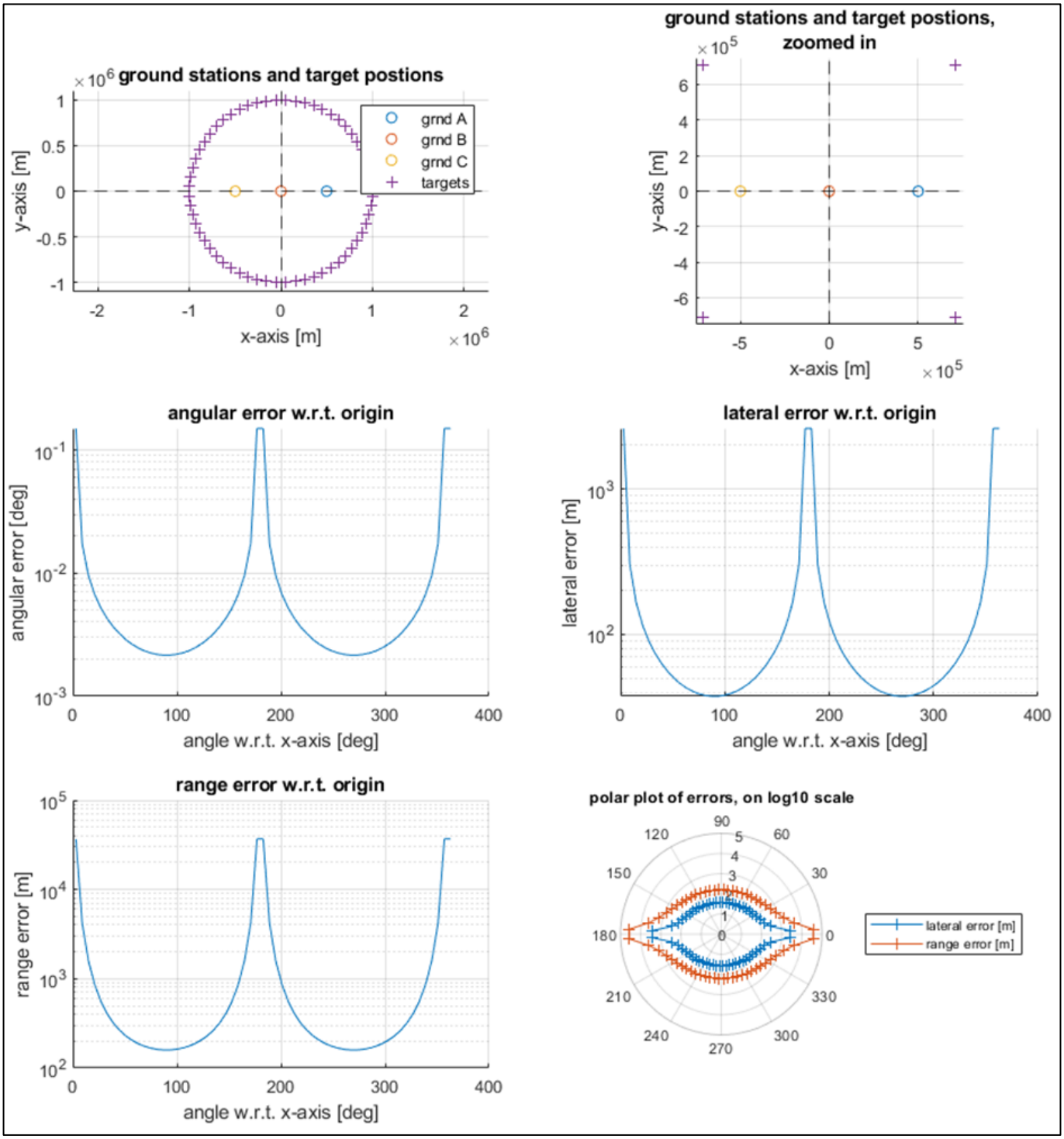

Figure 17: summary plots of the results of the quantitative Matlab script with inputs: Ax=500000, Ay=0, Bx=0, By=0, Cx=-500000, Cy=0, target_range=1000000, time_noise=0.000000028, box=5000000, mesh=151, target_angle = 3:6:366;

In Figure 16 ground station are place in an L-shape whereas in Figure 17 they are placed in a line, this can best be seen by looking at the two upper subplots in each of the figures.
In Figure 16 and Figure 17 one can observe that the performance of the TDOA system with respect to target location, orientation and ground station geometry. This is perhaps most clear in the two lower subplots, enlarged for clarity in Figure 18.

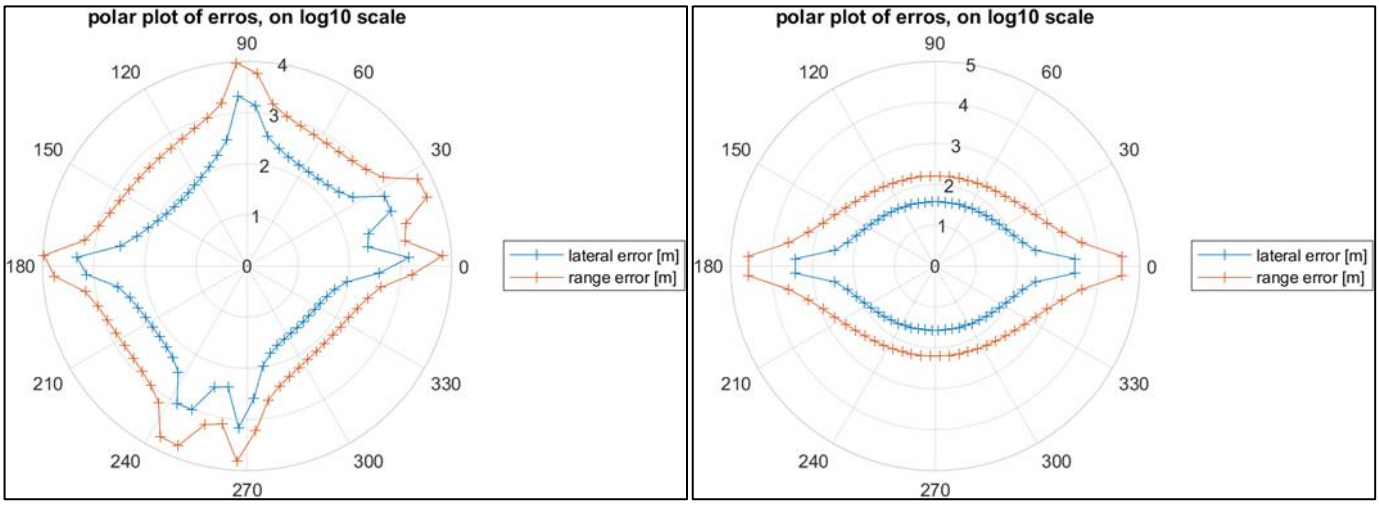

Figure 18: enlarged sub plots of Figure 16 and Figure 17

As discussed previously the error in range is noticeably larger than the lateral errors. But in Figure 18 one can also observe that the left plot is not symmetric whereas the plot on the right is. This is due to the different arrangement of the 3 ground stations.
One can also observe that the accuracy of the system is highly dependent on the target location. Even though all targets are located at the same distance from the origin, the errors (both lateral and range) vary by at least one order of magnitude and usually more than two. This points to the geometry and arrangement of the ground stations being one of the determining factors of a TDOA tracking system.

However here we run into the one of the weaknesses of this Matlab script: it is strictly two dimensional. This is a problem when the geometry of the ground stations plays such a big role in the overall system accuracy. There are several other limitations of this script. The code cannot correctly identify target points on the extension of the line connecting the two ground stations being used to establish equation 5-6 or 5-7, this is because for these cases when a noise error is applied the range error can become so large (see also Figure 16 and Figure 17) that it would fall beyond the bounds established by the box.
Only two of the 3 possible TDOA equations/hyperboles are used, and the same two equations/hyperboles are used for every target. This means that in some cases a sub-optimal combination of equations/ground station is used, leading to a larger apparent error.
Furthermore, the Matlab script is not a stochastic simulation, as such only limited conclusions can be drawn regarding the overall system accuracy.

5.3.2 Feasibility Consideration

In this section the feasibility of implementing a TDOA system will be discussed. All requirements will be dealt with in order.

ACC.1
This requirement is met for some target locations in Figure 16 and Figure 17. From section 5.3.1 we know that the accuracy can be improved by increasing the baseline, reducing the noise levels, etc. It is also important to note that having additional ground stations is expected to improve the system accuracy.

SAT.1
The TDOA system is expected to utilize the existing satellite radio communications system, so this requirement is met.

SAT.2
This requirement is closely linked with the ACC.1 requirement since the distance between the radio ground stations and the target satellite is a factor in the accuracy as shown in 5.3.1. For a satellite in an orbit of 500 km the minimum range between the satellite and ground station is 500 km, when the satellite is directly overhead. Or 2573 km maximum when the satellite is at 0 degrees above the horizon. In Figure 16 and Figure 17 the target satellite to ground station range is set to 1000 km, since this is considered a reasonable range value. As explained above the required accuracy is met for some target locations.
We know from equation 5-8 that the lateral errors are proportional to the noise and the distance between the target satellite and the ground stations, and inversely proportional to the baseline.
So, we can conclude that the required accuracy (ACC.1) can be met, for the required satellite orbital altitude SAT.2 for some combinations of baseline, noise, and range. Hence this requirement is achievable.

Before we cover the Ground station requirements, it is important to elucidate what a TDOA ground station requires to function:

1) Antenna and associated radio equipment to receive the signal.
2) GPS or GNSS receiver to establish the ground station position and provide an accurate reference timing.
3) Internet connection or other means of communication with other ground stations or a central hub.
4) Processing capacity to identify the time of arrival, estimate the target position based on the TDOA measurements and run all the systems mentioned above.

These are all commercial of the shelf components. No problems are foreseen in implementing these into a typical radio ground station. As such we foresee no problems in meeting the ground stations requirements: GRND.1, GRND.2, GRND.3.

In summary from a hardware perspective the TDOA tracking system meets the requirements set forth. However, the question of the system accuracy in a 3D system and with additional ground station remains.

From these results the decision was made to investigate the error present in a TDOA system (see chapter 6) And to develop an improved TDOA simulation tool (see chapter 7).

6) Sources of Noise and Measurement Errors in TDOA

From section 5.3.1 in the previous chapter we know that the noise and measurement errors play an important role in the overall TDOA system accuracy.
So, a more advanced TDOA simulation tool needs to account for the noise and measurement errors as part of the system. In this chapter a number of noise and measurement errors sources will be discussed and combined into an overall error to be used in the 3D TDOA simulation tool developed in chapter 7).

6.1 Total Electron Content (TEC)

Space-ground communications using radio are affected by the ionosphere [31]. Specifically, the total number of electrons present along the path between the transmitter and receiver, or the Total Electron Content (TEC) [31]. The electrons affect the path and time of flight of the radio signals. According to the National Oceanic and Atmospheric Administration (NOAA) ignoring TEC can lead to positioning errors for GPS on the order of tens of meters [31]. Note that the TEC is also dependent on the transmissions path length through the atmosphere and depends on solar cycle, geomagnetic conditions, etc.

The following equation is adapted from [32]:

$$R = \rho + \frac{40.3}{f^2} * TEC \qquad 6\text{-}1$$

From which the following equation can be derived

$$ranging\ error\ due\ to\ TEC = \frac{40.3}{f^2} * TEC \qquad 6\text{-}2$$

Where:

R	Range measured by the receiver
ρ	True geometric range
f	Operating frequency
TEC	Total electron content, $1\ TEC = 10^{16}\ electrons/m^2$, note in some literature this unit is called TECU.

From equation 6-2 the error induced by total electron content can be calculated for a range of different frequencies and TEC levels, see Table 3.

	0	50	100	150	200	250	300	350	400	450	500	TEC
	0	5E+17	1E+18	1.5E+18	2E+18	2.5E+18	3E+18	3.5E+18	4E+18	4.5E+18	5E+18	electrons/m^2
30	0	22389	44778	67167	89556	111944	134333	156722	179111	201500	223889	
100	0	2015	4030	6045	8060	10075	12090	14105	16120	18135	20150	
200	0	504	1008	1511	2015	2519	3023	3526	4030	4534	5038	
300	0	224	448	672	896	1119	1343	1567	1791	2015	2239	
400	0	126	252	378	504	630	756	882	1008	1133	1259	
500	0	81	161	242	322	403	484	564	645	725	806	
600	0	56	112	168	224	280	336	392	448	504	560	
700	0	41	82	123	164	206	247	288	329	370	411	
800	0	31	63	94	126	157	189	220	252	283	315	
900	0	25	50	75	100	124	149	174	199	224	249	
1000	0	20	40	60	81	101	121	141	161	181	202	

frequency [MHz] plot area: range error due to TEC in meters

Table 3: plot showing the range error in meters due to total electron content (TEC) for a range of TEC and frequencies, calculated based on equation.

As can be seen in Table 3, TEC errors can play a significant role in the accuracy of a radio-based positioning system, depending on the frequency and electron content.
However, these errors can be compensated for in several ways, three will be given below:

1) Have Delfi-PQ transmit on two different frequencies simultaneously. Since TEC affects different frequencies in a predictable way, the difference in arrival time between the two signals at different frequencies can be used to calculate the TEC along the signal path [32]. By knowing the TEC along the path, the effects of TEC can be compensated for. Note that that is applied to the so-called dual frequency GPS [32].
   This mitigation is considered highly unlikely, since it would probably require two separate antennae tuned to different frequencies to be carried by Delfi-PQ, and in any case greatly increases the complexity of the communications system. These changes to the communications system would mean not complying with requirement SAT.1.
2) Alternatively, publicly available data on the ionosphere can be used to correct for TEC. NOAA published TEC forecasts [33] and ESA publishes near real-time TEC maps [34]. Models also exist to correct for TEC errors such as the Ionospheric Correction Algorithm for Galileo Single Frequency Users [35].
3) Conversely the dual-frequency nature of the GPS signal can be used to calculate the TEC from a certain ground station to any GPS satellite. From this calculation an estimate can be made of the TEC to the target satellite by applying corrections for difference in elevation and azimuth of the target satellite with respect to the GPS satellite.

In summary the error from TEC can be significant and must be compensated for, this compensation can be achieved in many ways. TEC is not expected to be a dominant noise source, due to the aforementioned compensation and is not considered in the rest of the thesis.

6.2 Detection Error

In a TDOA ranging system it is important to measure the time of arrival of a given signal with high temporal precision. In our case specifically we want to measure the time of arrival of a specific bit or symbol. In Figure 19 a visual representation is given of how noise can lead to a ranging error (or measurement error) in pulse arrival time. This is analogous to the error in detecting symbols or bits. Note that this error can cause a measurement to register a signal arrival too early (as in Figure 19) or as too late due to the stochastic nature of the noise.

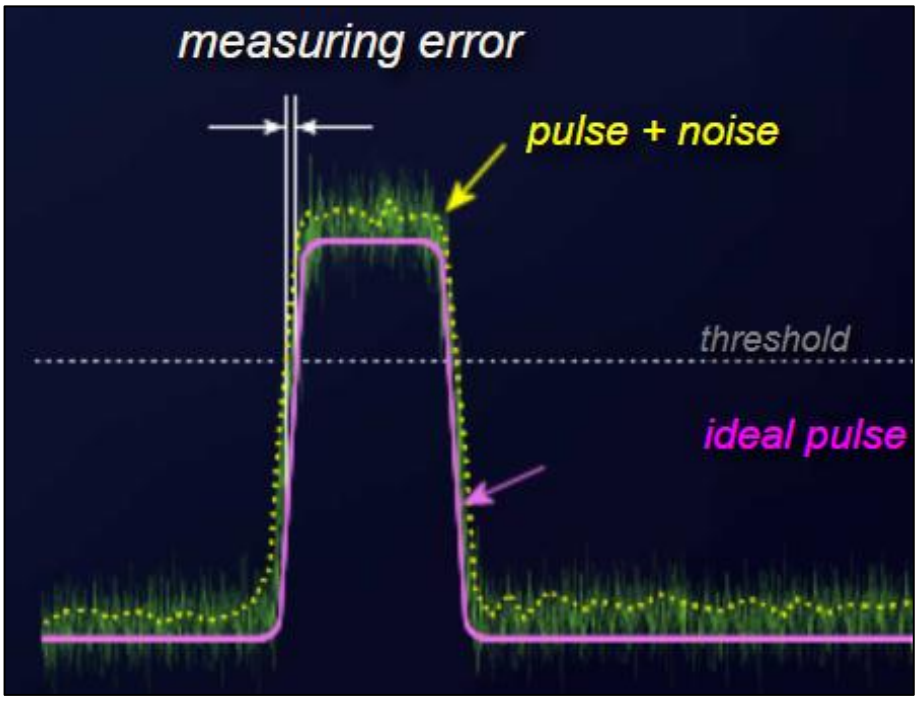

Figure 19: visual representation of a pulse measuring error (ranging error) due to noise, from [36]

Several equations [37] exist to calculate the two-way ranging error standard deviation. These equations require many inputs which are intrinsically related to the satellite communication system and the ground station design. Such as the modulation scheme used, signal to noise ratio, doppler shift, using a correlator VS a symbol loop, symbol rate, etc.
A full design of the satellite and ground station communications and ranging is beyond the scope of this thesis. However, the paper does present two examples, see Figure 20 below. From these examples we can conclude that the ranging error standard deviation (range jitter) varies from 10^4 to 10^{-2} m for a two-way ranging system. Note that the TDOA system is a one-way system, the results above will be converted to one-way in section 6.4.

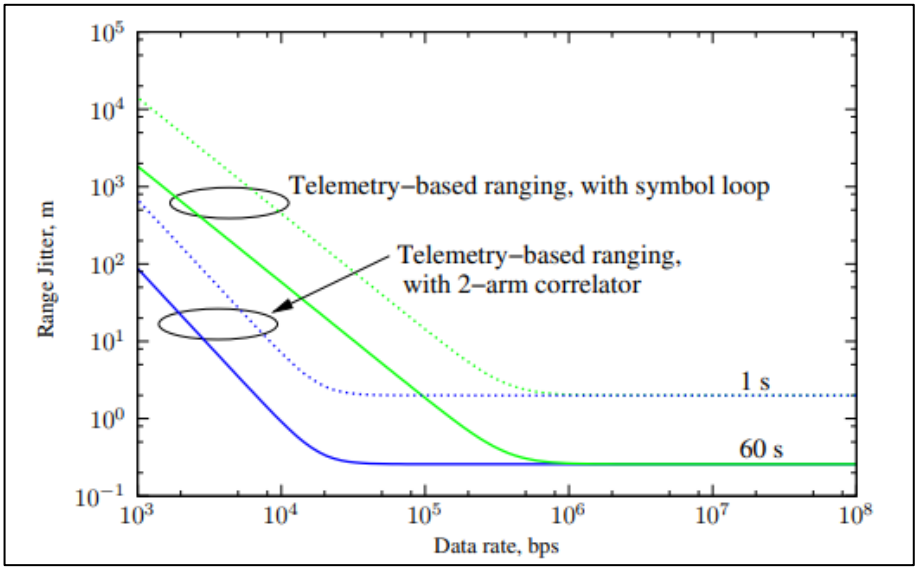

Figure 20: plots of the Range Jitter (or ranging error standard deviation) in meters wr.t. the data rate in bits per second (bps), source: [37]

6.3 GPS Timing Error

The final source of error is related to uncertainties of the time at the ground station. Since light travels at 299 792 458 meters per second [38] even milli- or nano-second uncertainties in time can heavily influence the system accuracy.
For the system being considered, it is assumed that the ground station clock synchronized via a GNSS receive (Global Navigation Satellite System) since this allows for high time precision at relatively low cost, using commercial of the shelf components as per requirement GRND.1. According to the operator of the GPS (Global Positioning System) system, the United States government, the temporal accuracy is $\leq 30\ nano\ seconds$ 95% of the time [39] for specialized receiver at a fixed location. The assumption is made that the accuracy follows a normal distribution and hence the empirical rule for normal distribution [40] can be applied. From this we can concluded that a single standard deviation for GPS time errors is 15 nano seconds with mean zero. Note since 95% corresponds to two sigma deviation we must dived the 30 ns by two to find the one sigma or 68% deviation to be 15 ns.

6.4 Combining the Error and Noise Factors for TDOA

In the previous sections several sources of noise in the time and range domain were elaborated. These are by no means exhaustive but covers a range of possible environmental and system error sources deemed most important.

First it is important to realize that ranging errors and timing error are linked through the following formulas [30]:

$$range = time\ of\ flight * c \tag{6-3}$$

Which can be modified to:

$$range\ error = time\ of\ flight\ error * c \tag{6-4}$$

Where:

c Speed of light in a vacuum

The next issue is how to combine the disparate error sources into a single error distribution. This is done by assuming that each error source follows a normal distribution and is uncorrelated with the others. Then applying the following relation successively on each error source (from [41]):

$For\ uncorrelated\ variables$:

$$N(\mu_x, \sigma_x^2) + N(\mu_y, \sigma_y^2) = N(\mu_x + \mu_y, \sigma_x^2 + \sigma_y^2) \tag{6-5}$$

Where:

N Normal distribution or Gaussian distribution, the first term is the mean, and the second term is the variance.
μ_x Mean of normal distribution x
μ_y Mean of normal distribution y
σ_x^2 Variance of normal distribution x
σ_y^2 Variance of normal distribution y
σ Standard deviation

Note that the equation above states that the sum of two normal distribution is another normal distribution.

This equation can also be inverted to convert the ranging error standard deviation found in section 6.2 to a one-way error by assuming the two-way error is the sum of two uncorrelated one-way errors that follow a normal distribution. See Table 4 for the results of this approach.

Two-way detection error SD [m]	One-way detection error SD [m]
10000	7071
1000	707
100	71
10	7
1	0.7
0.1	0.07
0.01	0.007

Table 4: table comparing the two-way ranging error with the one-way ranging error.

From table Table 4 one can conclude that one-way ranging can be expected to be noticeably more accurate than two-way. This result can then be combined by using equation 6-4 into a total standard deviation (SD) error as given in Table 5 below. Note that the mean of the individual and total errors is zero.

Two-way detection error SD [m]	One-way detection error SD [m]	GPS timing error SD [m]	Total error SD [m]	Total error SD [ns]
10000	7071	4.5	7071	23587
1000	707	4.5	707	2359
100	71	4.5	71	236
10	7	4.5	8	28
1	0.7	4.5	5	15
0.1	0.07	4.5	4	15
0.01	0.007	4.5	4	15

Table 5: table listing the total standard deviation error composed of the GPS timing error and the one-way (ranging) error).

The table above gives a range of plausible standard deviation errors for TDOA. Note that for low detection errors the GPS timing error becomes dominant and vice versa, see also Figure 21 below.

Figure 21: figure showing the one-way detection error SD [m], GPS timing error SD [m] and total error SD [m] with respect to two-way detection error SD [m]. Based on data from Table 4 and Table 5.

7) 3D Time Difference of Arrival

In this chapter TDOA in 3D is modeled in a Matlab script by application of linearized least squares. First in the preamble a simple qualitative script is used to explore TDOA in 3D. Then the implementation of a 3D Quantitative TDOA simulator is explained, followed by verification, validation, and results.

7.1 Preamble: Qualitative 3D Matlab Script

Similar to the approach taken in chapter 5) a qualitative Matlab script was first written. Even though this script was not used to generate numerical results, it did lead to two important observations applicable to implementing a full 3D TDOA simulator. This Qualitative 3D Matlab Script will be briefly covered in this preamble before diving into the more advanced code it was a steppingstone to.

The code plots the 3D hypersurface(s) (adapted from the 2D TDOA relation introduced in 5.1):

$$r_{grnd,A} - r_{grnd,B} \pm c * noise_{time} = \sqrt{(x - x_A)^2 + (y - y_A)^2 + (z - z_A)^2} - \sqrt{(x - x_B)^2 + (y - y_B)^2 - (z - z_B)^2} \quad 7\text{-}1$$

The user can specify four ground stations and one target, then the equation above can be plotted as a hyper surface for any combination of two ground station. One of these hypersurfaces is plotted in Figure 22 below:

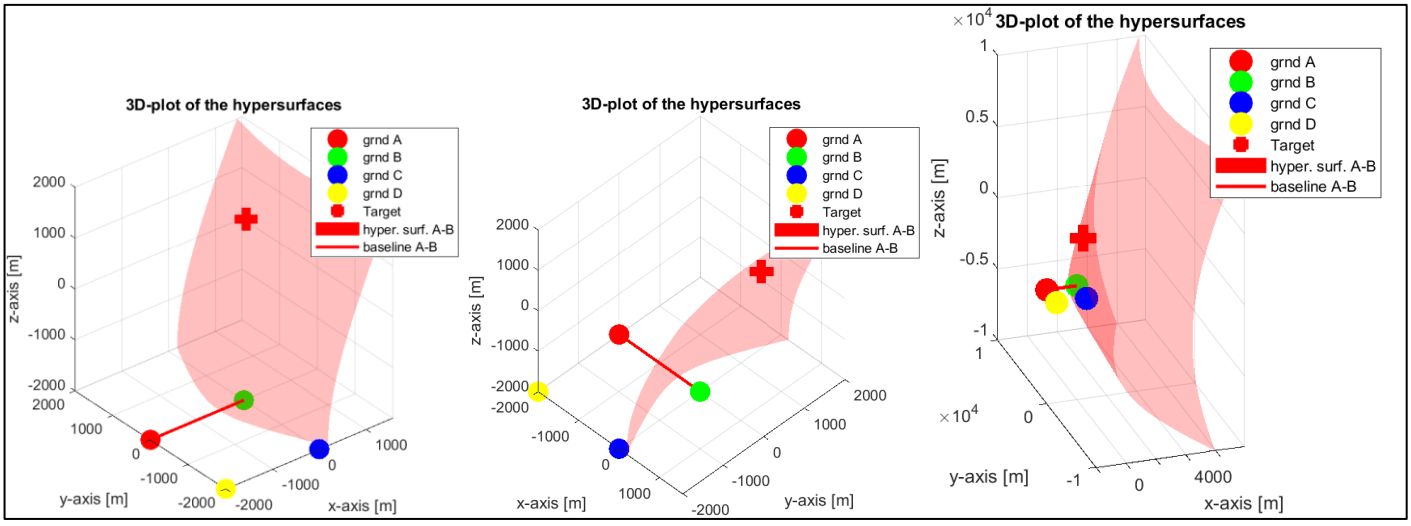

Figure 22: several views of a single hypersurface, including zoomed out view. Generated with the qualitative Matlab script, inputs: Ax -2000, Ay 0, Az -2000, Bx 0, By 0, Bz -2000, Cx 0, Cy -2000, Cz -2000, Dx -2000, Dy -2000, Dz -2000, Tx 700, Ty 800, Tz 900, bound x min -2000, bound x max 2000, bound y min -2000, bound y max 2000, bound z min -2000, bound z max 2000 all units in meters, with A, B, C and D ground stations and T the target. Left: view 1, centre: view 2, right view 3, zoomed out view, bounds were multiplied with 5.

Since four ground stations can be combined into six unique pairs, this means that there are 6 hypersurfaces that can be plotted. This leads us to our first important observation: for each additional ground station (in view of the target satellite) the number of additional TDOA measurements increases with the number of ground stations already present. For example, if there if a fifth ground station is added, 4 additional TDOA measurements are made available, meaning 4 additional hypersurfaces can be constructed. The effect of this is shown visually in Figure 23 below. Note that the number of TDOA measurements increases quadratically: $TDOA\ measurements = \frac{L^2}{2} - \frac{L}{2}$ where L is the number of ground stations [42].

This is an important effect since it implies that each ground station added to the system greatly increases the number of measurements available for the position estimation. Since the errors / noise follows a normal

distribution as per chapter 6) , having more measurements increases the confidence and accuracy of the position estimation. As more measurements are used; more information is available on the target satellite position. Or to make the link with chapter 4) effectively we can increase the integration gain by taking more measurements through multiple ground stations. This is further elaborated upon in section 7.4.1.

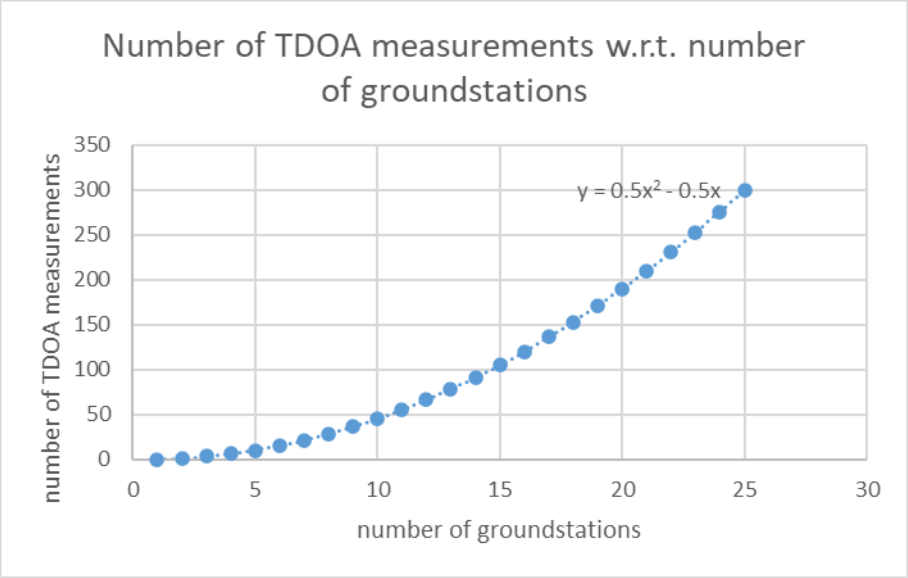

Figure 23: plot of the number of TDOA measurements with respect to the number of ground stations.

The Matlab tool also lets us visualize a counter-intuitive feature of TDOA, namely that 4 or more ground stations are necessary to localize a target in 3D space [42], see Figure 24 below. In this figure one can clearly see that if only three ground stations are used to constitute the TDOA measurements, the hypersurfaces do not intersect in only 1 point as in Figure 25 below, but they intersect in an infinitely long curve. This means that mathematically there are infinite intersections and there is insufficient information to localize the target in 3D space. Note that it is possible to locate an object in 3D space if additional information is known. For example, if the TDOA system is used to locate a target on the surface of the earth it can be located by using 3 ground stations and finding the intersection of the curve with the surface of the earth.

Note that in this chapter we are treating the TDOA tracking as a positioning problem, in other words the target satellite is assumed to transmit one message, this message is received by the ground stations and the satellite position at the time of transmission is estimated. Effectively the problem is simplified to a positioning problem. In chapter 8) a method is presented for future implementation which utilize multiple measurements in time to estimate not just the target satellite position but also its velocity, from this the orbit of the target satellite can be predicted.

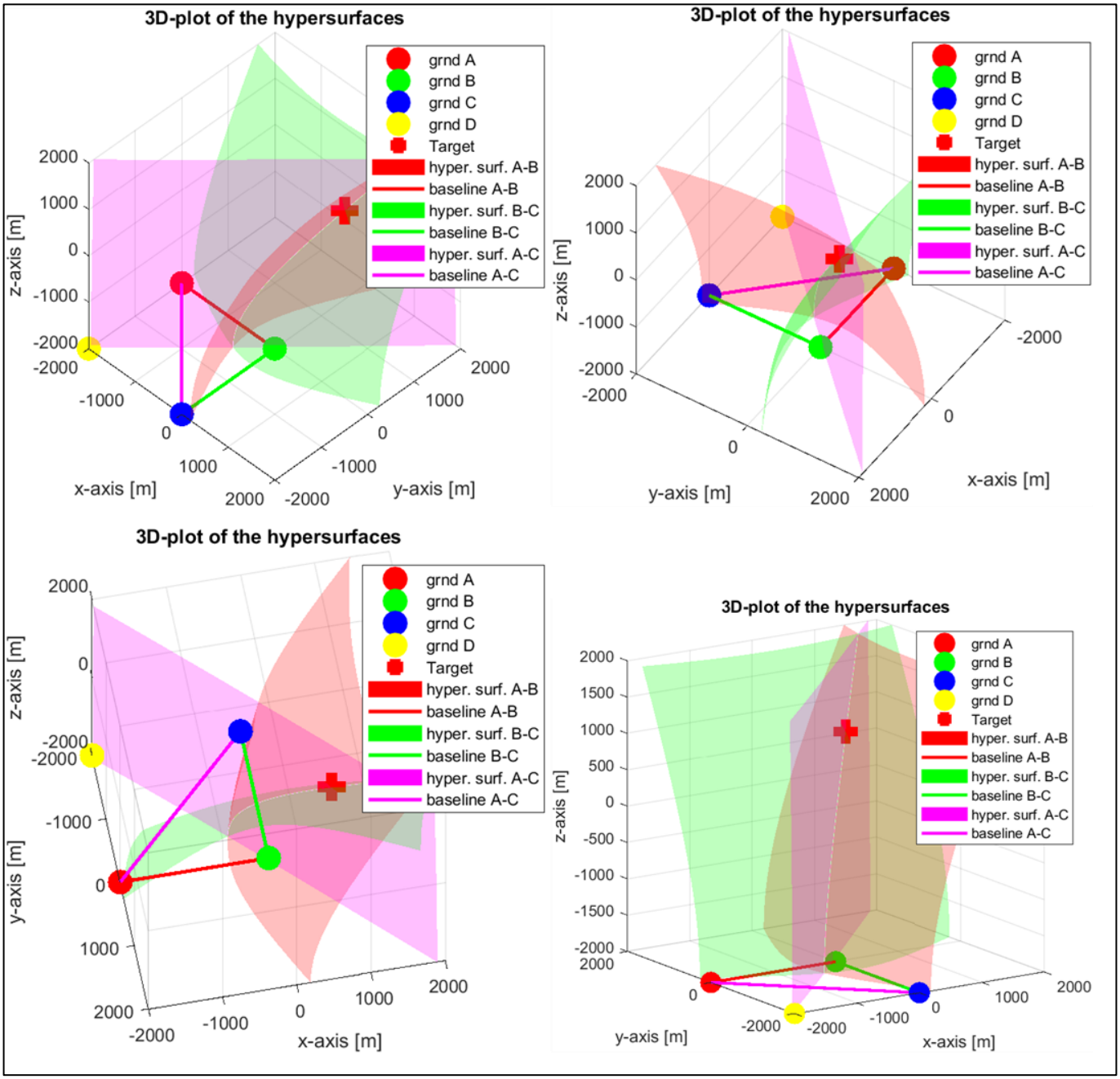

Figure 24: visualization of the linear dependence of the 3 TDOA measurement derived from 3 ground stations. inputs: Ax -2000, Ay 0, Az -2000, Bx 0, By 0, Bz -2000, Cx 0, Cy -2000, Cz -2000, Dx -2000, Dy -2000, Dz -2000, Tx 700, Ty 800, Tz 900, bound x min -2000, bound x max 2000, bound y min -2000, bound y max 2000, bound z min -2000, bound z max 2000 all units in meters, with subscripts A, B, C and D indicating ground stations and T the target.

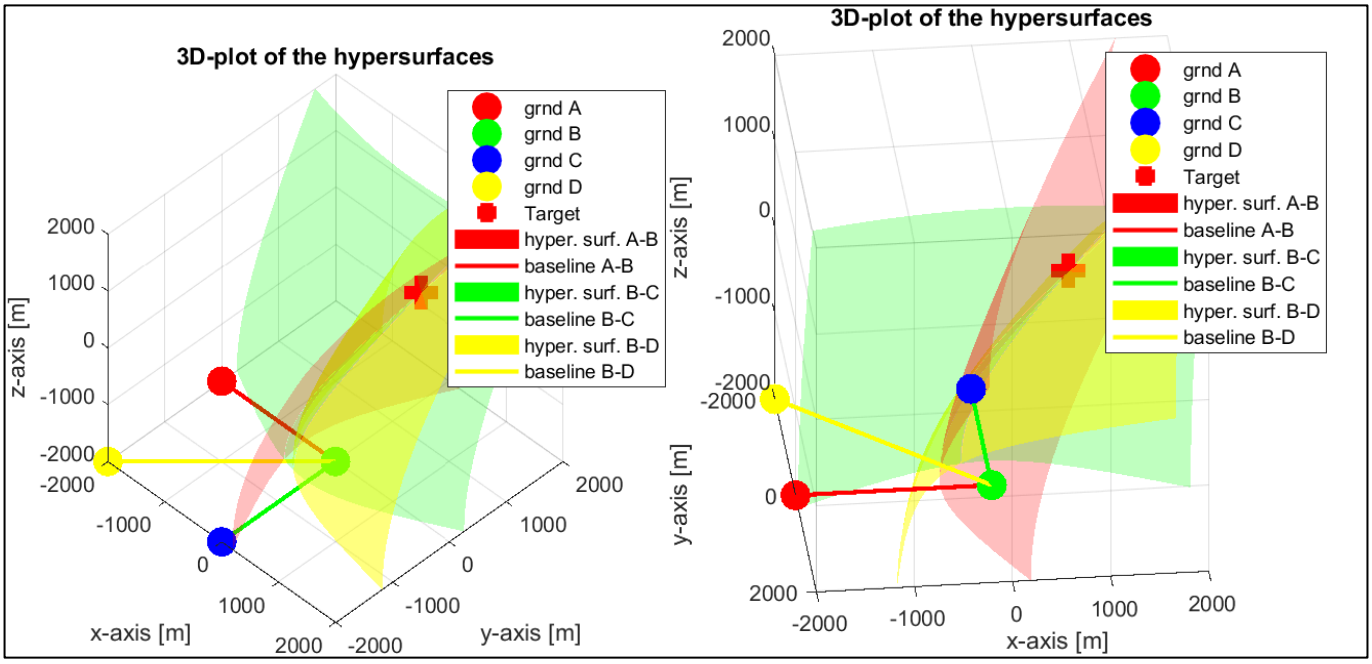

Figure 25: visualization of the linear independence of the 3 TDOA measurement derived from 4 ground stations. inputs: Ax -2000, Ay 0, Az -2000, Bx 0, By 0, Bz -2000, Cx 0, Cy -2000, Cz -2000, Dx -2000, Dy -2000, Dz -2000, Tx 700, Ty 800, Tz 900, bound x min -2000, bound x max 2000, bound y min -2000, bound y max 2000, bound z min -2000, bound z max 2000 all units in meters, with subscripts A, B, C and D indicating ground stations and T the target.

Attempts were made to find the intersection of the hypersurfaces in 3D, using a 3D variant of the techniques used in section 5.1.2, but this proved to be excessively computationally intensive and was a contributing factor to the utilization of linearized least squares approach in the advanced code covered in the next section.

7.2 Implementation of 3D TDOA

In this section, the implementation of the main code will be elaborated.

The purpose of this code is to provide a first order estimate TDOA tracking techniques as implemented to a satellite, specifically:

- The impact of ground station positions w.r.t accuracy and coverage area
- Accuracy (in various forms) w.r.t ground stations, timing accuracy/noise, etc.
- The impact of the "optical ground station" on accuracy and coverage

In addition, the code is:

- Fully three dimensional
- Able to use information from up to 25 ground stations to better estimate the target position. If more than 25 ground stations are required, then it is possible to change the "supporting code".

Due to the complexity of the 3D TDOA code, it is split into three parts. The first part listed in section 7.2.1 reads and loads the input data, keeps records of the outputs, and generally supports the other two parts. In the section 7.2.2 the 3D TDOA problem is solved numerically by application of linearized least square and Cholesky decomposition. In the last section: 7.2.3 the results of the least squares are processed and converted to quantified and aggregated system accuracies.

7.2.1 Supporting Code

A schematic overview of this part of the code is given in Figure 26 below. Each of the elements of the code diagram will we explained this section to give the reader an overview of the code and its functioning.

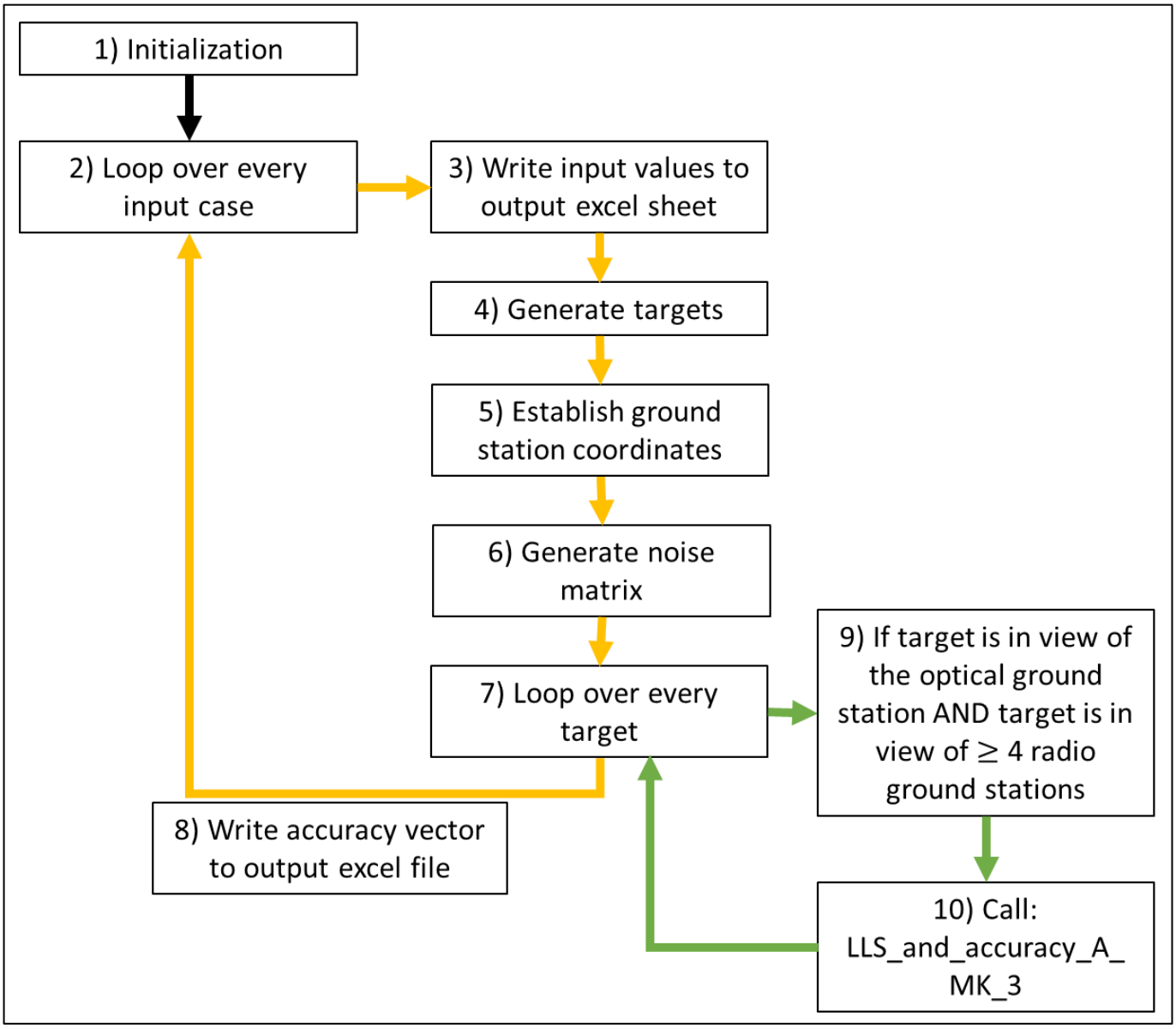

Figure 26: diagram of the supporting code

1) **Initialization**
   The TDOA code requires many inputs (minimum 31, typically close to 100), such as target satellite altitude, ground station coordinates, etc. It would be impractical to enter all these manually into Matlab for each test case. Hence the inputs are entered into an excel sheet which Matlab can then read the input values out of. An example of (part of) such an excel sheet is given in Figure 27 below. Note that formulas and formatting can be applied to generate this input excel sheet quickly and clearly. Hence the user only has to enter 4 inputs into Matlab:
   a. path (the path of the location of the excel file)
   b. excel_file (the name of the excel file including .xlsx at the end)
   c. sheet_name (the name of the sheet in the excel file containing the inputs to be used
   d. range (the range of the input values in the excel sheet, for example: "C3:I122"). Note that each column in the range is treated as a separate input case

These inputs are then used to read the input values from excel and store them in Matlab.

Identifiying information	batch_name [-]	"validation_1"	"validation_1"	"validation_1"	"validation_1"	"validation_1"	"validation_1"	"validation_1"
	run_name [-]	"baseline"	"noise to zero"	"optical out of bounds"	"optical out of bounds + angle = -90"	"radio 89"	"radio -90"	"radio to far apart"
	date [dd/mm/yyyy]	16/07/2021	16/07/2021	16/07/2021	16/07/2021	16/07/2021	16/07/2021	16/07/2021
Location of the results	filename of excel with results [-]	"C:\Users\timna	"C:\Users\timna	"C:\Users\timna	"C:\Users\timna	"C:\Users\timna	"C:\Users\timna	"C:\Users\timna
	tab of the excel sheet containing the results [-]	1	2	3	4	5	6	7
Targets population	latitude_step_size [deg]	5	5	5	5	5	5	5
	longitude_step_size [deg]	5	5	5	5	5	5	5
	altitude [m]	1000000	1000000	1000000	1000000	1000000	1000000	1000000
noise matrix	noise_matrix_length [rows]	1000	1000	1000	1000	1000	1000	1000
	noise_time [sec]	4.00E-08	0	4.00E-08	4.00E-08	4.00E-08	4.00E-08	4.00E-08
	reference_area [m^2]	7854	7853.981634	7853.981634	7853.981634	7853.981634	7853.981634	7853.981634
	rng seed	"default"	"default"	"default"	"default"	"default"	"default"	"default"
LLS solver inputs	max_steps [-]	100	100	100	100	100	100	100
	max_step_size [m]	500	500	500	500	500	500	500
	tolerance [m]	0.01	0.01	0.01	0.01	0.01	0.01	0.01
Accuracy_groundstation_lla	lat [deg]	51.51457032	51.51457032	-41.19742966	-41.19742966	51.51457032	51.51457032	51.51457032
	long [deg]	5.643491173	5.643491173	174.8925586	174.8925586	5.643491173	5.643491173	5.643491173
	alt [m]	149.7034467	149.7034467	0	0	149.7034467	149.7034467	149.7034467
	Accuracy Groundstations min elevation [deg]	-90	-90	20	-90	-90	-90	-90
	Number of groundstations [-]	16	16	16	16	16	8	8
Groundstations_lla	lat [deg]	64.01384978	64.01384978	64.01384978	64.01384978	64.01384978	45	45
	long [deg]	-22.51309868	-22.51309868	-22.51309868	-22.51309868	-22.51309868	0	0
	alt [m]	20	20	20	20	20	0	0
	min elevation angle [deg]	10	10	10	10	89	-90	**30**
	etc.	65.57621954	65.57621954	65.57621954	65.57621954	65.57621954	45	45
		-13.81737035	-13.81737035	-13.81737035	-13.81737035	-13.81737035	90	90
		20	20	20	20	20	0	0
		10	10	10	10	89	-90	**30**

Figure 27: Matlab inputs excel sheet example, note the formatting and that excel formulas can be used to generate this sheet.

2) Loop over every input case

This section initiates the primary loop and is indicated in yellow in Figure 26. In this loop each test case defined in the input excel sheet is sequentially treated.

3) Write input values to output excel sheet

In this section the input values are written into the output excel sheet for reproducibility.

4) Generate targets

The code assesses the system performance by generating a large target population and subsequently (attempting to) estimate the position of each target through TDOA. These targets are placed at a predefined height above the surface of the earth and in a grid defined by a latitude steps size and a longitude steps size, as can be seen in Figure 28 below.

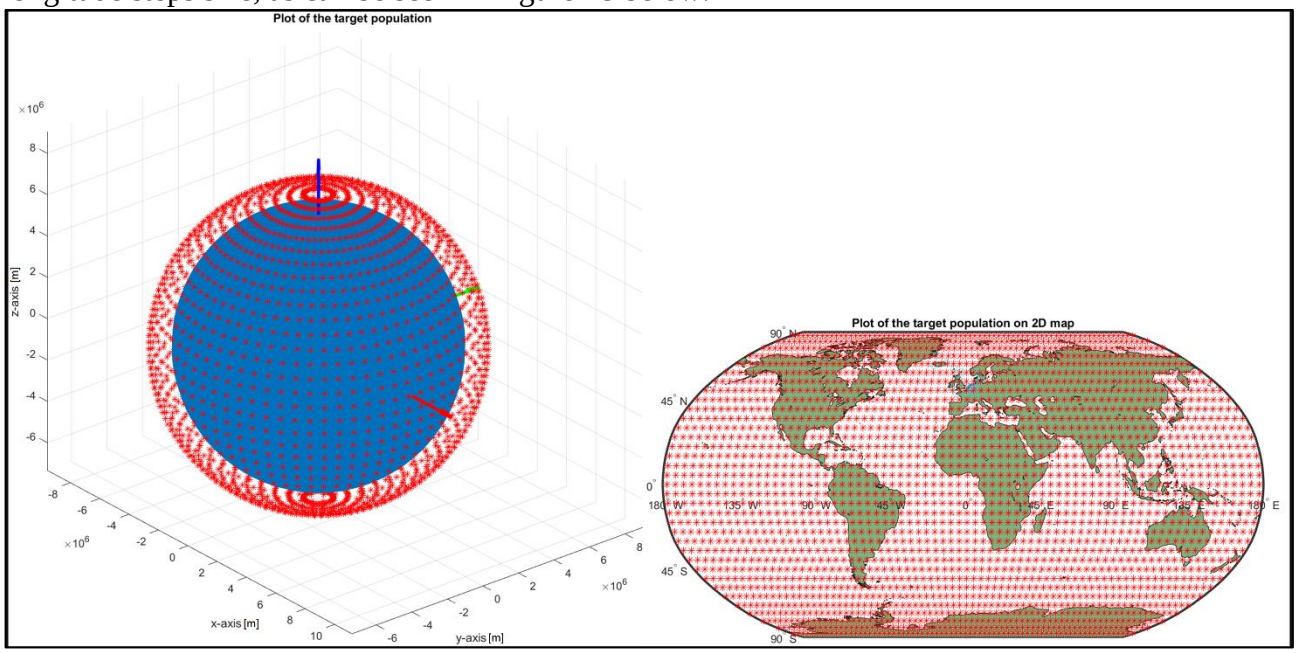

Figure 28: plot of the target population for latitude and longitude step size at 5 deg and altitude set to 1000 km. The left-hand plot gives a 3D view whereas the right-hand plot shows the target population on a map of the earth.

5) **Establish ground station coordinates**

Each ground station is defined by four inputs: the location of the ground station in latitude, longitude and altitude and the ground station minimum elevation angle.

Note that the term "altitude" is used to indicate the height of a ground station above the surface of the earth, the term "elevation" is reserved for the angle related to tracking/poisoning. It is important to note that the input altitude used is the altitude above sea level of the antennae. In the input excel sheets a separate tab called: "coordinated generator" is supplied to facilitate the generation of the inputs, note that the Matlab function elevation(…) [43] can be used to quickly find the elevation above sea level of latitude and longitude coordinates.

In the Matlab code the altitude above sea level is converted to the altitude above the ellipsoid, to enable later conversion of the latitude – longitude – altitude coordinates to the earth-centered-earth-fixed (ECEF) coordinate frame. As can be seen in Figure 29 this requires the addition of the geoid height, Matlab function geoidheight(…) is used for this.

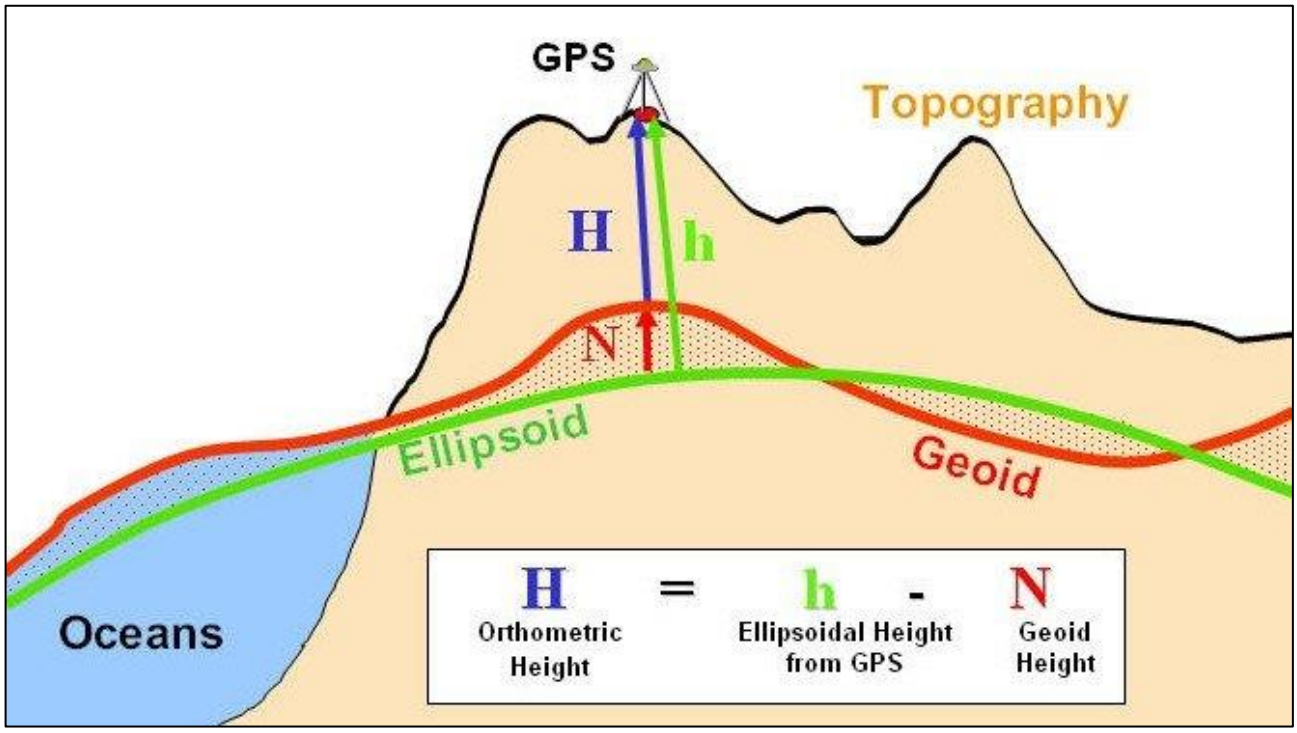

Figure 29: diagram of the relation between the ellipsoidal, geoid and orthometric height source: [44]

The Matlab function lla2ecef(…) is used to convert the ground station coordinates to the earth-centered-earth-fixed coordinate frame, by using the WGS84 ellipsoid model.

6) **Generate noise matrix**

As explained in 6), several different noise and measurement errors can affect the system under consideration, these are called noise from here on. These are stochastic in nature and are represented in the code through the noise matrix. This is a matrix where each column corresponds to a certain ground station and the number of rows can be specified by the user. Each row corresponds to a "case" for which the simulation will be run.

The user must also specify the noise_time this is the sample standard deviation use to generate the values in the noise matrix. Each element in the noise matrix corresponds to a certain ground station (column) and a certain "case" (row) for which it represents noise present in the TDOA measurement. This noise is also referred to as the noise time since it is representing the timing inaccuracy in measuring the time of arrival at each ground station which is used to calculate the TDOA measurements.

7) **Loop over every target**

Here the secondary loop is initiated where each target location generated in: "4) generate targets" is considered in turn.

8) **Write accuracy vector to output excel file**
   The accuracy vector is the output of the LLS_and_accuracy_A_MK_3 function. It is written into the output excel file for future analysis, plotting, etc.
9) **If target is in view of the optical ground station AND target is in view of ≥ 4 radio ground stations**
   This check is performed to prevent wasting computational power on targets that cannot be detected or tracked. Note that for TDOA to track a point in 3D it needs at least 4 independent measurements, implying at least 4 ground stations are needed, see also 7.1.
10) **Call: LLS_and_accuracy_A_MK_3**
    Here the separate function **LLS_and_accuracy_A_MK_3** is called. This function performs the linearized least squares to determine where the TDOA systems estimates the target satellite to be. This function also assesses the accuracy of this position estimate by comparing it with the true position of the target satellite. These topics are however extensive enough to warrant their own sections, see 7.2.2 and 7.2.3.

7.2.2 Linearize Least Squares

The linchpin of the 3D TDOA approach is the implementation of a Linearize Least Squares (LLS) algorithm. This is a mathematical algorithm that has several advantages over the previous method used (finding the intersections of 2D hyperbolic functions, see 5). One of the advantages of linearized least squares is that it is orders of magnitude faster than the intersection finding method. It can also utilize many baselines simultaneously, allowing for additional measurements to be used, leading to better accuracy. In other words, LLS can handle "over constrained" problems. Consider the 2D case: we have 3 hyperbolic curves then they will theoretically intersect in the same point (the target), but in reality, due to the presence of noise there will probably be 3 intersections near the target. With least square we can use the 3 hyperbolic curves simultaneous to find the most probable target location.

The background and approach of LLS presented in this chapter are based on E. Gill and O. Montenbruck's excellent book: Satellite Orbits Models, Methods and Applications [45] and on B. D. Tapley, B. E. Schutz, and G. H. Born' very extensive book Statistical Orbit Determination [46]. The publicly available MATLAB code "TDOA simulation" by Ufuk Tamer [47] was also used as a starting point for the code and modified and expanded upon.

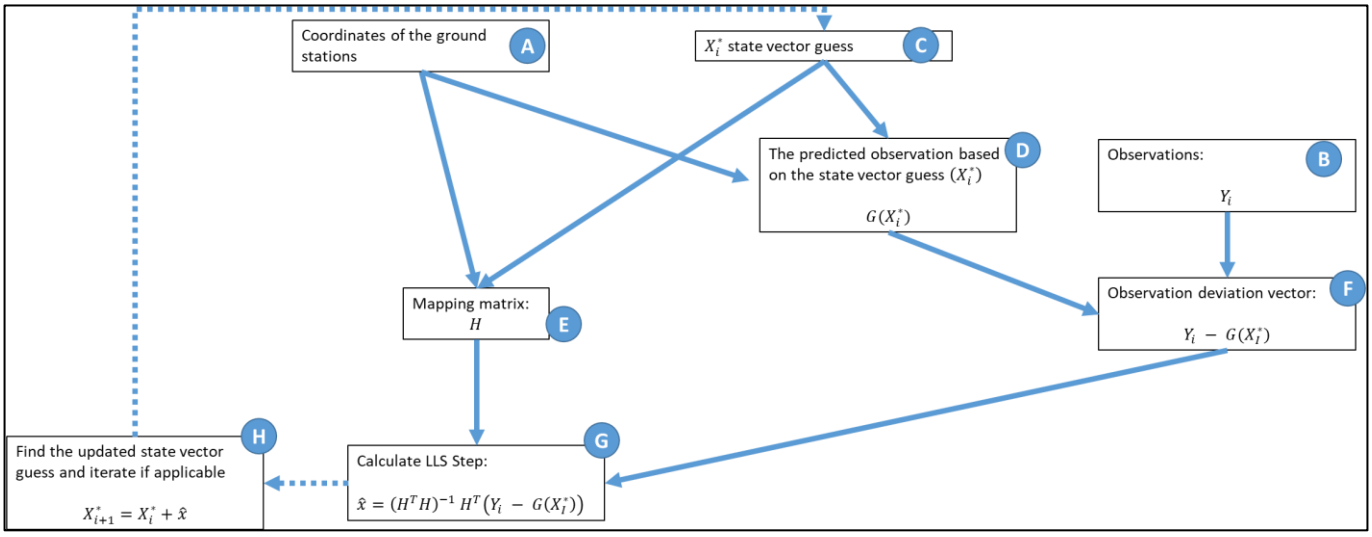

Figure 30: schematic representation of the LLS algorithm, each block is indicated with a number to facilitate the written explanation.

Figure 30 presents the algorithm. Note that the coordinate system used is earth-centred earth-fixed.

The coordinates of the ground stations (A) are taken as an input (in matrix format) as are the observations Y_i

(B). These observations are the time of arrival measurements taken at every ground station and degraded with the noise/measurement errors as explained in point **6) Generate noise matrix** in section 7.2.1. In effect these measurements are ambiguous and will be pointing towards different points in space as being the position of the target satellite. How LLS operates and how it deals with this will be covered later in this section.
The last input is X_i^* (C), the state vector guess, this vector contains the (initial) guess for the state vector describing the satellite position. During the LLS process an initial guess is required for the target position. This initial guess is taken to be the true target position. This implicitly assumes that an initial guess is present that is close to the true target. Note that in practice the code will usually still converge to a mathematically correct solution even if the initial guess is far from the target. But this will require (significantly) more computing power and runs the risk of getting stuck in a local minima or phantom/alternate solution (see Figure 10).

In (D) the vector $G(X_i^*)$ is generated, this vector contains the predicted observations based on the state vector guess X_i^*. The observations simulated by calculating the distance between the state vector guess and each ground station. This can then be converted to TDOA measurements.

The next step (E) is to establish the mapping matrix H this matrix maps how a change in the state vector guess X_i^* will lead to a change in the predicted observations. The formula used is adapted from [46]:

$$H = \begin{bmatrix} \frac{X - X_{grnd(1)}}{\rho_1} - \frac{X - X_{grnd(2)}}{\rho_2} & \frac{Y - Y_{grnd(1)}}{\rho_1} - \frac{Y - Y_{grnd(2)}}{\rho_2} & \frac{Z - Z_{grnd(1)}}{\rho_1} - \frac{Z - Z_{grnd(2)}}{\rho_2} \\ \vdots & \vdots & \vdots \\ \frac{X - X_{grnd(i-1)}}{\rho_{i-1}} - \frac{X - X_{grnd(i-1)}}{\rho_i} & \frac{Y - Y_{grnd(i-1)}}{\rho_{i-1}} - \frac{Y - Y_{grnd(i)}}{\rho_i} & \frac{Z - Z_{grnd(i)}}{\rho_{i-1}} - \frac{Z - Z_{grnd(i)}}{\rho_i} \end{bmatrix} \quad 7\text{-}2$$

With:

$$\rho_1 = \sqrt{\left(X - X_{grnd(1)}\right)^2 + \left(Y - Y_{grnd(1)}\right)^2 + \left(Z - Z_{grnd(1)}\right)^2} \quad 7\text{-}3$$

And:

$$\rho_2 = \sqrt{\left(X - X_{grnd(2)}\right)^2 + \left(Y - Y_{grnd(2)}\right)^2 + \left(Z - Z_{grnd(2)}\right)^2} \quad 7\text{-}4$$

Etc.

X, Y, Z	The Cartesian ECEF coordinates of the target guess, note that $X_i^* = [X, Y, Z]$
$X_{grnd(1)}, Y_{grnd(1)}, Z_{grnd(1)}$	The Cartesian ECEF coordinates of the first ground station
$X_{grnd(2)}, Y_{grnd(2)}, Z_{grnd(2)}$	The Cartesian ECEF coordinates of the second ground station
Etc.	Etc.

Note that in the three equations above the multiplication with c is omitted for clarity, and the equations above can be converted from distance to time-of-flight via [30]:

$$range = time\ of\ flight * c \quad 7\text{-}5$$

The matrix H contains information on how a change in the initial state vector guess X_i^* will change the predicted observations $G(X_i^*)$. This is one of the assets of the LLS approach, it has information on how a change in the state vector guess will lead to a change in predicted observations.

The speed of light used in this script was take from [38].

The observation deviation vector (F) is simply the difference between the (measured) observations and predicted observations, it may also be called the cost function since it is what the LLS algorithm is trying to minimize.

Subsequently in (G) the LLS step is calculated by applying the formula [46]:

$$\hat{x} = (H^T H)^{-1} H^T \left(Y_i - G(X_I^*)\right) \quad 7\text{-}6$$

And finally, in (H) the state vector guess is updated by applying

$$X_{i+1}^* = X_i^* + \hat{x} \quad 7\text{-}7$$

In (G) the formula is estimating the changes that must be made to the state vector guess X_i^* by trying to minimize the observation deviation vector $Y_i - G(X_I^*)$, if this vector is zero (the estimated position corresponds exactly to the observations) then $\hat{x} = 0$ and the problem has converged. If measurements contradict each other (which is inevitable when observation errors are considered), the LLS algorithm will try to minimize the observation deviation vector. This means that all observation data will be used to estimate the target position. Observations can be contradictory or noisy and yet the algorithm will still be able to generate an estimated position for the target satellite based on all observations. A visual representation of a simplified case is given in Figure 31 below, here a similar algorithm to the one described above is used to draw the linear trend line. As can be seen a linear trend line can be generated out of noisy data.

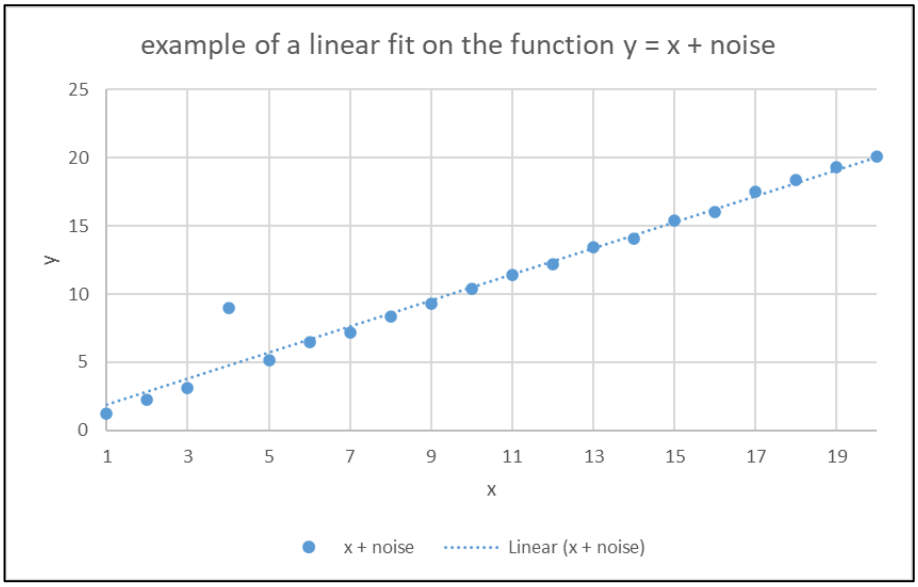

Figure 31: example of a linear fit on the function y = x + noise using least squares, made in excel.

In Figure 30 in step (H) it is mentioned that the solution should be iterated this is because LLS usually does not converge in one step and will need multiple iterations to converge. In our application, the convergence to an observation deviation vector of zero is not feasible because of the noisy data set. Hence a tolerance is defined that enables the LLS iterations to stop iterating when appropriate. If the $\hat{x}$ step size is smaller than the tolerance the iterations are stopped. If the $\hat{x}$ step is larger than the tolerance the algorithm is repeated with the updated state vector guess, this is indicated with a dashed arrow in the diagram.

Conceptually, the LLS algorithm is iteratively modifying the state vector guess to ensure that the predicted observations based on the state vector guess match the true observations as closely as possible. How the state vector must be modified to achieve this is extrapolated from the mapping matrix which predicts how a change in the state vector will lead to a change in the predicted observations.

7.2.2.1 Cholesky Decomposition

Recall equation 7-6:

$$\hat{x} = (H^T H)^{-1} H^T \left(Y_i - G(X_I^*)\right) \quad 7\text{-}6$$

This equation requires a matrix to be inverted, this is done via a Cholesky decomposition [46], which will be explained in this section. This is faster and more accurate than a conventional inversion [46].

First, we define the matrix M [46]:

$$M = H^T H \quad 7\text{-}8$$

and the matrix N [46]:

$$N = H^T \left(Y_i - G(X_I^*)\right) \quad 7\text{-}9$$

Simplifying equation 7-6 into:

$$M * \hat{x} = N \quad 7\text{-}10$$

Then we use Cholesky decomposition [46]:

$$R^T * R = M \quad 7\text{-}11$$

Where R is an upper triangular matrix.
An example is given below, where A, B, C, D, E and F represent unknowns.

R^T

A	0	0
B	D	0
C	E	F

*

R

A	B	C
0	D	E
0	0	F

=

M

29641.089	-31626.75	18984.37
-31626.75	36988.505	-21707.48
18984.37	-21707.48	17437.124

This matrix operation can now easily be converted to a purely algebraic problem: $A^2 = 29641.089$, $A * B = -31626.75$, etc.

Subsequently we can apply [46]:

$$R^T * Z = N \quad 7\text{-}12$$

Which can again be expressed in matrix form, with the unknowns G, H, and I. Which can be solved for algebraically: $172.16588 * G = -7205632$, etc.

R^T

172.16588	0	0
-183.6993	56.948058	0
110.2679	-25.48537	68.033888

*

Z

G
H
I

=

N

-7205632
6791849
-6290636

And finally we can find $\hat{x}$ with [46]:

$$R * \hat{x} = Z \quad 7\text{-}13$$

Which can again be expressed in matrix form, with the unknowns J, K and L. Which can be found algebraically (in reverse order) $68.033888 * L = -30526$, etc.

R

172.16588	-183.6993	110.2679
0	56.948058	-25.48537
0	0	68.033888

*

x\hat

J
K
L

=

Z

-41853
-15742
-30526

Note that the equations: 7-11, 7-12, and 7-13 solve for $\hat{x}$, without inverting any matrices and each of these equations can be solved through algebraic relations, making the computational execution very fast.

For a more extensive explanation, including derivations, see G. H. B. Byron D. Tapley, Bob E. Schutz' book Statistical Orbit Determination [46], chapter 5. For the 1924 paper introducing Cholesky decomposition see [48].

7.2.3 Accuracy Assessment

In this section the way the accuracy is assessed is given. The procedure outlined in 7.2.2 is repeated for each case (row) in the noise matrix to stochastically simulate the behaviour of the TDOA system. In Figure 32 an example of the spread of the estimated target positions with respect to the ground stations can be seen.

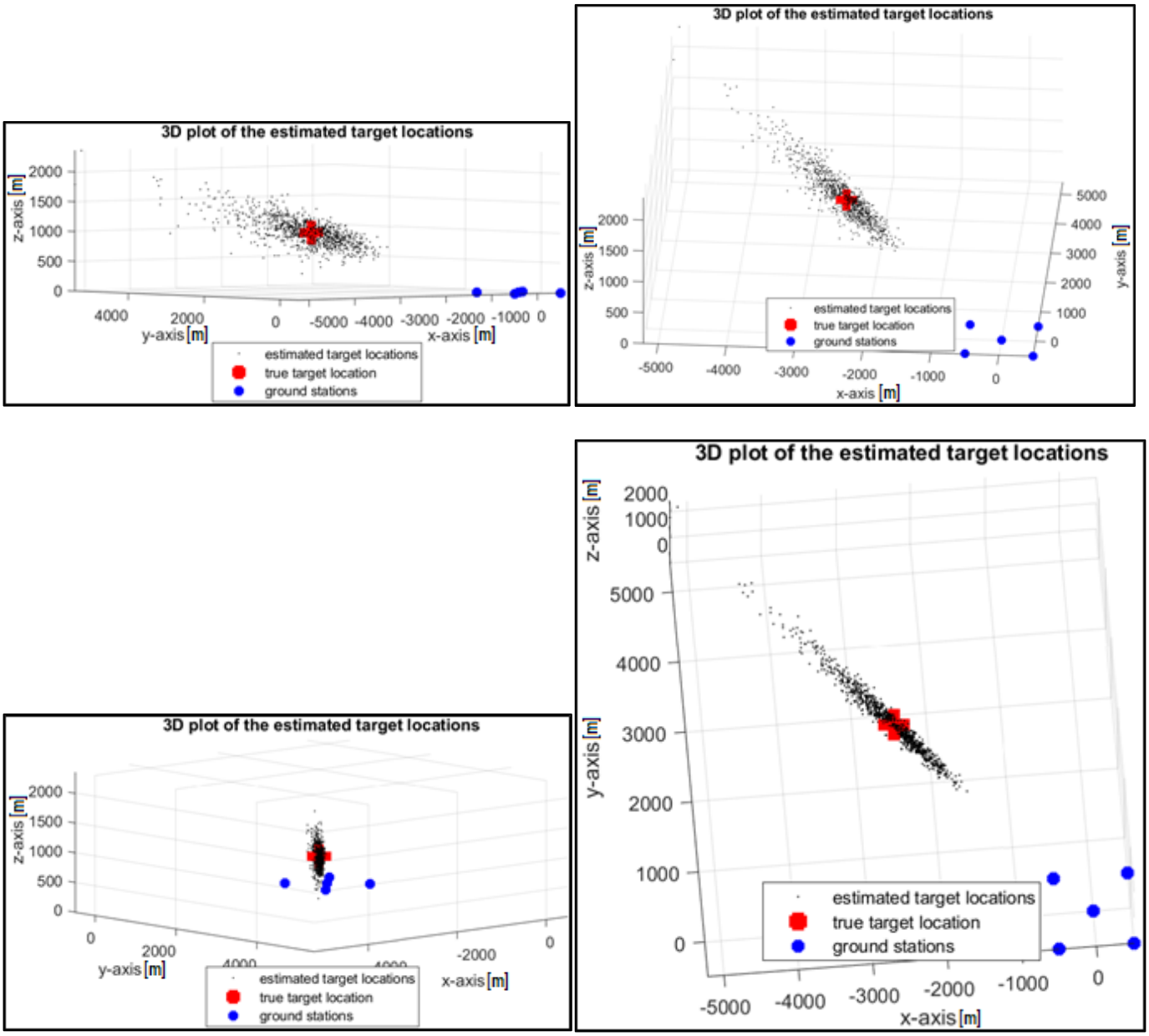

*Figure 32: a number of 3D plots demonstrating the spread of estimated target locations, made in a (unit) test environment, with inputs: rng('default'); Groundstations = [[0;0;0],[500;500;0],[-500;500;0],[-500;-500;0],[500;-500;0]] Target = [-2465;2500;1000]; noise_time = 1 * 37*10^-9; noise_matrix = zeros(1000,length(Groundstations));noise_matrix = normrnd(0, noise_time , size(noise_matrix));max_steps = 100;max_step_size = 5000;tolerance = 0.01; Ground_accuracy_coordinates = [1;1;1]; reference_area = 83*83*pi();*

It is clear from Figure 32 that the system error cannot be represented as merely the mean distance from the target. The estimated target positions are spread out much more towards and away from the (radio) ground stations than in other directions. This behaviour was already observed in 5.1.1.

Hence the accuracy must be quantified in different dimensions. We know from 2.4 that our overall system is much more sensitive to lateral errors as seen from the optical ground station than range errors. As can be seen in Figure 32 if the optical ground station is collocated with the central radio ground station, then the lateral or angular errors would be relatively small. If, however the optical ground station was located at for example [-4000,0,0], the angular errors would be much larger.

Hence the concept of an accuracy ground station or optical ground station is introduced. This is an input to the 3D TDOA simulator, the accuracy or errors are determined with respect to this point in the manner described in the rest of this chapter.

First range error is dealt with. Specifically by using the formula below, adapted from [49]:

$$d = -\frac{(A * x_1 + B * y_2 + C * y_3) + (-A * x_0 - B * y_0 - C * z_0)}{\sqrt{A^2 + B^2 + C^2}} \quad \text{7-14}$$

With:

A, B, C	Cartesian ECEF coordinates of the normal vector connecting the accuracy ground station and the true target position
x_0, y_0, z_0	Cartesian ECEF coordinates of the target true position
x_1, y_1, z_1	Cartesian ECEF coordinates of the estimated target position

This formula gives the orthogonal distance between the estimated target position and the plane defined by the target true position and normal vector A, B, C. From this, the range sample standard deviation can be derived. The assumption is made that the range errors follow a normal distribution.

Then the lateral errors are quantified which is explained below.

First the estimated target locations are orthogonally projected on to a plane located on the optical ground station. This plane is perpendicular to the vector connecting the optical ground station with the true position of the target satellite. This converts the problem from a 3D one to a 2D one.
Subsequently the Matlab function pca() is used to perform a principal component analysis of the estimated target locations [50]. The principal component analysis finds the vector along which the variance of the estimated target locations is largest. See Figure 33, here a principal component analysis is performed on an example of a bivariate data set. One can clearly see that the variance of the data is larger in one direction than in the other. The principal component is also displayed as a dotted line.

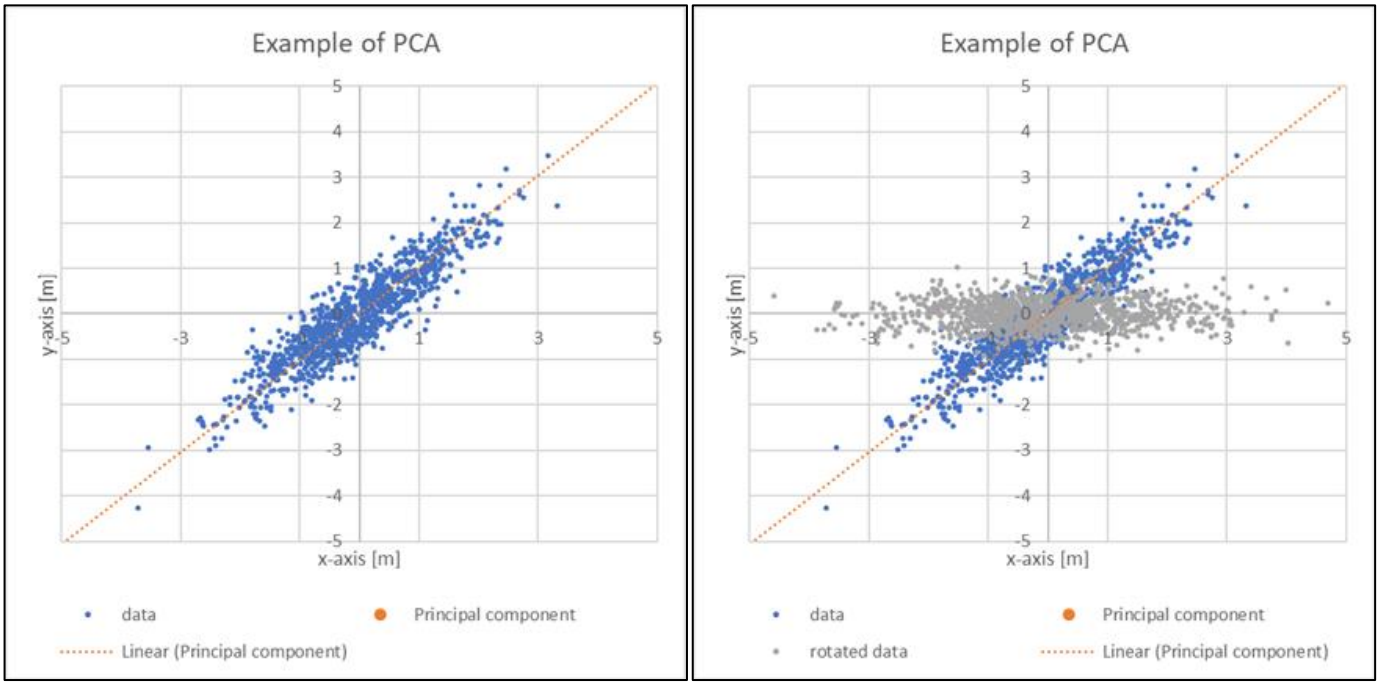

Figure 33: (left) excel plot showing 1000 data points and the principal axis of these data points. One can clearly see the principal axis is along the dimension of highest variance. In the right hand plot the rotated data has been rotated to align the principal component with the x-axis Based on the Matlab example [50].

Then the dot product can be used to find the angle between the principal component and the x-axis. Subsequently a rotation matrix can be used to rotate all data points [51]:

$$R = \begin{bmatrix} \cos(\theta) & \sin(\theta) \\ -\sin(\theta) & \cos(\theta) \end{bmatrix} \qquad 7\text{-}15$$

This is also represented visually in Figure 33.

Now the sample standard deviation can be found along the principal axis and the secondary axis. This gives us an indication of the area across which the estimated targets are spread. Which is of interest to us since it relates to the area our optical system will have to search through to identify and/or communicate with the targeted satellite.

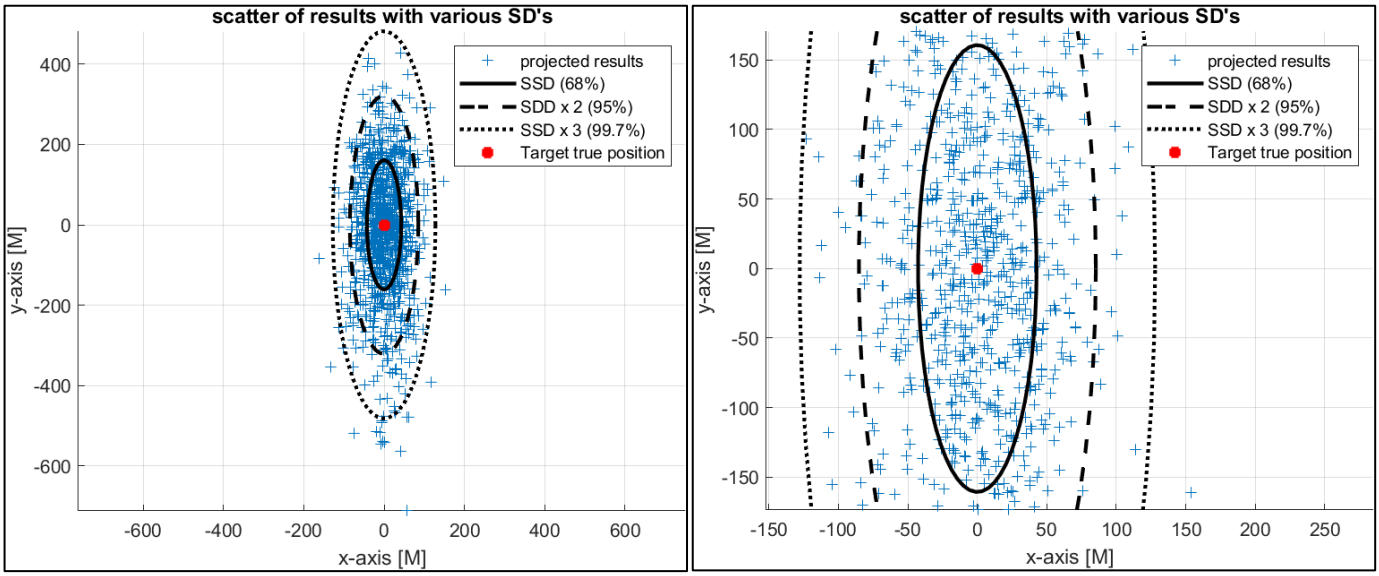

*Figure 34: (left) showing a scatter plot of the projected estimated target locations with elliptical SD's, (right) same plot but zoomed in. Made in a (unit) test environment, with inputs: rng(7); Groundstations = [[0;0;0],[500;500;0],[-500;500;0],[-500;-500;0],[500;-500;0]] Target = [-2465;2500;1000]; noise_time = 1 * 37*10^-9; noise_matrix = zeros(1000,length(Groundstations));noise_matrix = normrnd(0, noise_time , size(noise_matrix));max_steps = 100;max_step_size = 5000;tolerance = 0.01; Ground_accuracy_coordinates = [1;1;1]; reference_area = 83*83*pi();*

The assumption is made there that an ellipse is a good representation of the (projected) area the optical system will have to search. This may be an interesting topic to be further investigated but fits well with the spreads of estimated target positions found, see for example Figure 34. Note that the ellipse semi-major and semi-minor axis are taken to be respectively the sample standard deviation across the principal axis and the axis orthogonal to the principal axis.

In addition, the area of the ellipse defined by the SD, 2*SD and 3*SD is calculated and the area of this with respect to the reference area is found. The reference area is the area the optical system can search through in a certain time, it is used to evaluate the system performance. For example, if the surface area of the ellipse SD is equal to the reference area, then the optical ground station has a 68% change of finding the satellite in its search area.
Note that the implicit assumption is made here that the area the optical ground station can search through is not affected by the shape of the area it needs to search.

7.3 Verification & Validation

In this section the verification and validation of the Matlab code will be elaborated.

First of all, when the noise is set to zero the 3D TDOA code reacts as expected namely that the target position estimation errors are all very close to zero. The maximum range error is on order of 10^{-8} m (or about 10 nano meters) with lateral errors one order of magnitude smaller. Or in other words the 3D TDOA code converges (almost) perfectly to the target coordinates when its measurements are not subjected to noise. This is a very strong indication that the code is functioning properly.

An additional verification performed is to compare the performance of the 3D TDOA simulator with the 2D quantitative Matlab scrip introduced in 5.1.2.
The results of this comparison can be found in Table 6.
Note that a direct comparison of these results is not possible since, the 3D code requires 4 ground stations to be able to generate an estimated target location in 3D. From these 4 ground stations 3 linearly independent measurements can be derived and 3 more linearly dependent measurements. The 2D code can only use 3 ground stations and only uses 2 linearly independent measurements.
Related to the difference in number of measurements is the ground stations geometry or configuration. This cannot be identical in the 2D, and 3D code. In Figure 35 the chosen 3D configuration used is shown. This specific 3D configuration was used since: it closely resembles the 2D configuration, show in Figure 36.
When all ground stations are placed in the XY plane, and the target is some distance above the direct centre of the square defined by the ground station. Then the problem cannot be solved in the 3D Matlab script. Specifically, the Cholesky decomposition becomes impossible since the H matrix has a column full of zeros. This means that the solution space has become an infinitely long line and a unique solution is not possible. This makes sense when one considers that in this configuration each ground station must receive the transmission at the exact same time (if there is no noise present). Then the target must be located on a line orthogonal to the XY plane and passing through the centre of the square formed by the ground stations. This is an infinitely large solution space (the target can be anywhere on the Z-axis) so the solver cannot converge.
Note that the target must be offset slightly in the case 3D to ensure convergence in the LLS solver. For some combinations of ground stations and target geometry there are “blind spots” where the LLS solver cannot converge or struggles to converge see for example Figure 62. In reality it is unlikely that a satellite will remain in such a “blind spot” for any appreciable length of time.
In addition, the 3D code is stochastic in nature, simulating 1000 different noise cases, whereas the 2D code simulates only 4 specific cases.
Furthermore, the 2D code is operating on very different assumption and using a different method to estimate the target location then the 3D code. As such even if exactly the same input values could be used it is unreasonable to expect the 2D and 3D code to have identical results.

3D			
	Range SD [m]	Primary-axis SD [m]	Secondary-axis SD [m]
3D TDOA	87	24	45
2D			
	Ranging error [m]	Lateral error [m]	
2D TDOA quantitative Matlab script	137	35	

Table 6: table comparing the predicted errors for the 3D TDOA and 2D TDOA quantitative Matlab script
inputs for 3D: Groundstations = 1000[[0;0;-250],[0;500;0],[0;0;250],[500;0;0]];Target = [700000;710000;0];noise_time = 28*10^-9; noise_matrix = zeros(1000,length(Groundstations));noise_matrix = normrnd(0, noise_time , size(noise_matrix));max_steps = 500;max_step_size = 5000*2;tolerance = 0.01; Ground_accuracy_coordinates = [0;0;0]; reference_area = 83*83*pi();*
inputs for 2D: Ax=0, Ay=500000, Bx=0, By=0, Cx=500000, Cy=0, target_range=1000000, time_noise=0.000000028, box=5000000, mesh=151,

Taking all these difference in mind the 2D and 3D case give similar results, as can be seen in Table 6. The range errors vary by about 50%. Note that lateral error has no direct comparison in the 3D solver, which has primary and secondary axis SD errors. But the 2D lateral error is between the Primary- and Secondary axis SD from the 3D case. This is a very good sign of the similar behavior of the 2D, and 3D code.
In summary even though a direct comparison of the 2D and 3D code since is not possible, one can conclude that they show consistent and similar behavior.

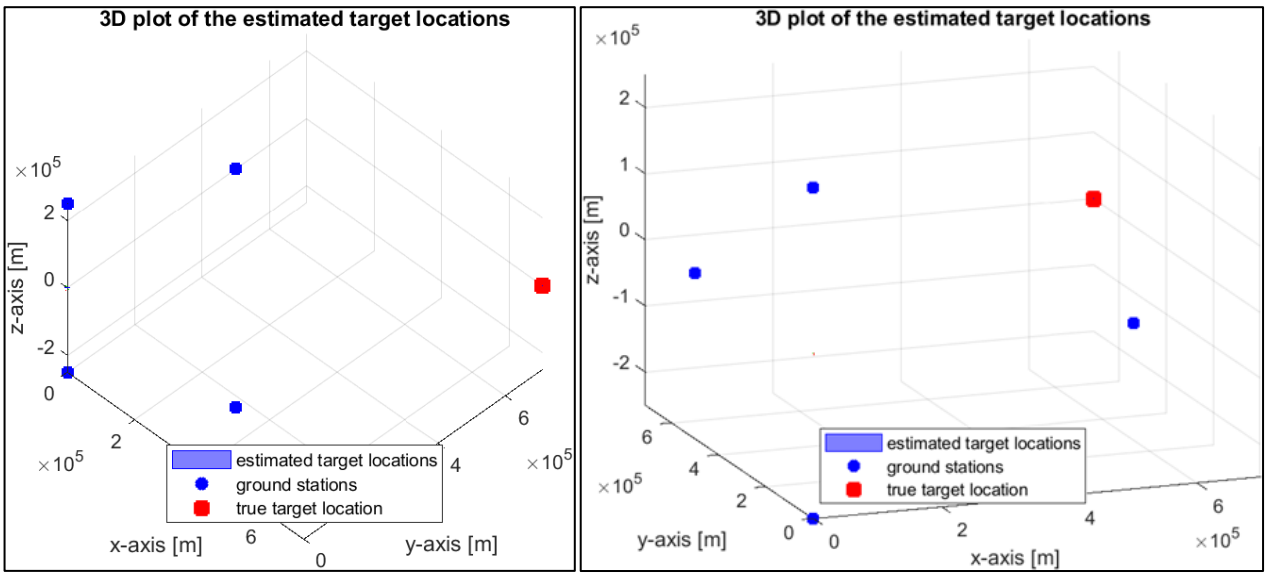

Figure 35: figure showing the positions of the ground stations and targets of the 3D case in Table 6. See Table 6 for the input values.

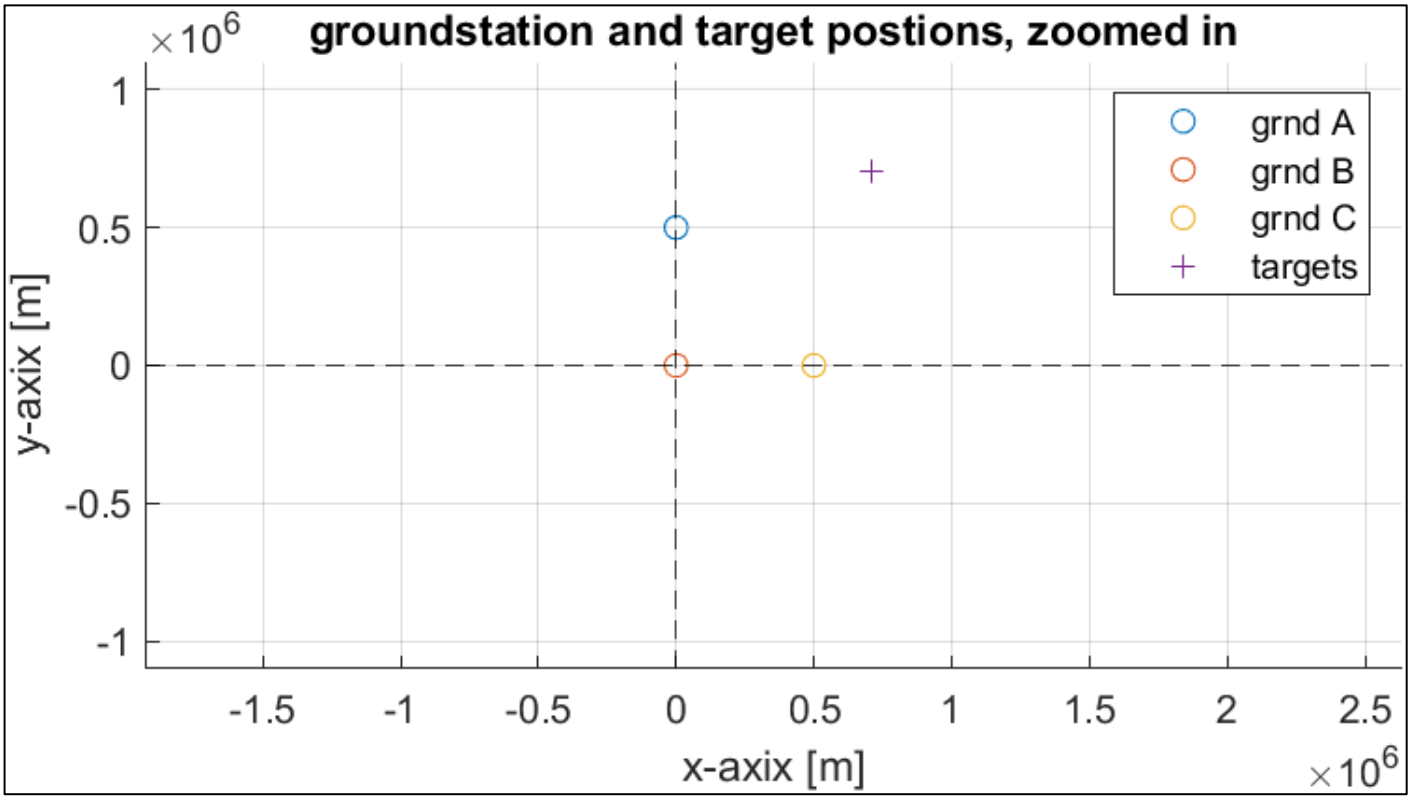

Figure 36: figure showing the positions of the ground stations and targets of the 2D case in Table 6. See Table 6 for the input values

Another method of verification applied is to visually compare the results and shape of the 3D TDOA simulator with the 2D quantitative Matlab scrip introduced in 5.1.2.

The simulation was run for 1000 noise cases with stochastic noise applied to each ground station as outlined in the previous sections. In Figure 38 one can see the 3D shape taken by the estimated target points. In the plots the 3D shape is shown from other angles, to show the spread of the individual data points. One can observe that the 2D plot (Figure 37) has a pronounced higher range error then latter error. This same behavior can be seen in the 3D plot.

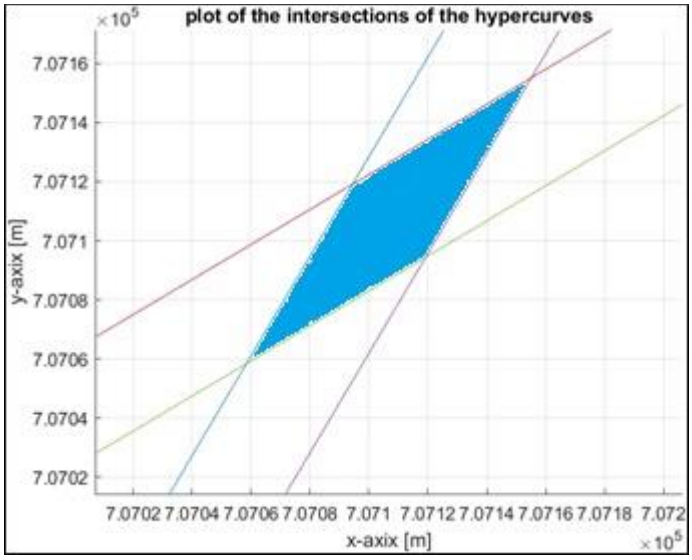

Figure 37: top right: figure showing the hyperbolic curves intersections from the 2D TDOA code, the area between the intersection is coloured in blue.

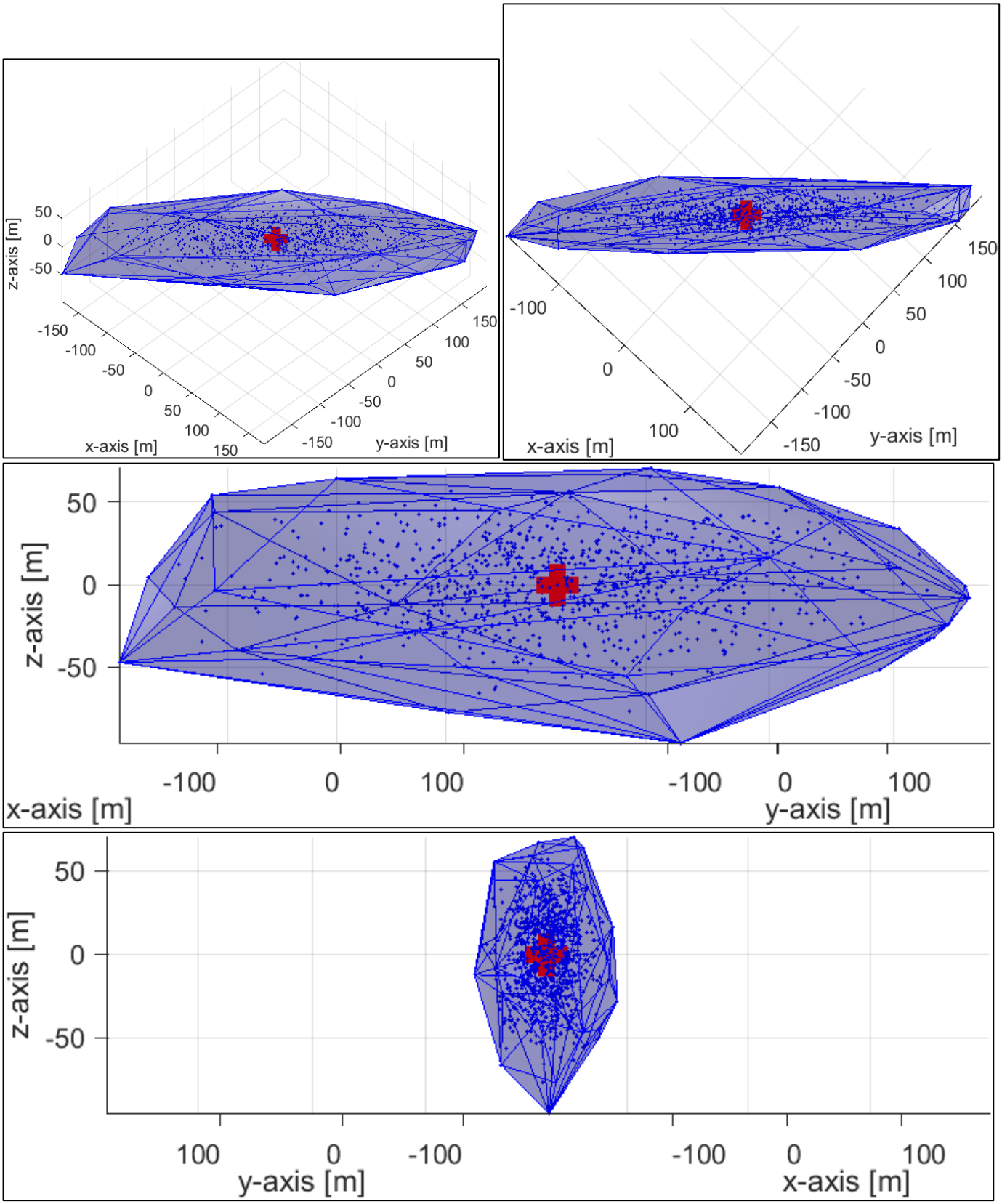

Figure 38: Isometric, top, side, and front view of the results of the 3D TDOA code. See Table 6 for the input values.

Finally, several verification tests were performed. The input values of these test cases can be found in Appendix . For each test case the behavior was as expected, some examples will be given below:

- Reducing the maximum step size from 5000 m to 50 m for the LLS solver leads to a higher mean number of steps needed for convergence, as expected. In addition, there was no change in the amount of target that were visible, which is to be expected since there was no change in the parameters affecting ground station visibility.
- Additional ground stations increased the accuracy of the system.
- Ground stations spread over a larger geographical area leads to a more accurate system that can see more target satellites (up to a point, since if the baseline gets too big the ground stations get pushed so far apart that fewer of them can track the satellite at any one time, which lead to a less accurate system.
- Reduced noise/error levels lead to a more accurate 3D TDOA system. Setting the ground noise/error levels to zero lead to zero results in an target position estimation with (almost) zero errors. Furthermore, this also leads to the LLS solver converging in one step, every time.

In addition, unit tests were performed whenever feasible on parts of the code.

In summary the 3D TDOA code is considered validated.

7.4 Results

In this section the 3D TDOA Matlab script is used to analyze the behavior of a 3D TDOA system.

7.4.1 Only Non-Redundant TDOA Measurements or All TDOA Measurements

This section will elaborate upon an interesting and unexpected conclusion drawn from the 3D TDOA code. As explained in pervious sections the TDOA method relies on measuring the time of arrival of a radio message from the target satellite at a number of ground stations. These arrival times are then subtracted from each other to convert them to TDOA measurements. Hence each TDOA measurement relies on two ground stations. This is represented visually in Figure 39 below.

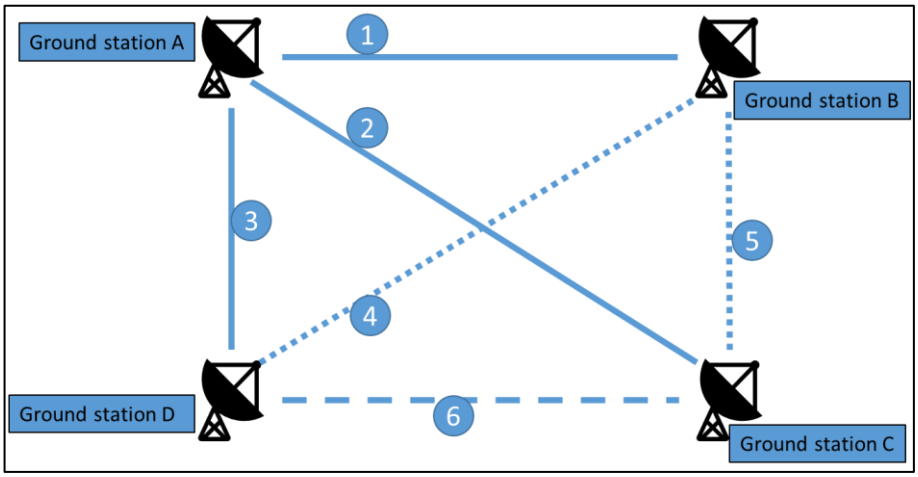

Figure 39: the ground stations A, B, C, and D are shown schematically and the TDOA measurements are shown with lines and indicated with 1, 2, 3, 4, 5, and 6.

According to [42]:

$$number\ of\ TDOA\ measurements = \frac{L^2}{2} - \frac{L}{2} \qquad 7\text{-}16$$

But:

$$number\ of\ non-redundant\ TDOA\ measurements = L - 1 \qquad 7\text{-}17$$

Or consider Figure 39, there are 4 ground station and hence 6 TDOA measurements. But only 3 of these are

non-redundant, let's take 1, 2, and 3 as the non-redundant measurements (but note that for example 2, 5, and 6 are also non-redundant). Consider TDOA measurement 4 between ground stations B and D. The time of arrival of the message at B and D is already used in respectively TDOA measurements 1 and 3. And since the ground station locations are known TDOA measurement 4 can be perfectly reconstructed from the non-redundant measurements. Or in other words, measurement 4 is adding no new information. Hence [42] states to only use non-redundant measurements and that this will not lead to a loss of generality. In fact this is how Ufuk Tamer [47] implemented it in his code.

Figure 40 one can see the target-point by target-point comparison of using all measurements or only non-redundant measurements for four ground stations. The difference in behavior is trivial (note that the percentual differences range from $-0.1 * 10^{-9}\%$ to $0.2 * 10^{-9}\%$).

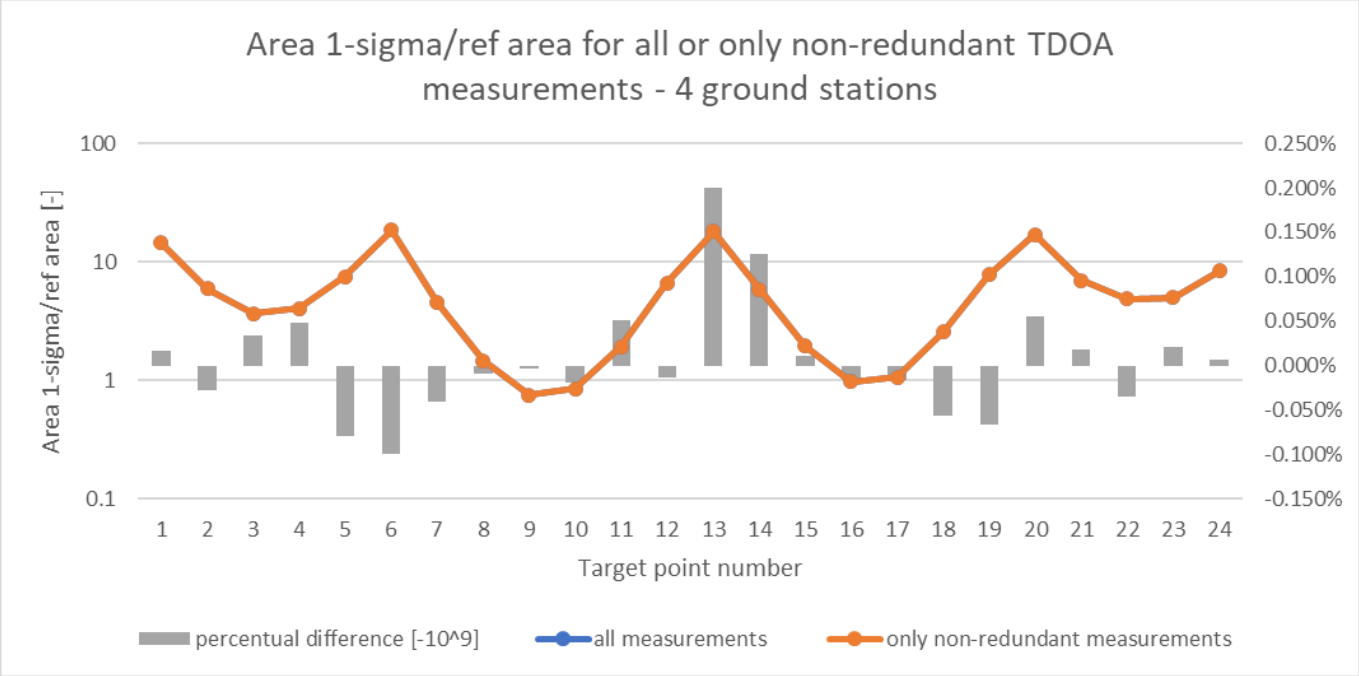

Figure 40: plot comparing the area 1-sigma of using all measurements or only non-redundant measurements for 4 ground stations, baseline 100 km, see Appendix C for all inputs. Note that in this plot the performance is plotted for each target point.

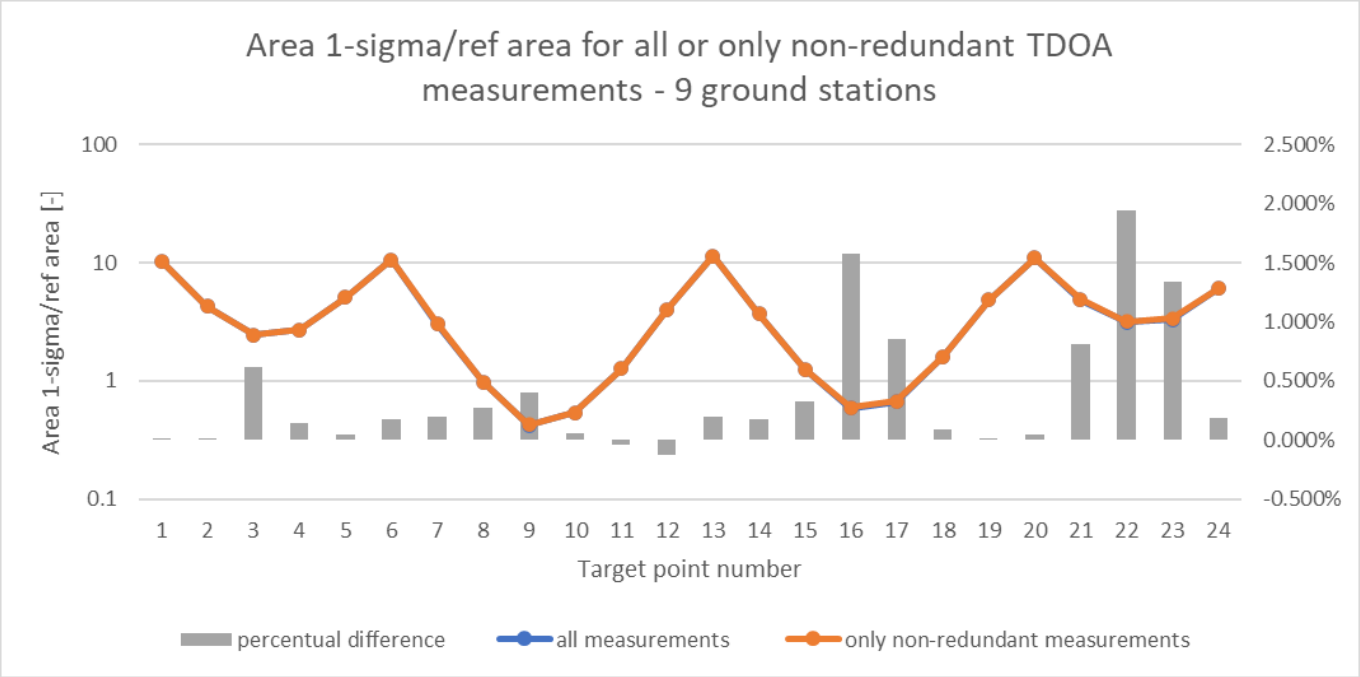

Figure 41:plot comparing the area 1-sigma of using all measurements or only non-redundant measurements for 9 ground stations, baseline 100 km, see Appendix C for all inputs. Note that in this plot the performance is plotted for each target point, only points present in Figure 40 are shown.

Figure 41 shows the target-point by target-point comparison of using all measurements or only non-redundant measurements for nine ground stations. For most cases using all measurements gives the best result, with difference up to 2%. Only for Target points 11 and 12 is it more accurate to use only the non-redundant equation, by about a tenth of a percent.

In Figure 42 one can see that using all measurements is noticeably outperforming using only non-redundant measurements by up to 73%. The smallest improvement is 3% and the average improvement across all target points is 37%.

In Figure 43 the 9 ground stations case is repeated (with slightly different coordinates) and with a 1000 km baseline rather than 100 km. Here we can see that using all equation is again significantly outperforming using only non-redundant equations. Here the largest improvement is 23% and the average is 7%. There are 3 target points which have a smaller area 1-sigma but they are all on the order of 10^{-12}% or less.

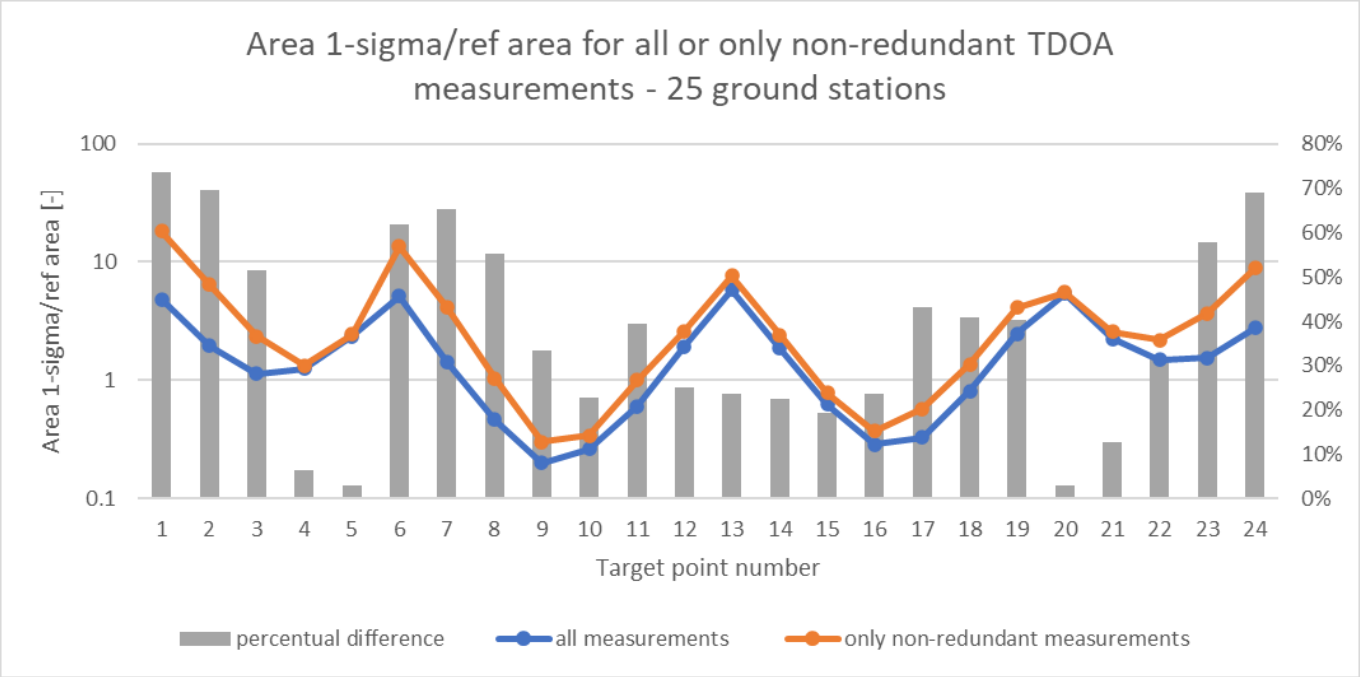

Figure 42: plot comparing the area 1-sigma of using all measurements or only non-redundant measurements for 25 ground stations, baseline 100 km, see Appendix C for all inputs. Note that in this plot the performance is plotted for each target point, only points present in Figure 40 are shown.

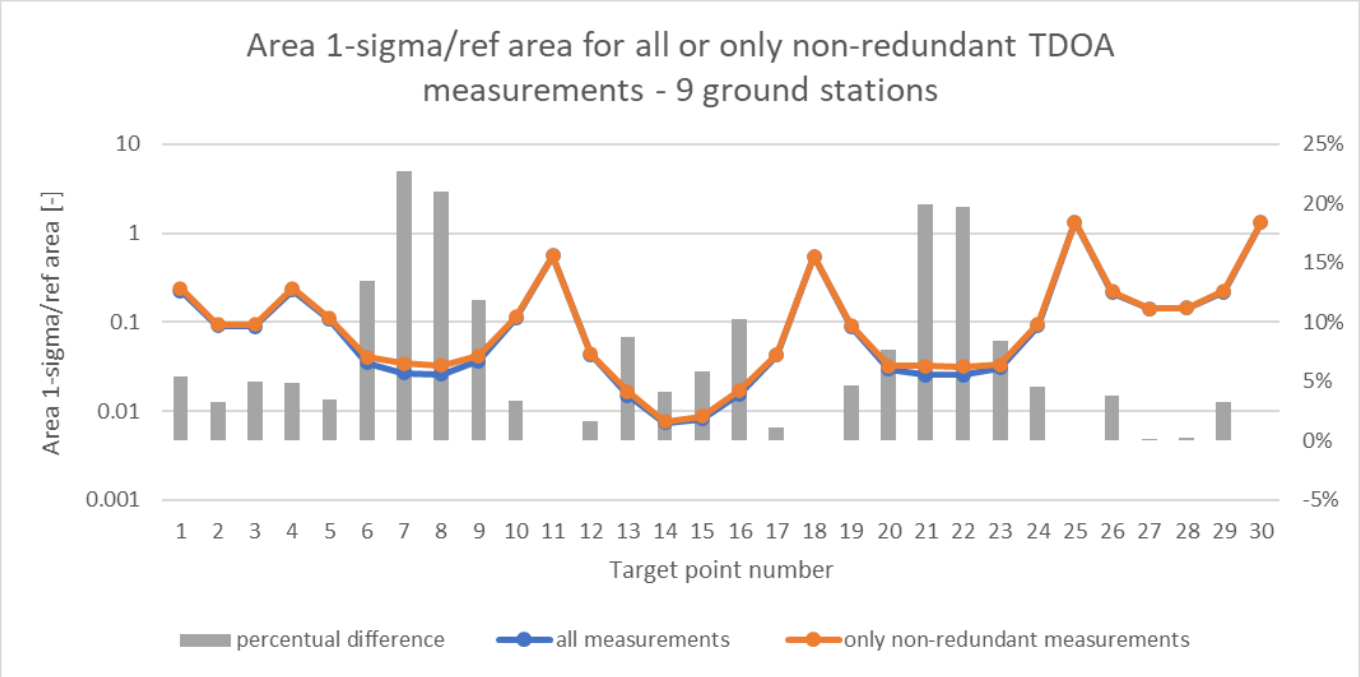

Figure 43: plot comparing the area 1-sigma of using all measurements or only non-redundant measurements for 9 ground stations, baseline 1000 km, see Appendix C for all inputs. Note that in this plot the performance is plotted for each target point, only points present in Figure 40 are shown.

In the rest of this thesis all measurements will be used, since utilizing only the non-trivial measurements will in most cases lead to a worse performing TDOA system, as explained above. There are situations where the difference between the two systems is trivial, and rare cases were using only the non-trivial measurements will give a very slight advantage. But this advantage pales in comparison to the performance gains made by using all available measurements.

7.4.2 Numerical Results

In this section the numerical results are presented. There are four main factors of interest to the TDOA system viability:

- the noise levels
- the number of ground station
- the ground stations baseline
- the ground stations geometry

Each of these will be analysed in turn in this section. Below the approach and input values will be listed. See also Appendix C for the input values in table form.

Please see section 7.2 for a detailed explanation of how each of the inputs listed below is utilized in the code.

- The latitude and longitude step sizes are each set to 5 degrees. This step size was chosen to allow for a reasonable resolution of the TDOA system coverage area without requiring excessive computation time.
- Satellite altitude was set to 500 km as per requirement SAT.2
- The noise matrix length was set to 1000. This was again chosen to allow for a reasonable stochastic spread, without requiring excessive computations.
- The refence area is set to 21642 meters squared as per requirement ACC.1.
- The random seed that controls the noise in the noise matrix is set to 1. This is done to ensure the results are as comparable as possible.
- Max steps and max steps size are very closely related. They are sometimes varied for cases with poor convergence.
- Tolerance is set 0.01 m.
- Optical ground station min elevation is set to -90. This means the optical ground station can “see” everything and is unobstructed by the earth. This is done since we are focusing here on the TDOA system and do not want the optical ground station to affect these results. The optical ground station is defined to be located at 51.99009375 latitude by 4.375151609 longitude at an altitude of 20 m, which are the coordinates of the Aerospace Faculty of TU Delft.
- The radio ground stations are assumed to be located 20 m above ground level and to have a minimal elevation angle of 15 degrees, and the optical ground station is at the centre of the radio ground stations.
- The number of radio ground stations, their baseline and shape are varied to analyse the sensitivity of the system. In Figure 44 one can see 8 configurations of the ground stations. Note that the different shapes all have 9 ground stations to allow for comparison without having to correct for a different number of ground stations between configurations. All of these configurations have the same baseline size. The coordinates presented in Figure 44 are then multiplied by a baseline size factor and added to the central coordinate (at 51.99009375 latitude by 4.375151609 longitude). The baseline size factor is taken to be 0.09, 0.9 and 9 degrees representing respectively the 10, 100 and, 1000 km baseline size in longitude. In latitude the baselines are smaller. This approach was taken for convenience and consistency.

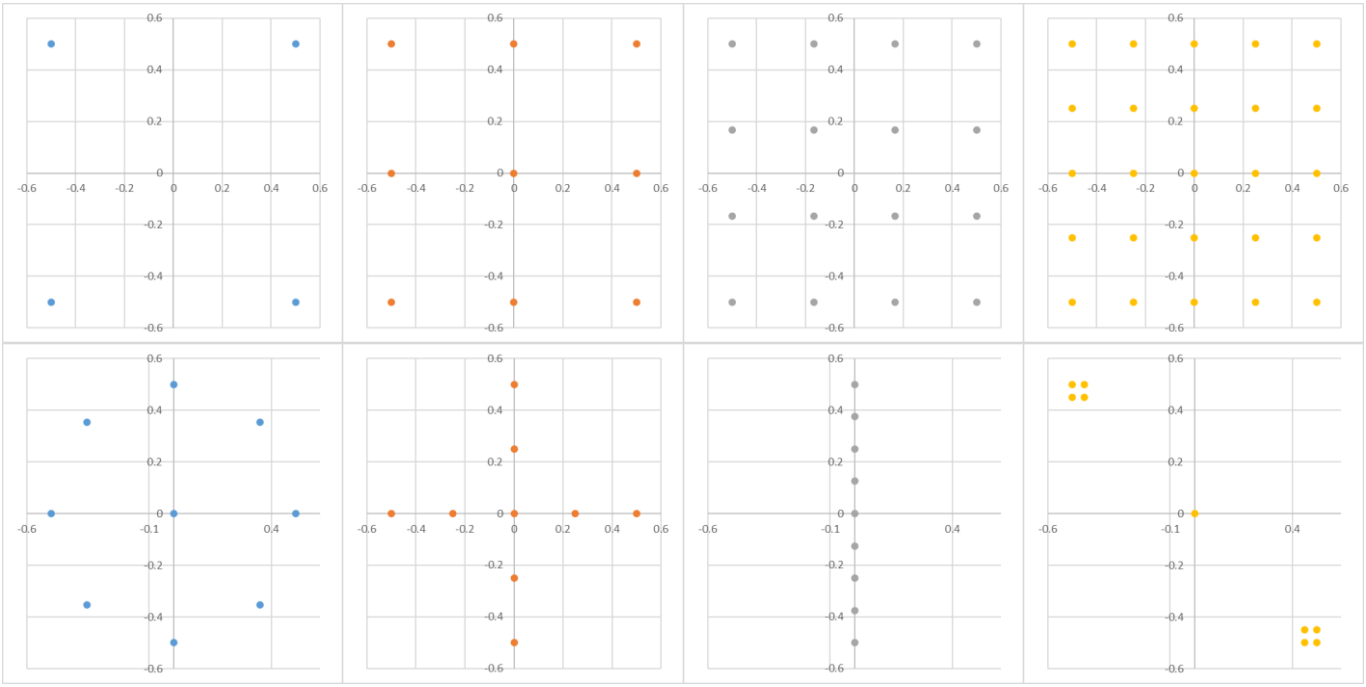

Figure 44: plot of the different geometrical configuration of the ground station: top row left to right: 4, 9, 16, 25 ground stations. Bottom row left to right: circle, cross, line and clustered. Note that these plots merely indicate the pattern as such the two axes have an arbitrary (but identical) scale.

7.4.2.1 Noise Levels

The noise levels were analysed in chapter: 6) and summarized in a table which is reproduced here, see Table 7 below.

Two-way detection error SD [m]	One-way detection error SD [m]	GPS timing error SD [m]	Total error SD [m]	Total error SD [ns]
10000	7071	4.5	7071	23587
1000	707	4.5	707	2359
100	71	4.5	71	236
10	7	4.5	8	28
1	0.7	4.5	5	15
0.1	0.07	4.5	4	15
0.01	0.007	4.5	4	15

Table 7: table listing the total standard deviation error composed of the GPS timing error and the one-way (ranging) error).

Looking at the last column of Table 7 four noise cases were chosen for further study: 15, 28, 236 and 2359 ns error. The results of this are presented in Figure 45 and Figure 46.

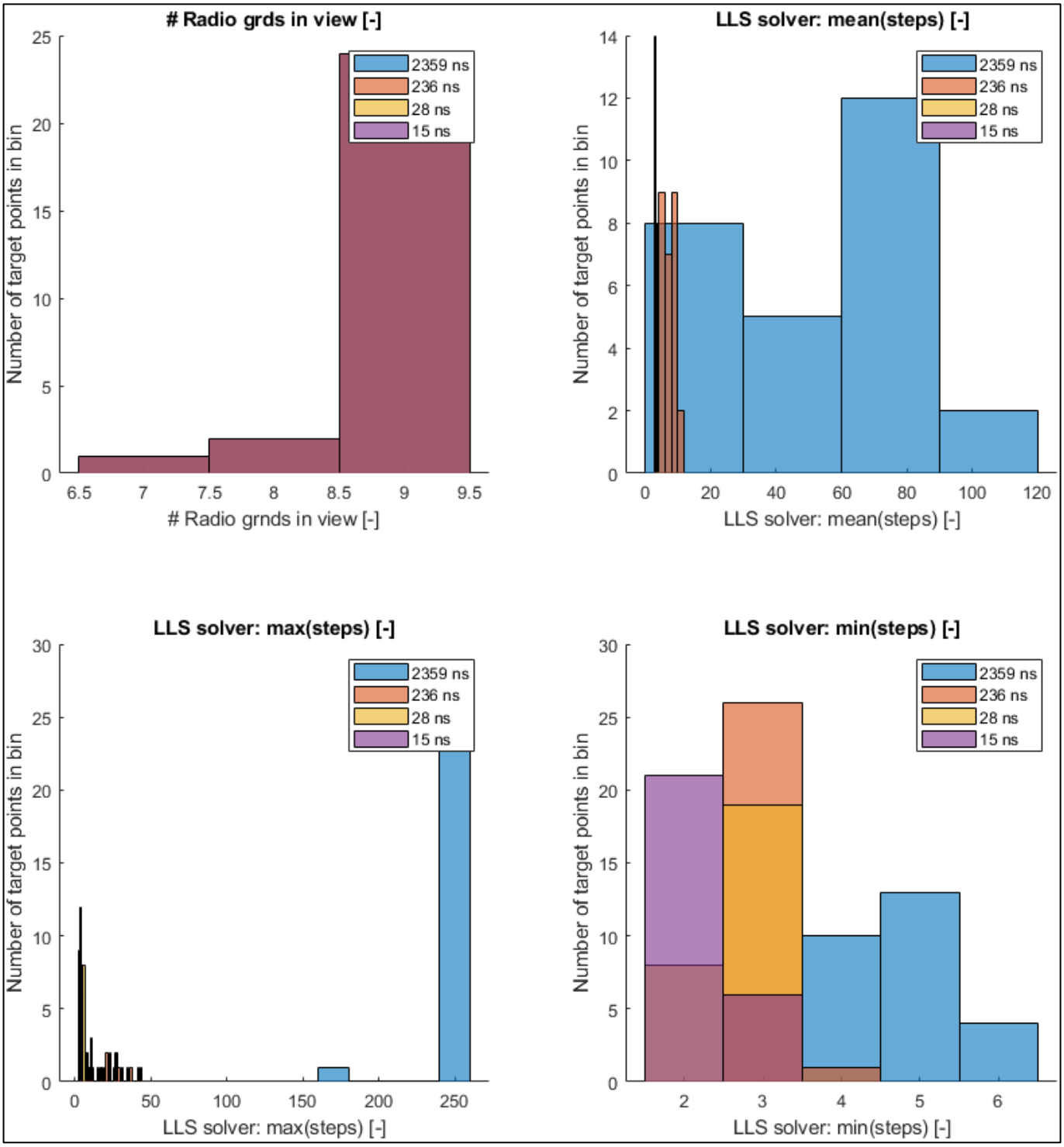

Figure 45: multiple histograms showing the impact of varying noise levels: 15, 28, 236 and 2359 ns, see Appendix C for all inputs.

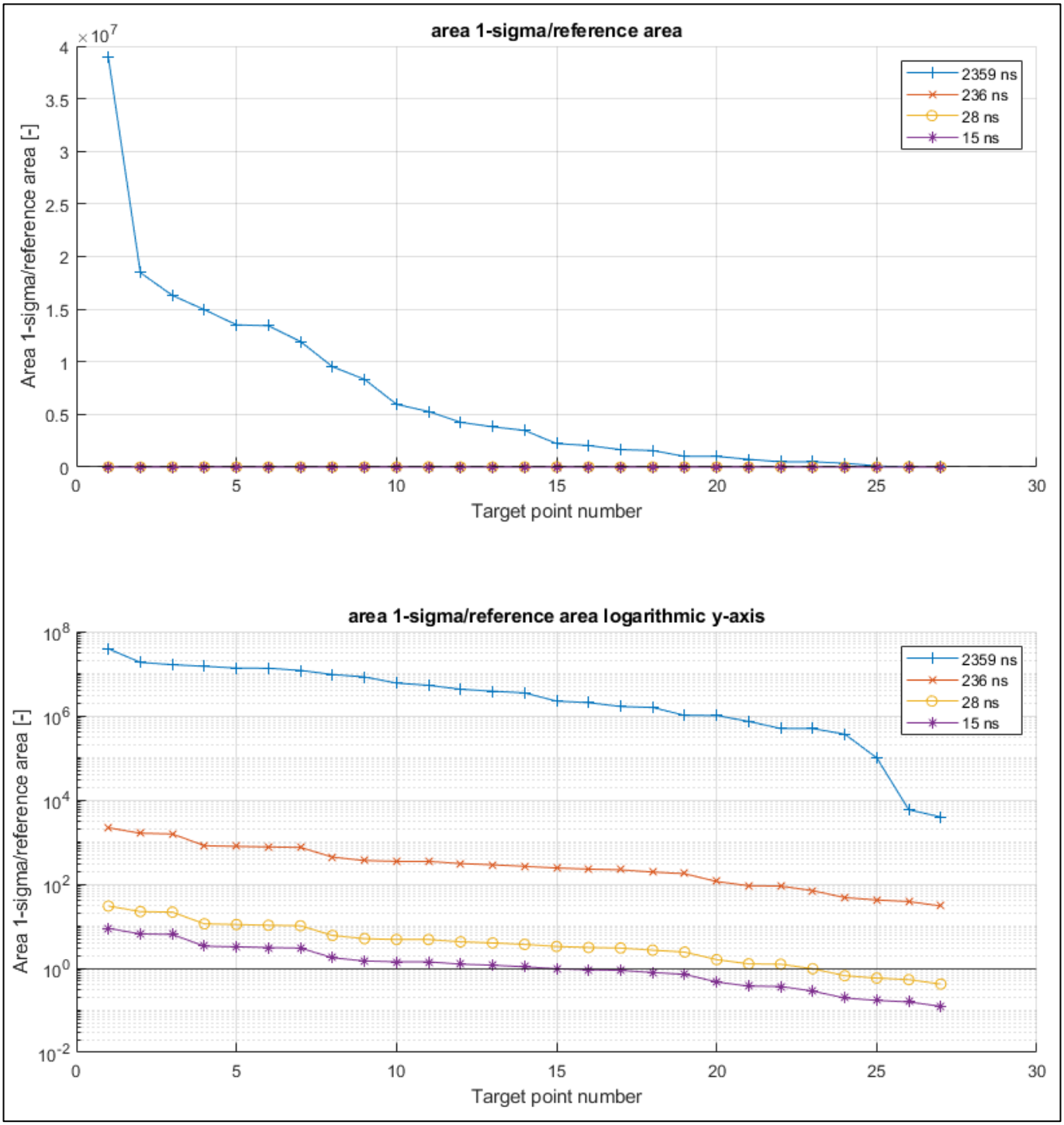

Figure 46: multiple plots showing the impact of varying noise levels: 15, 28, 236 and 2359 ns, see Appendix C for all inputs.

From Figure 45 we can draw several conclusions. Firstly, as expected changing the noise level does not affect target visibility (top left sub plot). Conversely a higher noise level leads to a higher mean and number of steps required. This also affects the minimum and maximum number of steps required.
More importantly we can observe in Figure 46 and in Figure 47 that only the 28 and 15 ns noise cases actually meet "area 1-sigma/ref area" is less than or equal to 1 as required by ACC.1. And of these two the 15 ns noise case meets the requirement for 48% of the coverage area and the 28 ns for 18.5%.

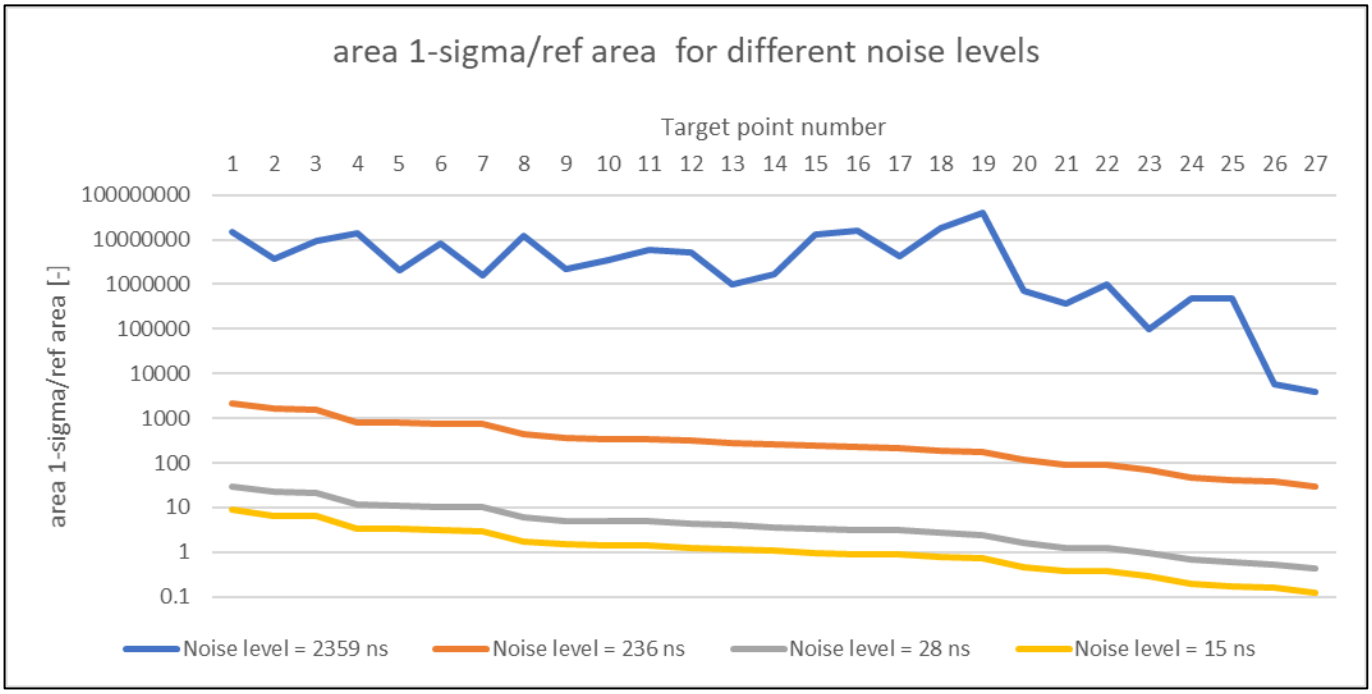

Figure 47: plot showing the impact of varying noise levels : 15, 28, 236 and 2359 ns, see Appendix C for all inputs. Note that the targets were sorted from largest to smallest for the 15 ns noise level.

One can also observe in Figure 47 that the 2359 ns noise level case shows some erratic behaviour and does not follow the same "shape" as the other noise cases. This is similar for the 1518 ns noise case in Figure 48. This is presumably due to a lack of convergence since both cases reach the maximum number of solver steps which confirms that the simulator had not yet converged or could not converge. In either case the results of these two cases should treated as unresolved and are not further used.

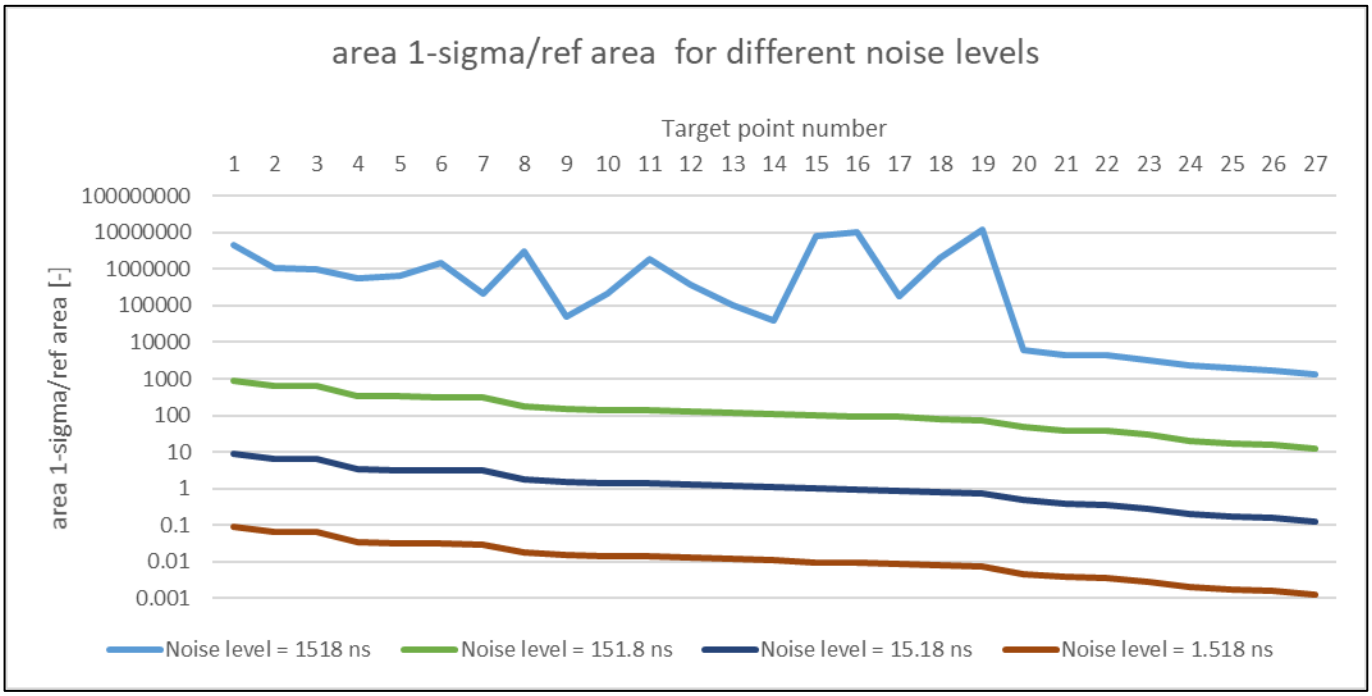

Figure 48: multiple plots showing the impact of varying noise levels: 1518, 151.8, 15.18, 1.518 ns on the TDOA system accuracy, see Appendix C for all inputs.

In Figure 48 one can see a clear relation between the "area 1-sigma ref" and the noise level. This can be summarized as the relation below.

$$error\ area \propto C_1 * \left(\frac{noise}{noise_{standard}}\right)^2 \qquad 7\text{-}18$$

where the subscript standard indicates the case for which the proportionality constant C1 was established

The relation above was formulated, based on the data in Figure 48 and summarized in Table 8 below. In this table in the first row the 151.8 ns noise case is compared with the 15.18 ns noise case. The ratio between these two is 10 as listed in the table. The average of the ratio of the "area 1-sigma/ref" is calculated by taking the average of the ratios between the "area 1-sigma/ref" of the 151.8 ns noise case and the "area 1-sigma/ref" of the 15.18 ns noise case, this is found to be 100.293 . The SD of these ratios is also found to be 0.282 . The same procedure is repeated for the second row.

Noise level 1 [ns]	Noise level 2 [ns]	Ratio noise levels [-]	Average of the ratios of the "area 1-sigma/ref" [-]	SD of the ratios of the "area 1-sigma/ref" [-]
151.8	15.18	10	100.293	0.282
15.18	1.518	10	99.996	0.021

Table 8: table comparing the effect of a change in noise level with respect to area 1-sigma /ref area.

7.4.2.2 Number of Ground Stations

The number of ground stations is an important parameter of the 3D TDOA system, its impact on the system performance will be assessed in this section.

First of all, the number of visible targets changes with the number of ground stations. This is logical when one considers that the 3D TDOA simulator requires at least 4 ground stations to be visible to resolve a target. In Figure 49 and Figure 50 one can see a summary of the effect of changing the number of ground station on various parameters. When the number of ground station increases, the number of ground stations visible for each target increases. The LLS calculator has the best convergence behaviour for 8 ground stations, this is partially because the 16 ground stations is able to (barely) detect an additional target, which is very hard to track, leading to seemingly worse convergence. Note that longer computation times are expected for more ground stations since the LLS problem is more complex and the operations to solve it increase exponentially. For example, a Cholesky decomposition of a 3 by 3 matrix requires 6 operations whereas a 4 by 4 matrix requires 10 and so on.

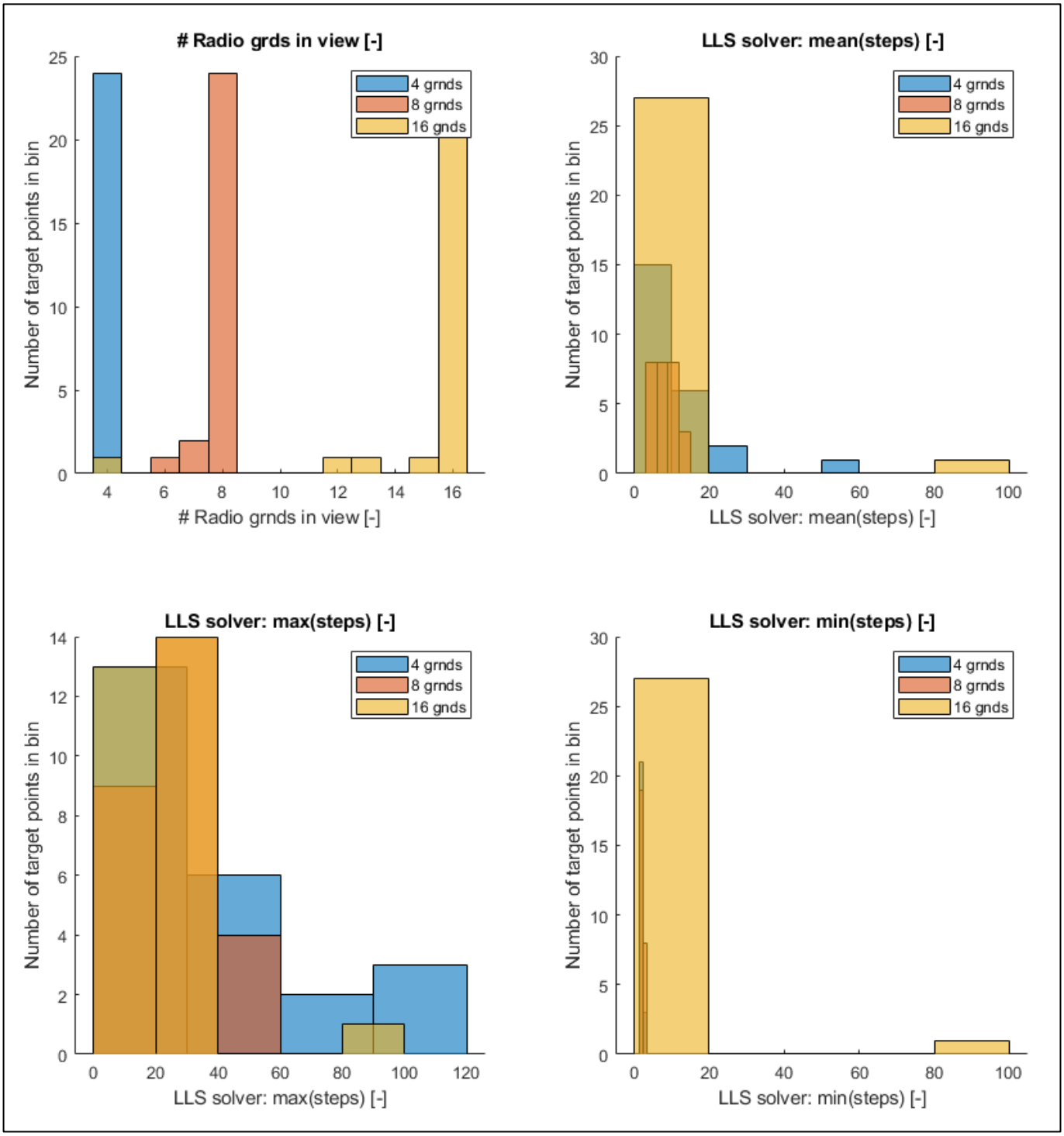

Figure 49: multiple histograms showing the impact of varying number of ground stations (4, 8 and 16), see Appendix C for all inputs

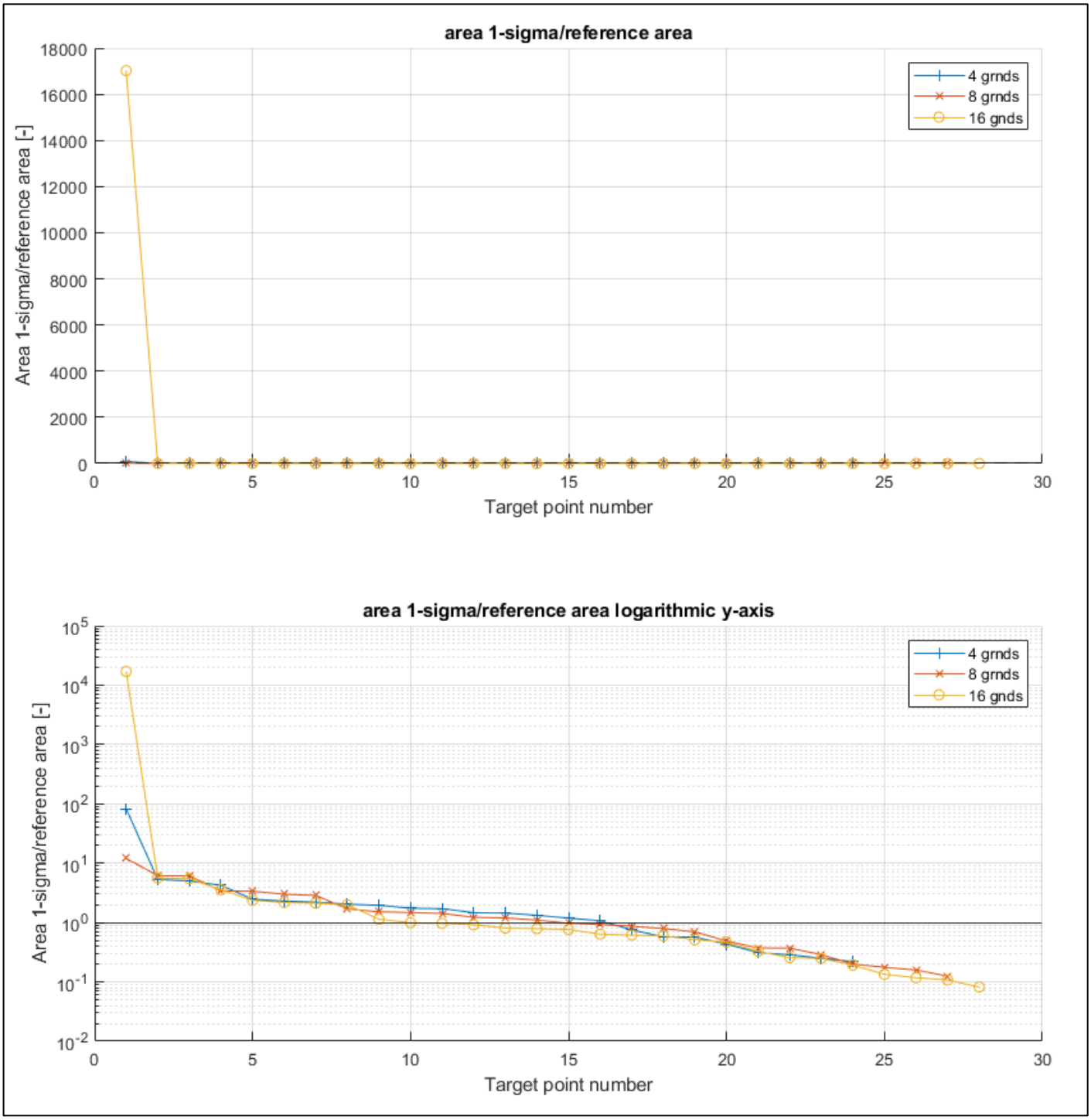

Figure 50: multiple plots showing the impact of varying number of ground stations (4, 8 and 16), see Appendix C for all inputs

In Figure 51 the additional target visible by adding ground stations are not considered. So, we are comparing the system performance with respect to the same target locations. Note the outlier for target number 6, the data point will be discarded in the proceeding analysis.

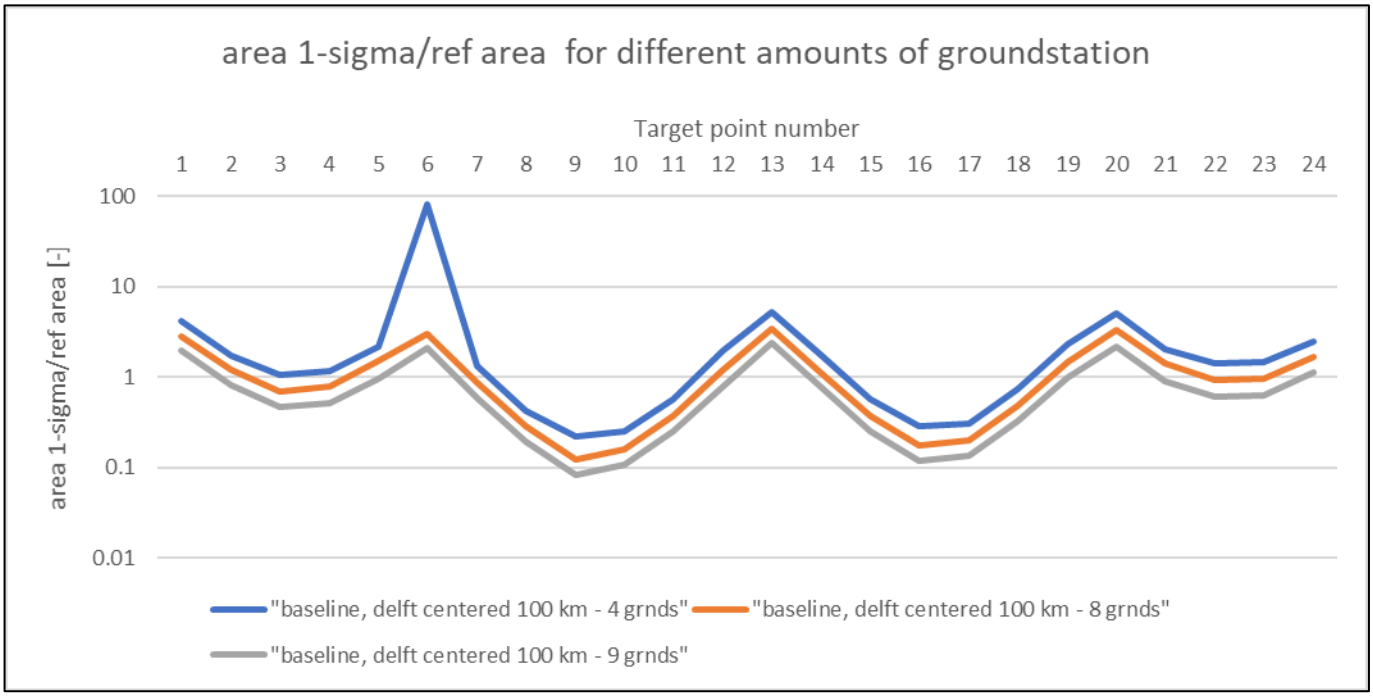

Figure 51: plot showing the impact of varying number of ground stations (4, 8 and 16) on the TDOA system accuracy, see Appendix C for all inputs.

Note that the 4 ground stations case meets requirement ACC.1 for 33% of the targets in its coverage area. For this same coverage area, the 8 and 16 ground stations cases achieve respectively 54% and 79% coverage.
In Table 9 the average and SD of the ratio between the results presented in Figure 51 is listed. From this we can concluded that doubling the number of ground stations reduce the area 1-sigma/ref area by a factor of approximately 1.5.

Number of ground station 1 [-]	Number of ground station 2 [-]	Ratio of number of ground stations [-]	Average of the ratios of the "area 1-sigma/ref" [-]	SD of the ratios of the "area 1-sigma/ref" [-]
4	8	0.5	1.536	0.069
8	16	0.5	1.494	0.042

Table 9: table comparing the effect of a change in number of ground stations with respect to area 1-sigma/ref area.

Or in equation form if the number of ground station is unchanged:

$$error\ area \propto C_1 * \left(\frac{noise}{noise_{standard}}\right)^2 \quad 7\text{-}19$$

If the number of ground stations doubles with respect to baseline:

$$error\ area \propto C_1 * \left(\frac{noise}{noise_{standard}}\right)^2 * \frac{1}{1.5} \quad 7\text{-}20$$

If the number of ground stations halves with respect to baseline:

$$error\ area \propto C_1 * \left(\frac{noise}{noise_{standard}}\right)^2 * 1.5 \quad 7\text{-}21$$

where the subscript standard indicates the case for which the proportionality constant C1 was established. Note that the number of ground stations effect was rounded to one decimal.

7.4.2.3 Ground Stations Baseline

The next question is how the ground stations baseline affects the 3D TDOA system performance. This was assessed by comparing 4 cases: 50, 100, 200, and 400 km baselines. The results are presented in Figure 52 and Figure 53.

One can see (in Figure 52) that the 3D TDOA system struggles to solve the 50 km baseline case (high mean number of steps, the number of max steps is at the limit of 100 steps for many target points) because a small baseline is correlates with poor accuracy, requiring more LLS steps to converge to a solution.

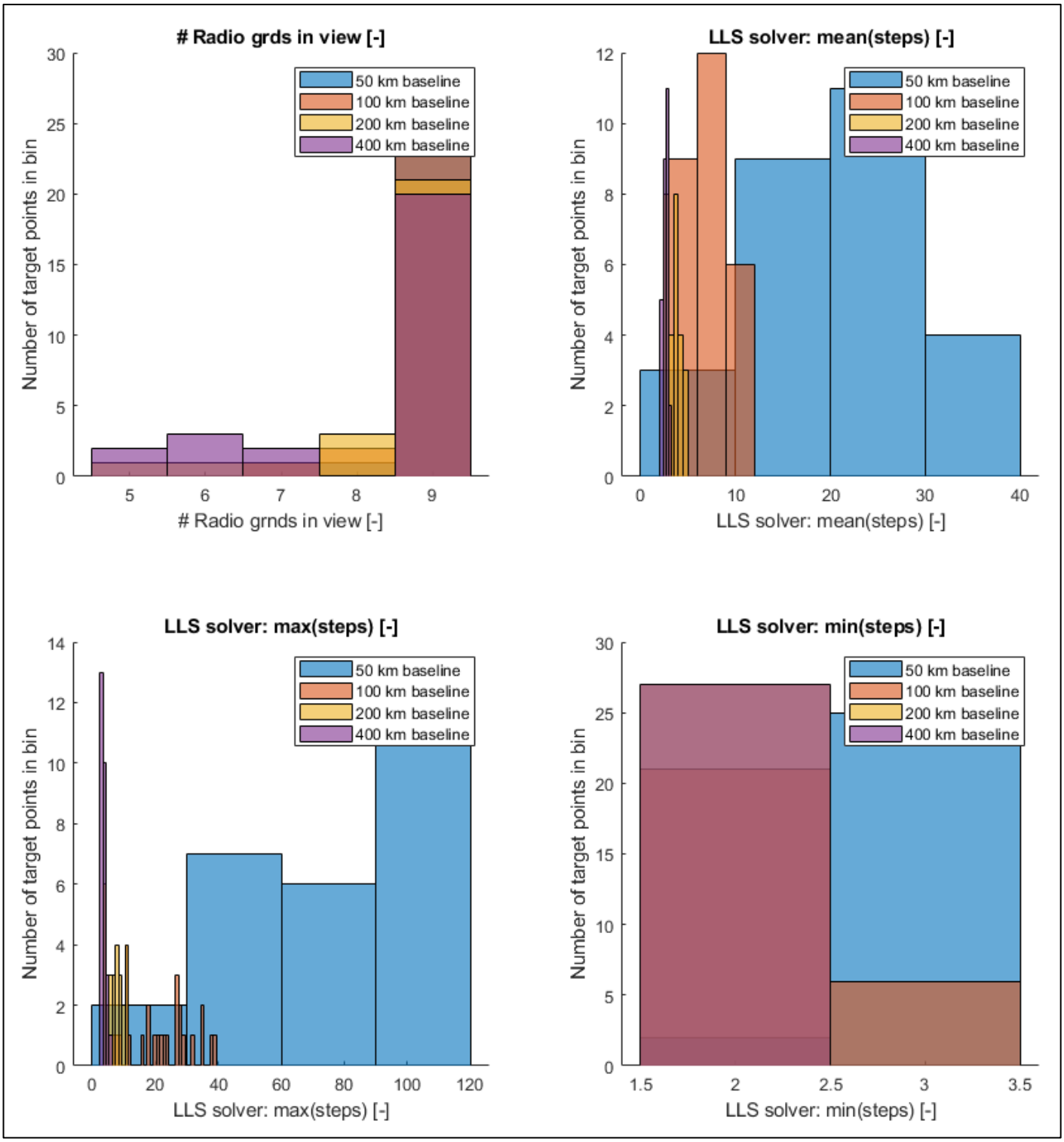

Figure 52: multiple histograms showing the impact of varying baseline size (50, 100, 200, and 400 km), see Appendix C for all inputs.

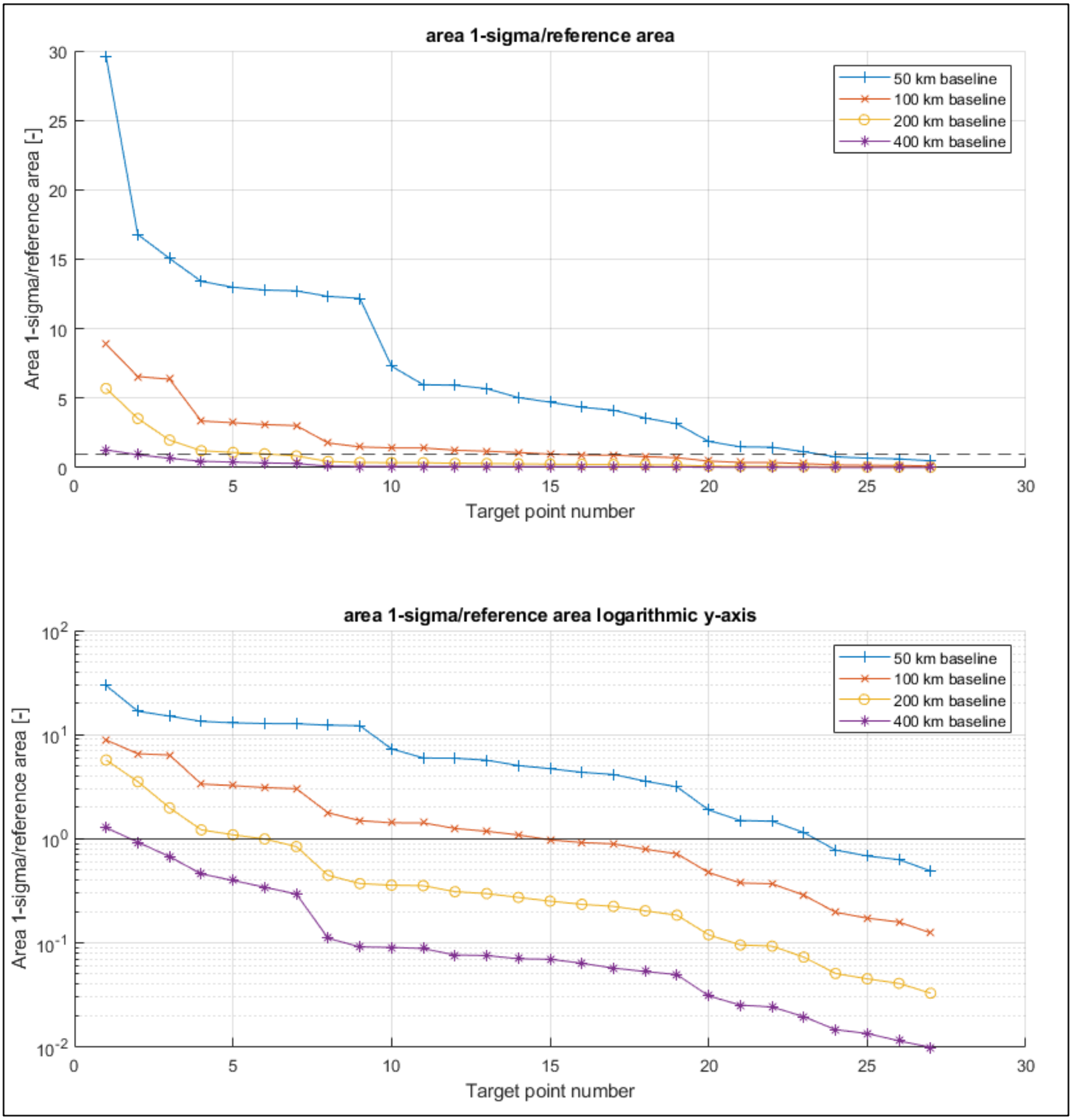

Figure 53: multiple plots showing the impact of varying baseline size (50, 100, 200, and 400 km), see Appendix C for all inputs.

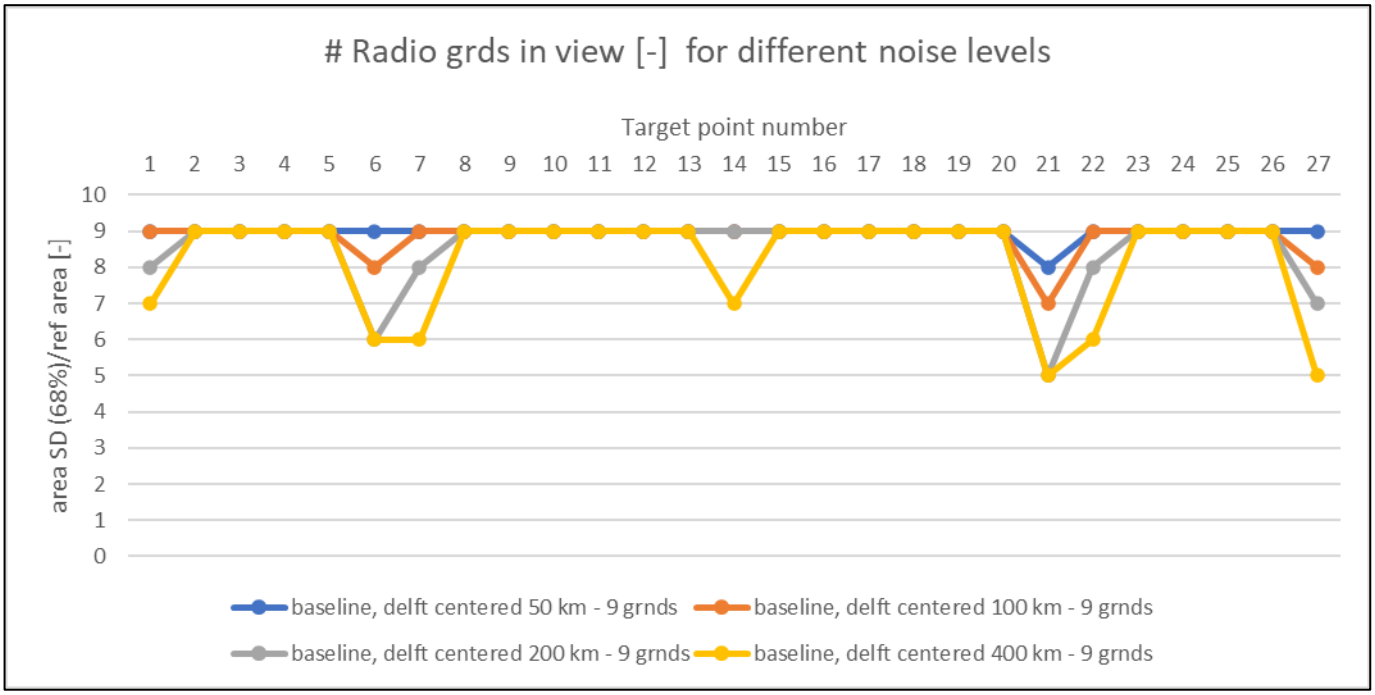

Figure 54: plot showing the impact of varying baseline size (50, 100, 200, and 400 km) on the number of radio ground station in view of each target, see Appendix C for all inputs.

In Figure 54 one can observe that a larger baseline size can lead to less ground stations being in view. We know from 7.4.2.2 that this has a negative impact on accuracy.

In Figure 55 one can see that the system performs better for longer baselines. The 50, 100, 200 and 400 km baseline meet the ACC.1 requirement for respectively 15%, 48%, 81% and 91 % of the coverage area. It is also interesting to note that no new targets become trackable for higher baselines, this is due to the targets being interspaced by 5 degrees, so due to discretization the coverage area appears to not expand (since no additional points are tracked by the ground stations) even though in reality the coverage area would be larger for a larger baseline.

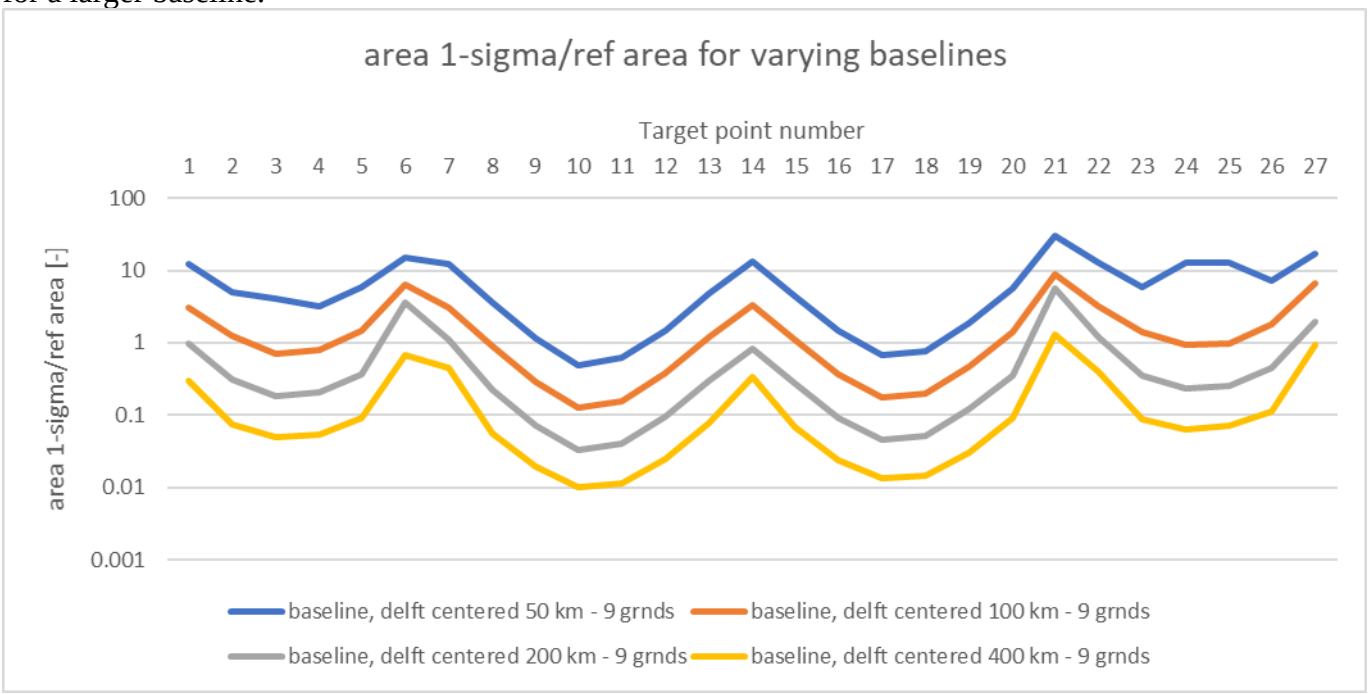

Figure 55: plot showing the impact of varying baseline size (50, 100, 200, and 400 km) on the TDOA system accuracy, see Appendix C for all inputs.

baseline size [km]	baseline size [km]	Ratio baselines [-]	Ratio average error [-]	Ratio SD error [-]
100	200	0.5	3.938	0.068
200	400	0.5	3.780	0.230

Table 10: table comparing the effect of a change in baseline size with respect to area 1-sigma/ref area. Note that target points 1, 6,7, 14, 21, 22 and 27 are not considered in this analysis.

From Table 10 one can conclude that doubling the baseline size reduces the target estimation error by approximately a factor of 4.
Note that target points 1, 6,7, 14, 21, 22 and 27 are not considered in this analysis because for these points the baseline changing alters the number of ground stations in view. The impact of the number of ground stations (in view) was analyzed in 7.4.2.2.

$$error\ area \propto \frac{C_2}{noise^2} * \left(\frac{baseline}{baseline_{standard}}\right)^{-2} \quad 7\text{-}22$$

Or in equation form if the number of ground station is unchanged:

$$error\ area \propto C_1 * \left(\frac{noise}{noise_{standard}}\right)^{2} * \left(\frac{baseline}{baseline_{standard}}\right)^{-2} \quad 7\text{-}23$$

If the number of ground stations doubles with respect to baseline:

$$error\ area \propto C_1 * \left(\frac{noise}{noise_{standard}}\right)^{2} * \frac{1}{1.5} * \left(\frac{baseline}{baseline_{standard}}\right)^{-2} \quad 7\text{-}24$$

If the number of ground stations halves with respect to baseline:

$$error\ area \propto C_1 * \left(\frac{noise}{noise_{standard}}\right)^{2} * 1.5 * \left(\frac{baseline}{baseline_{standard}}\right)^{-2} \quad 7\text{-}25$$

where the subscript standard indicates the case for which the proportionality constant C_1 was established.

It is also important to understand that this relation will not hold once an increase in baseline size leads to ground stations being located so far away that they can no longer acquire the satellite due to the curvature of the earth, see also Figure 54. So, the relation above only holds for those targets which remain in view of all ground stations.

7.4.2.4 Ground Stations Geometry

In this section the influence of the geometry or configuration of the ground stations is analysed. See Figure 44 for plots of the ground station geometry analysed in this section.
In Figure 56, Figure 57, Figure 58 and Figure 59 one can see how the effect of a change in geometry. The square, circle and cross are all have good convergence. Clustered behaves notably worse and the line configuration takes a large number of steps to converge. Note however that the line configuration is reaching the maximum number of steps for only 27 out of 27000 cases, hence the results give a reasonable impression of the system performance.

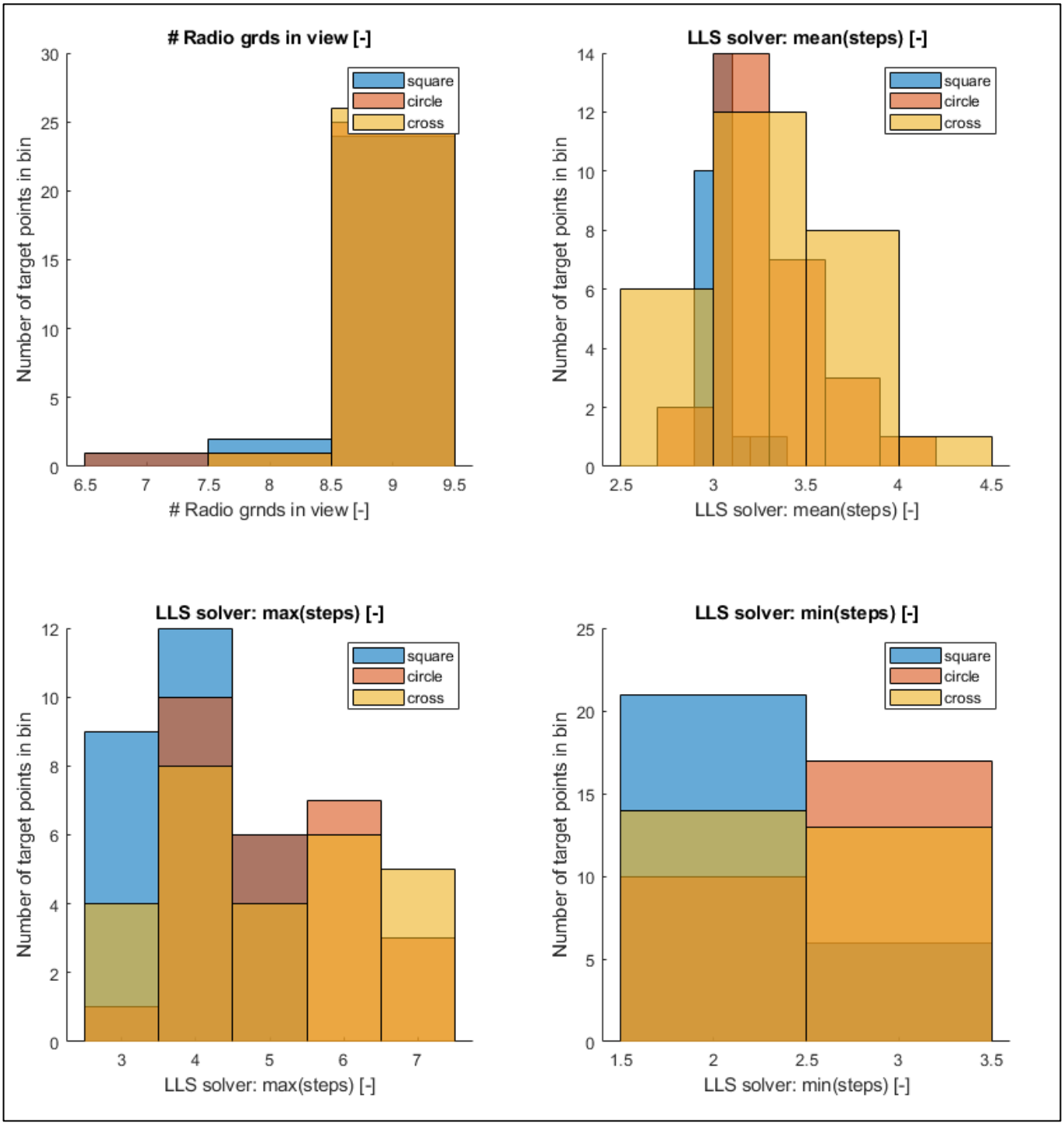

Figure 56: multiple histograms showing the impact of varying ground station geometry, see Appendix C for all inputs

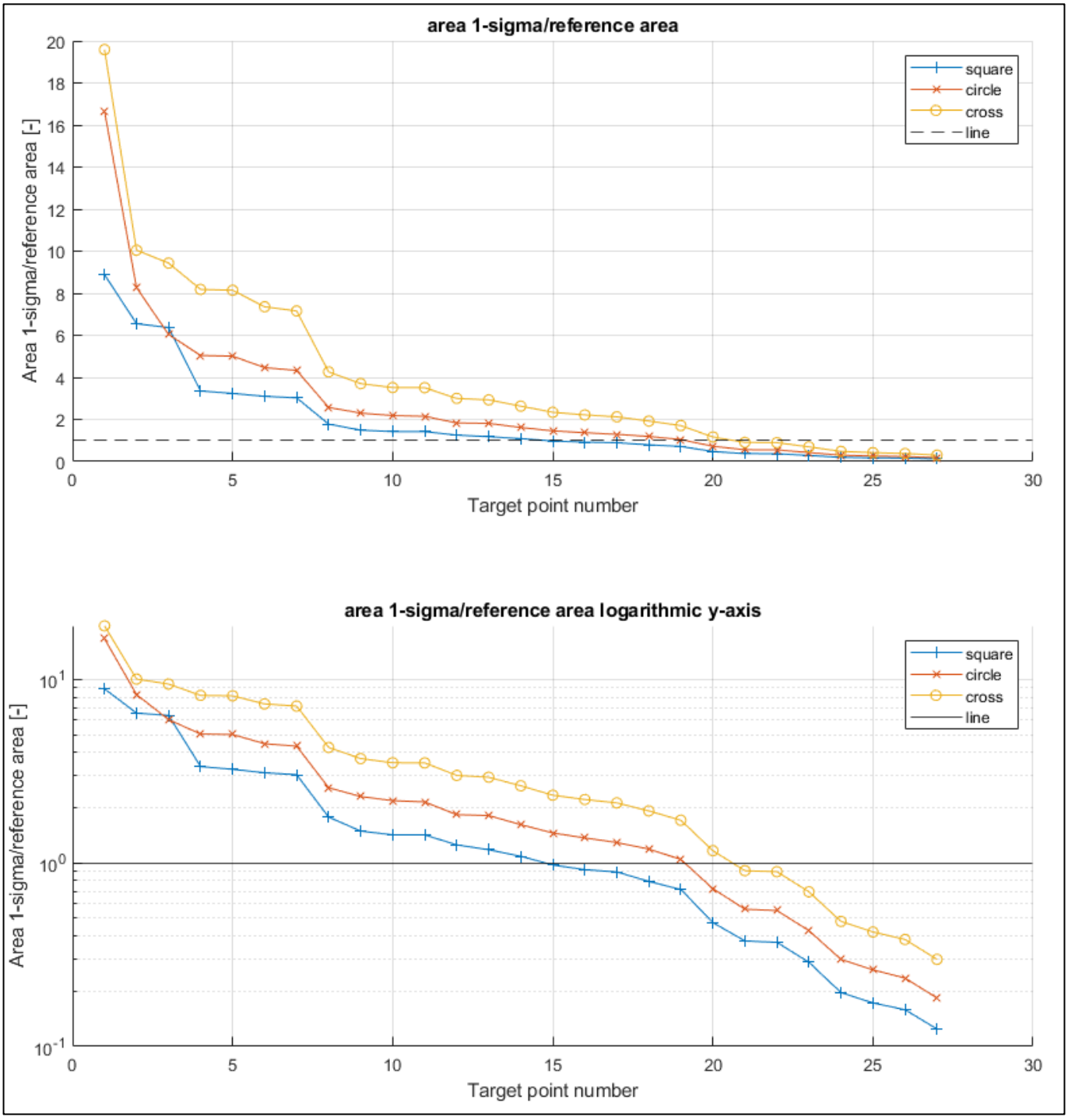

Figure 57: multiple plots showing the impact of varying ground station geometry, see Appendix C for all inputs.

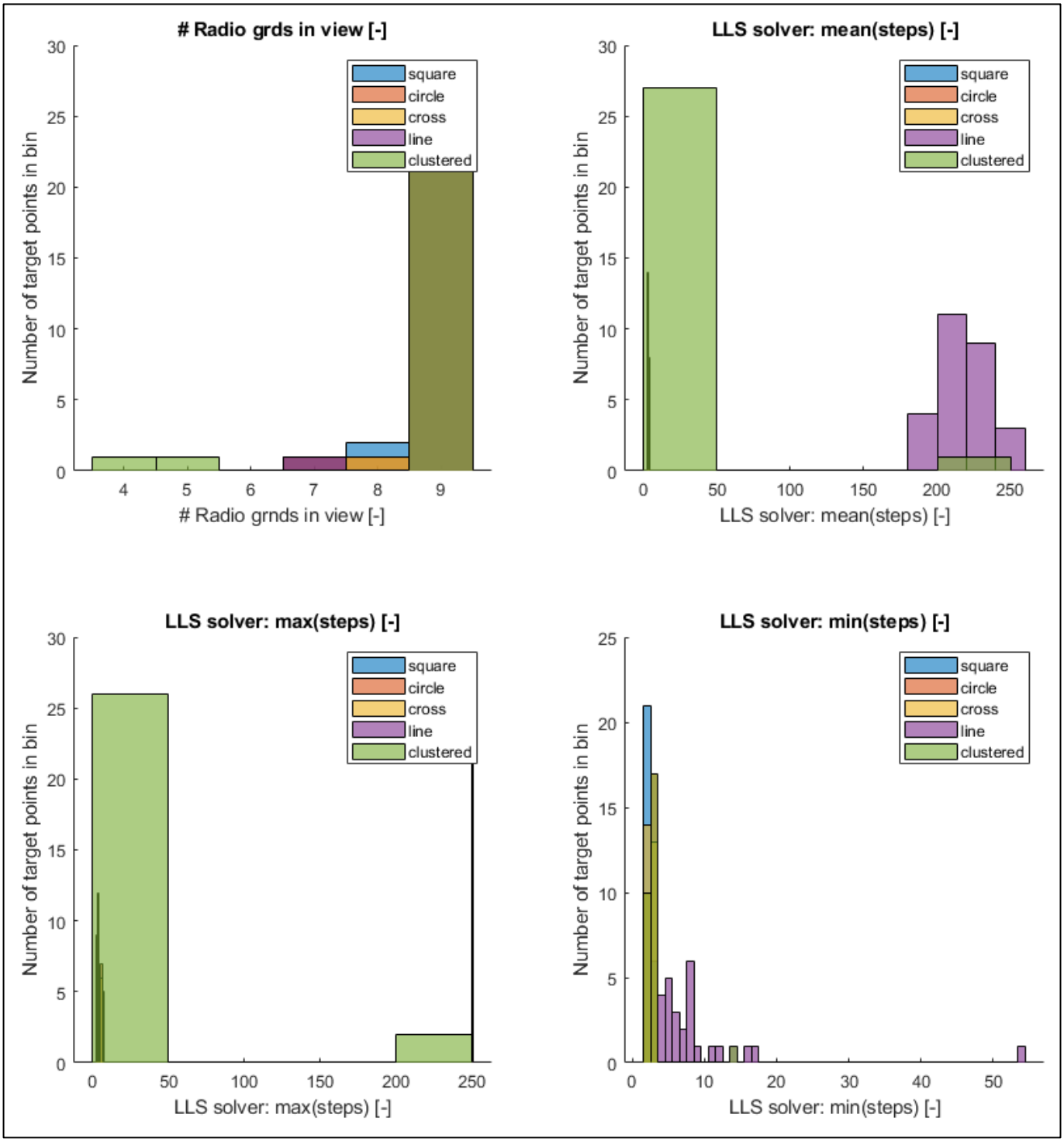

Figure 58: multiple histograms showing the impact of varying ground station geometry, see Appendix C for all inputs.

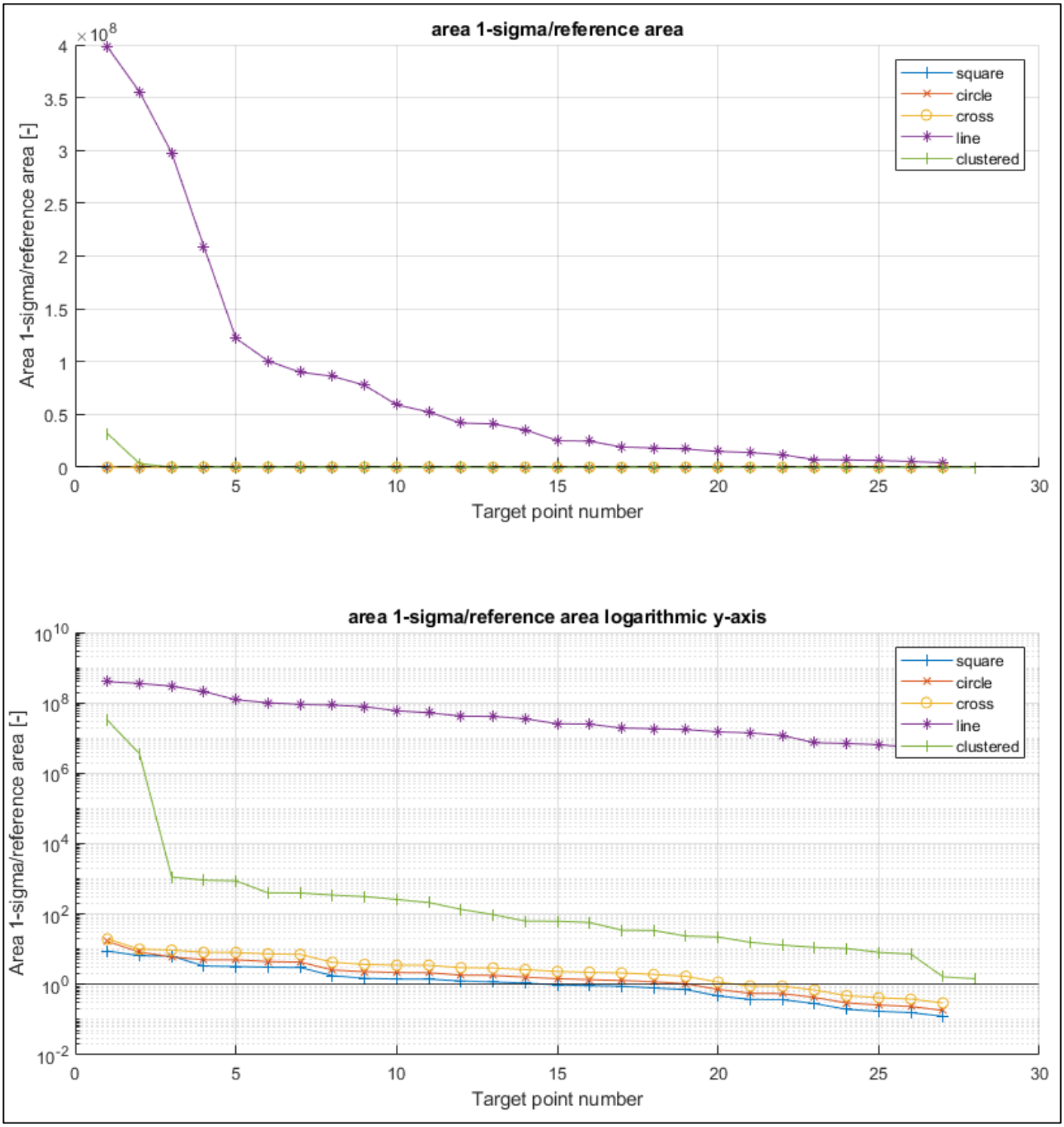

Figure 59: multiple plots showing the impact of varying ground station geometry, see Appendix C for all inputs.

The clustered configuration detects 1 additional target this is ignored in the subsequent analysis to allow for consistent comparisons.

In Figure 60 and Figure 61 the performance of the different ground stations geometries are compared. One of the important conclusions here is that the impact of the geometry for the square, circle and cross configurations is notable and should be accounted for in the 3D TDOA system design through simulation.

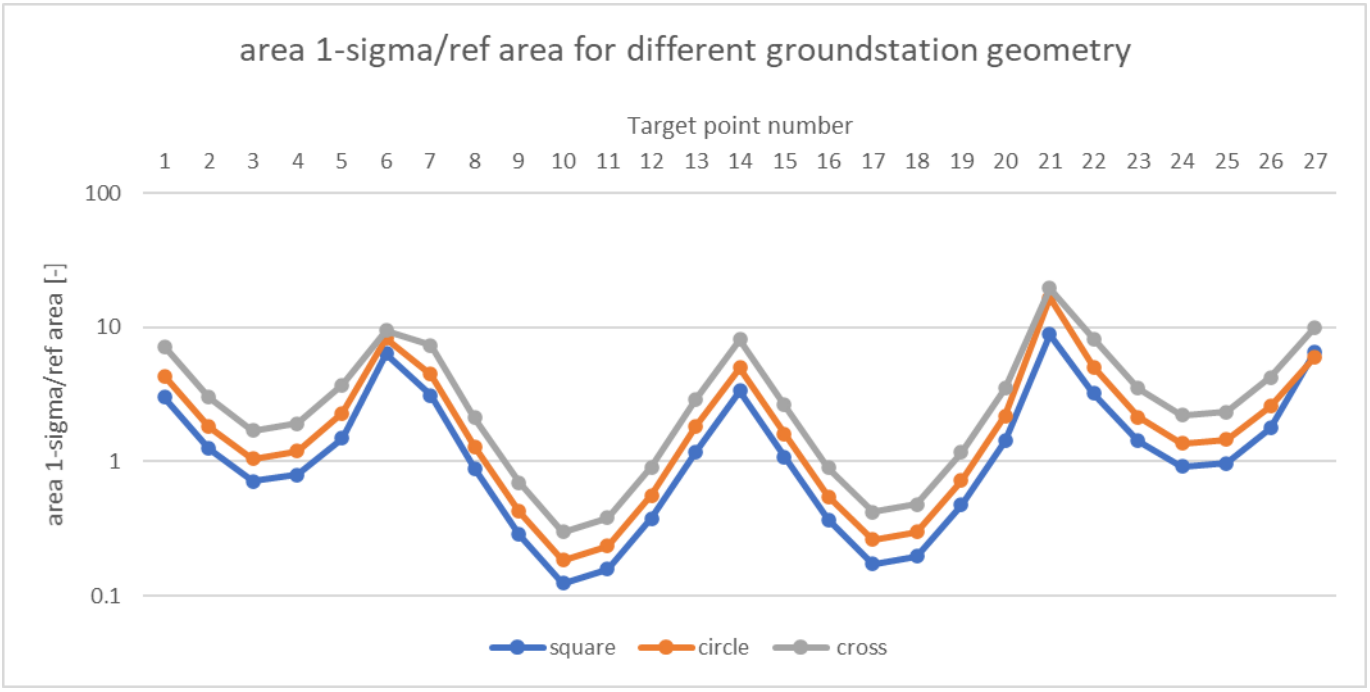

Figure 60: plot showing the impact of varying ground station geometry on the TDOA system accuracy, see Appendix C for all inputs.

However, when one considers either the clustered or line configuration the system performance worsens dramatically. For clustered the performance is sometimes close to the other configurations and other times more than 6 orders of magnitude worse. Meanwhile the line configuration is performing absolutely terrible, being about 6 orders of magnitude worse across the board.

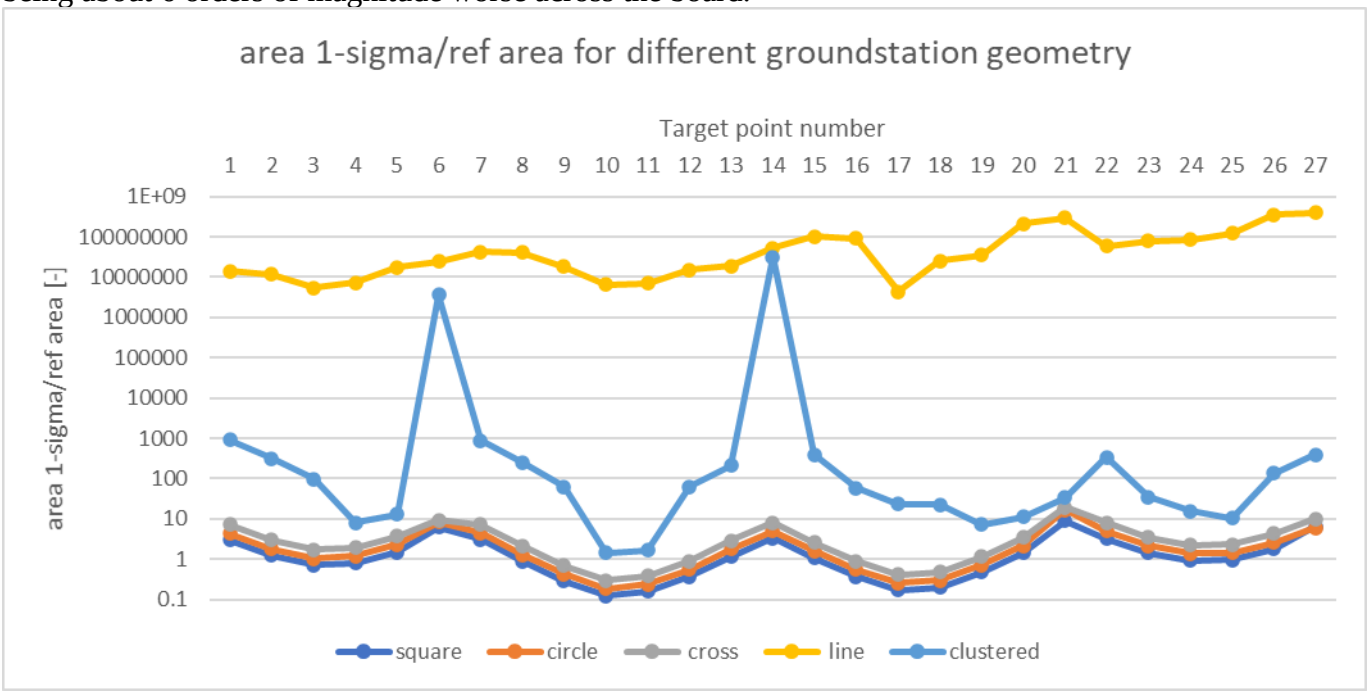

Figure 61: plots showing the impact of varying ground station geometry on the TDOA system accuracy, see Appendix C for all inputs

The reason for the poor performance by the line can be illustrated by using the qualitative 3D Matlab script from section 7.1, as show in Figure 62. Here 4 ground stations have been placed on a line with the target some distance away. Since these ground stations are all placed on the x-axis, they cannot resolve the target in 3D space. The reason the "line configuration" such as used to generate the results presented in Figure 61 can resolve targets in three-dimensional space is because the ground stations are placed on the surface of the earth. The means the ground stations follow the curvature of the earth and as such can estimate target positions in 3D space, albeit poorly.

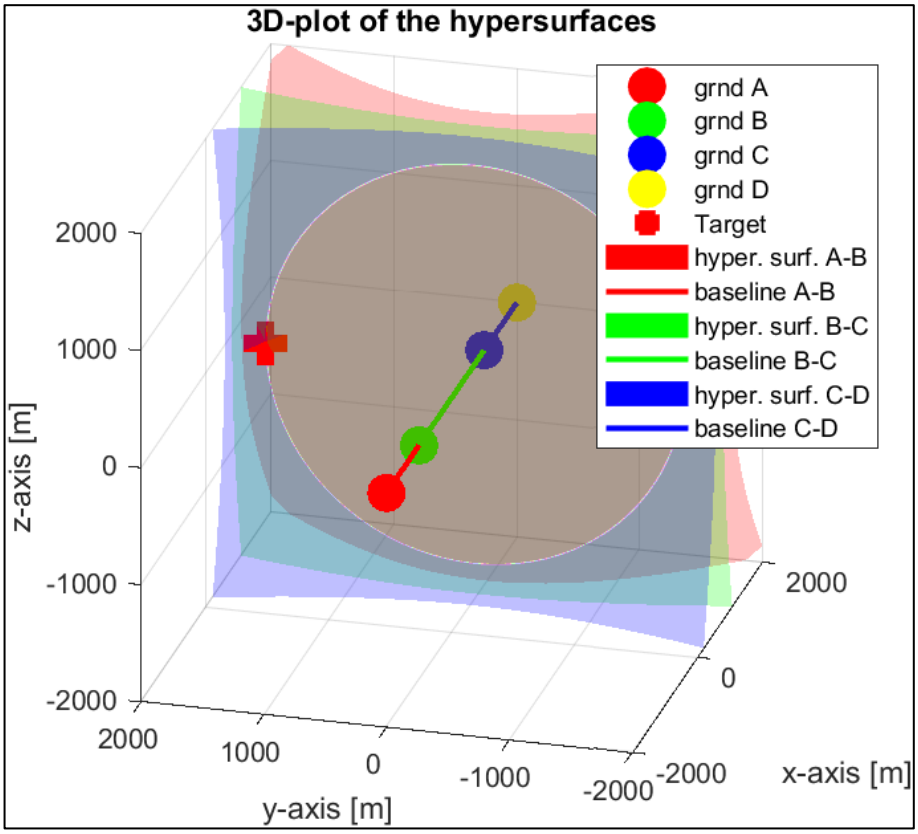

Figure 62: illustrative plot made in the qualitative 3D Matlab scipt with inputs: inputs: Ax -2000, Ay 0, Az 0, Bx -1000, By 0, Bz 0, Cx 1000, Cy 0, Cz 0, Dx 2000, Dy 0, Dz 0, Tx 700, Ty 1700, Tz 0, bound x min -2000, bound x max 2000, bound y min -2000, bound y max 2000, bound z min -2000, bound z max 2000 all units in meters, with A, B, C and D ground stations and T the target. Note that the axis uses arbitrary units, this plot is merely illustrative

The results of this section cannot be converted to a rule of thumb as in the previous sections. The geometry impact is certainly present and can be as relevant as the other factors considered such as when one considers either a circle or a cross geometry. Or it can be the most dominant factor by far, imposing heavy restrictions on the other parameters. This again underscores the importance of simulating a TDOA system prior to implementation since a poor ground station configuration can easily make the system untenable.

The relations established above remain unchanged given the erratic nature of the impact of the ground stations geometry.
Or in equation form if the number of ground station is unchanged:

$$error\ area \propto C_1 * \left(\frac{noise}{noise_{standard}}\right)^2 * \left(\frac{baseline}{baseline_{standard}}\right)^{-2} \quad 7\text{-}26$$

If the number of ground stations doubles with respect to baseline:

$$error\ area \propto C_1 * \left(\frac{noise}{noise_{standard}}\right)^2 * \frac{1}{1.5} * \left(\frac{baseline}{baseline_{standard}}\right)^{-2} \quad 7\text{-}27$$

If the number of ground stations halves with respect to baseline:

$$error\ area \propto C_1 * \left(\frac{noise}{noise_{standard}}\right)^2 * 1.5 * \left(\frac{baseline}{baseline_{standard}}\right)^{-2} \quad 7\text{-}28$$

where the subscript standard indicates the case for which the proportionality constant C1 was established

The relations presented above are only indicative, they predict how a TDOA system will respond to certain changes in input parameters, but they are based on a statistical analysis, not on a formal proof. As such it is still important to use the 3D TDOA software or other means to ensure the simulated performance is in line with the predictions. However, the relations above can be used to understand the relative impact of important system parameters.

In Figure 63 a scheme is presented to improve a given TDOA system based on the results presented in the previous sections.

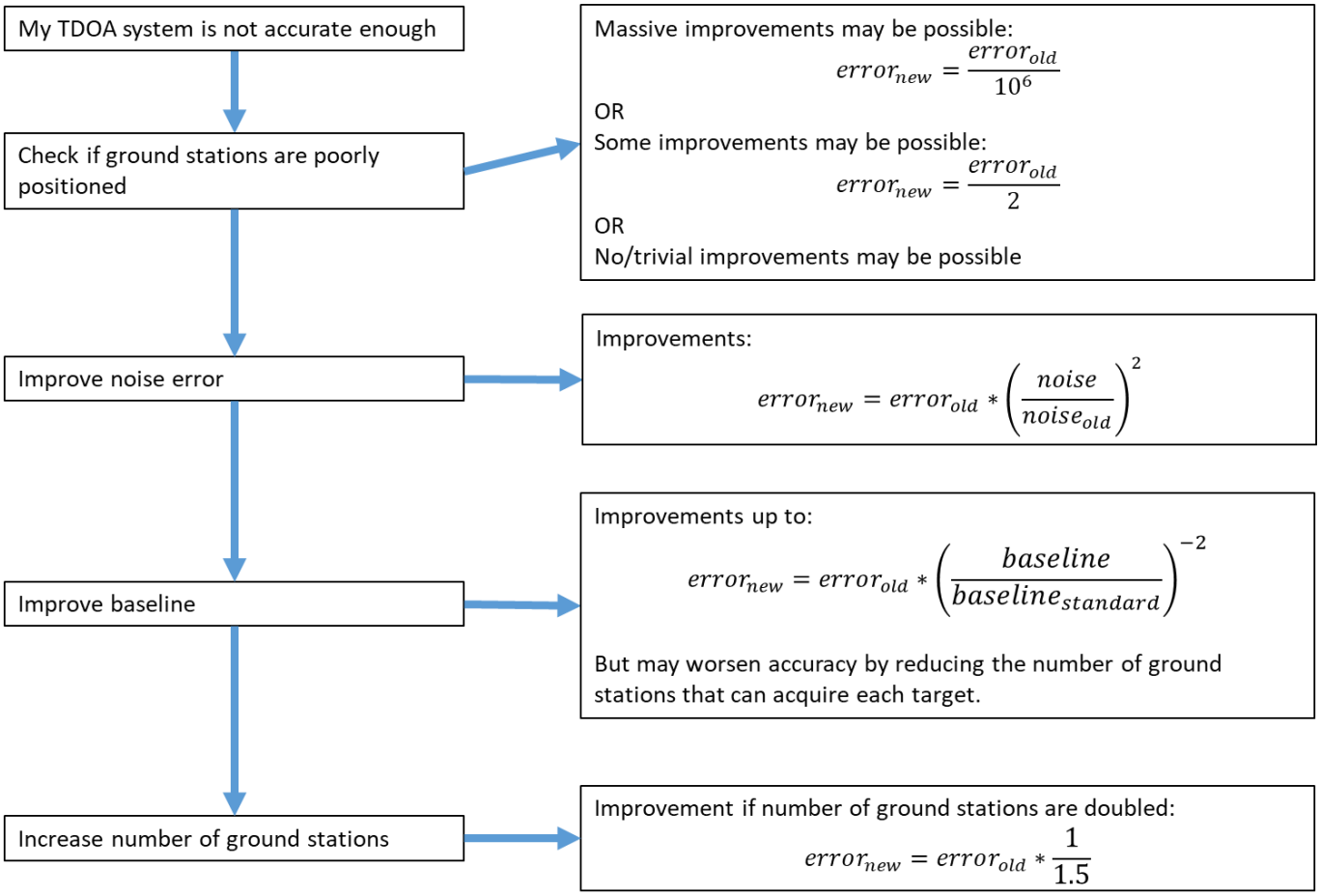

Figure 63: schematic representation of the recommended order to change parameters to improve a TDOA system performance.

Note that the different steps in Figure 63 are intertwined, one will probably improve the ground station positioning/geometry by adding some ground stations, these new ground stations will also affect the baseline, etc.

We can apply the 3D TDOA simulation tool to the latest TU Delft satellite (Delfi-PQ) to discover how well it can be tracked through a TDOA system with the required accuracy. Delfi-PQ has a data rate of up to 7.2 kbit per second [27] so by looking at Figure 20 we get a two-way range jitter of approximately 100 meters. This can be converted to the one-way range jitter and combined with the GPS timing error of 4.5 meters to find a total error SD of 236 ns (see section 6.4).
When this noise level is applied to a target satellite in a 500 km circular orbit (approximately Delfi-PQ orbit), then 18% of the coverage area (where the satellite can be received by a minimum of 4 ground stations) meets requirement ACC.1 when utilizing 25 ground stations in a square geometry with a baseline of 1000 km. See List of FiguresAppendix D for all input values.

7.4.3 Practical Considerations

In this section the feasibility of implementing a TDOA system will be discussed. All requirements will be dealt with in order but first a discussion of the coverage area will be given. Note that this section has similarities with section 5.3.2.

Another practical aspect that can now be in investigated by means of the 3D TDOA code is the coverage area of a certain 3D TDOA system. For example, in Figure 64 one can observe that the coverage area extends from roughly the Shetland islands in the north to Corsica in the south, covering most of Western Europe. This coverage area depends on several factors:

- The satellite altitude, a higher altitude satellite can be seen from farther away due to the curvature of the earth.
- The ground stations geographical spread. Ground station which are more spread out can cover a larger area (up to the point where there are less than 4 ground stations in view, then the code can no longer converge).
- The Ground stations (optical and radio) minimum elevation angle. They must be able to see and acquire the target satellite after all.

The coverage area is an important practical consideration when designing a TDOA tracking system. A target satellite in low earth orbit is visible from a ground station for 5 to 20 minutes per pass [52]. This means that there is a limited amount of time to acquire and track the satellite via the TDOA system and then subsequently acquire and communicate/identify with the optical ground station. As such it may be valuable to position the TDOA ground stations in such a way that they have achieved a high accuracy estimate of the target satellite orbit when it comes in view of the ground station. This can be done by using the 3D TDOA tool and by considering the orbit the target satellite is in. Alternatively, since the TDOA system does not require all ground stations to be in view to track the target it is possible to position the ground stations so that the satellite is in view longer.

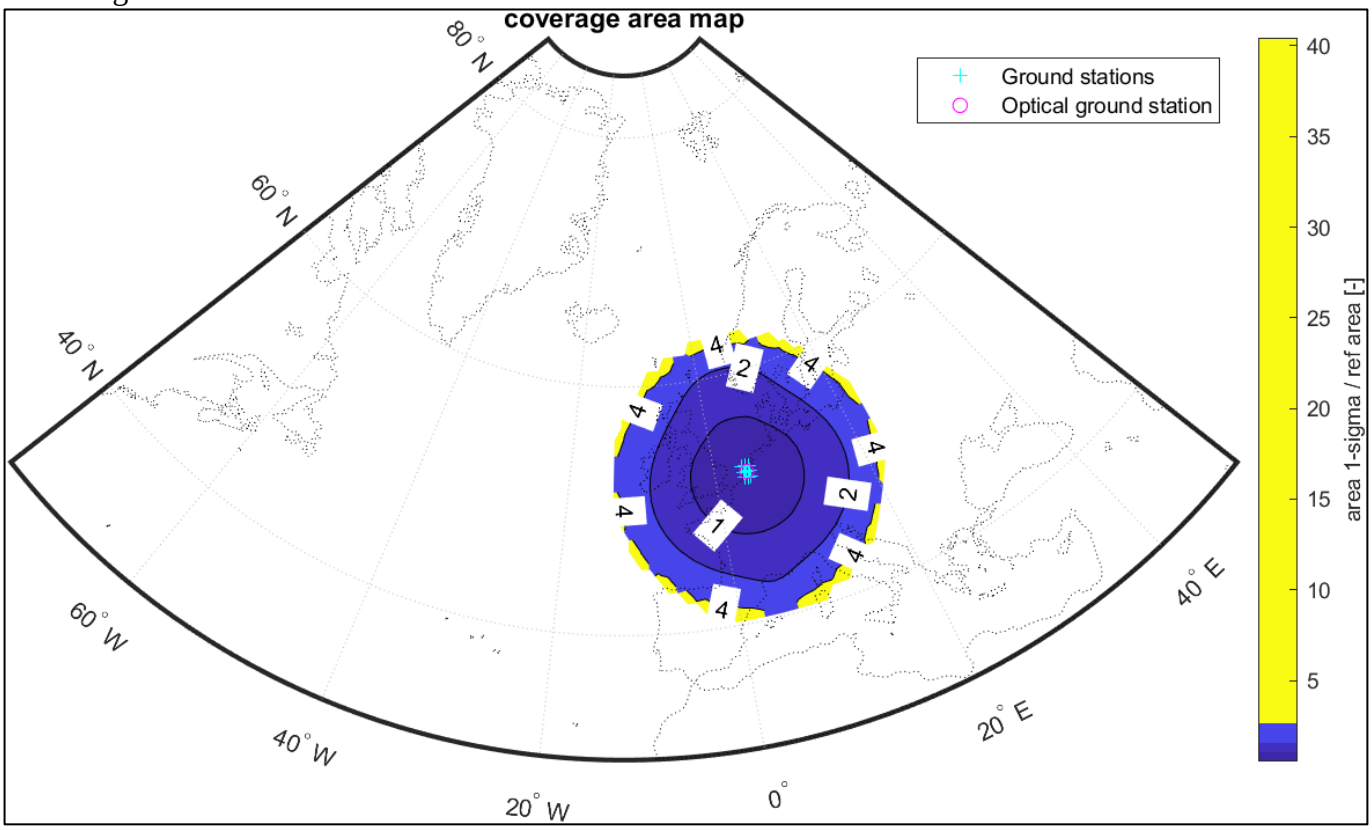

Figure 64: figure showing a map of Europe and the northern Atlantic ocean, with a contour map superimposed indicating the performance of the simulated 3D TDOA system (specifically the 4th case (Noise 15.1843093448556 ns), for all inputs see Appendix E

ACC.1
Note that usually the accuracy requirement can be met for part of the coverage area (see Figure 64). This partial coverage is (usually) unavoidable and must be considered during future development.
Meeting the accuracy requirement can be achieved by changing the ground station geometry, noise error level, baseline size and number of ground stations. As listed in Figure 63 these primary inputs to the 3D TDOA simulation are not equally effective at increasing the system accuracy.
In summary this requirement can be met, but this may impose constraints or requirements on the ground station and/or satellite. The 3D TDOA tool can be used to compare and contrast different implementation of a TDOA tracking system.

SAT.1
During the 2D analysis in section 5.3.2 it was stated that: TDOA system is expected to utilize the existing satellite radio communications system. This has remained unchanged, as such this requirement is met.

SAT.2
The satellite altitude was set to 500 km for all results presented in this chapter as per the requirement. Hence this requirement is met for part of the coverage area, for certain ground station amount, geometry, noise error level and baseline size.

No impediments to meeting ground station requirements have been uncovered in this chapter, they can be met as was concluded in section 5.3.2.

7.4.4 Answer to Research Question II

Research question II:

2) Is **Time Difference Of Arrival (TDOA)**, a **radio**-based **tracking** technologies applied to **cooperating spacecraft** in **low-earth orbit** a suitable technique to be used by TU Delft for the **DelfiSpace program**?
- 2A) What are the consequences with respect to the target satellite?
- 2B) What are the consequences with respect to the ground station(s)?
- 2C) What are the consequences with respect to the entire tracking system?

First the sub questions will be answered:
2A) What are the consequences of TDOA with respect to the target satellite?
The DelfiSpace program will almost certainly have a radio communication system on board. No obstacles were identified in integrating this system with a TDOA tracking system. But the performance of the TDOA tracking system does depend on the noise levels in the TDOA measurements. These in turn are related to the total communications system ground and space segments. Hence one of the recommendations for future work is integrate the ground and space communications segment into the future TDOA Tracking Tool, see also the next chapter. See also section 7.4.3 for a discussion on how the 3D TDOA tracking system performs with respect to the satellite requirements.

2B) What are the consequences of TDOA with respect to the ground station(s)?
The ground station configuration can be the dominant factor in the TDOA system performance if their geometry is poor. Otherwise, their baseline is a critical aspect of the TDOA system accuracy, and the number of ground stations is also important. In addition, the ground stations play a critical role in the satellite communications system, and as such also play a role in the noise levels in the TDOA measurements. Briefly the successful implementation of a TDOA tracking system will be heavily dependent on the ground stations. See also section 7.4.3 for a discussion on how the 3D TDOA tracking system performs with respect to the ground station.

2C) What are the consequences of TDOA with respect to the entire tracking system?
TDOA is a promising method for satellite tracking, the system performance is mostly dependent on the ground stations, not the satellite. This is a promising outcome since the restrictions on the space segment are usually more pertinent then on the ground segment in terms of mass, power budget, reliability etc. For example, the ground stations remain accessible, maintenance and modification can be made fairly easily, whereas the satellite is inaccessible once launched.

In summary in this chapter a 3D TDOA tracking system simulation was developed, however the simulation in this chapter treats the 3D TDOA tracking system as a localization problem. In other words, we are estimating the position in which the satellite was when a certain message was sent.
But in realty the satellite is moving rapidly though the sky. This means the satellite position is changing in time, this is an additional error source since we do not know where the satellite is, but rather where the satellite was when the message was sent, and from this we want to derive where the satellite is going to be so we can track and/or communicate with it optically.
In the next chapter: 8) recommendations are given on how to develop an advanced TDOA simulation tool, which track a moving target and directly predicts the satellite orbit. The nature of this tool means that will utilize multiple measurements in time (for example a 100 second observation span with 1 measurement per ground station per second). These additional measurements are expected to increase the system accuracy, as such the 3D TDOA tracking system accuracy results presented in this chapter may be considered conservative.

8) Future Work: 4D TDOA Simulation Tool

In chapter 5) a 2D TDOA simulation tool was developed, from these first order results the decision was made to develop a more sophisticated simulation tool. This is the 3D TDOA simulation tool which is the subject of chapter 7). This 3D TDOA tool was very different, utilizing linearize least square to process up to hundreds of TDOA measurements simultaneously, allowing for analysis of the coverage area and performance of larger, distributed 3D TDOA systems. In addition, it is a fundamentally 3D system which estimates the target location in 3D space (x, y, z) and uses a stochastic error approach to estimate the system performance.
This chapter deals with the proposed advanced TDOA simulation tool: 4D TDOA. This tool is to be developed as future work. A proposed code structure is presented, including aspects which may optionally be included. Note that elements of the advanced TDOA simulation tool can reuse aspects of the previous chapters.
The salient feature of the 4D TDOA simulation tool is that it estimates the target state vector directly: $(x, y, z, \dot{x}, \dot{y}, \dot{z})$. This means that the 4D TDOA simulation tool can be used to predict the target satellite position in the future, which is a critical part of the overall TDOA system. In effect the 4D TDOA simulation tool will be very similar to the operational code necessary for the actual 4D TDOA tracking system. In addition, it will be able to utilize measurements taken at different points in time and combine them into a target state vector, hence the name 4D TDOA. This greatly increase the number of measurements which can be used leading to higher accuracy.

8.1 Diagram of the 4D TDOA Simulation Tool

Figure 65 is a reproduction of Figure 30, which is a schematic representation of the LLS algorithm as implemented in 7.2. Figure 66 is the updated version of for the advanced TDOA simulation tool. Note that the new blocks are indicated in orange. Note that both these figures and the explanation below are based on on E. Gill and O. Montenbruck's excellent book: Satellite Orbits Models, Methods and Applications [45] and on B. D. Tapley, B. E. Schutz, and G. H. Born' very extensive book Statistical Orbit Determination [46].

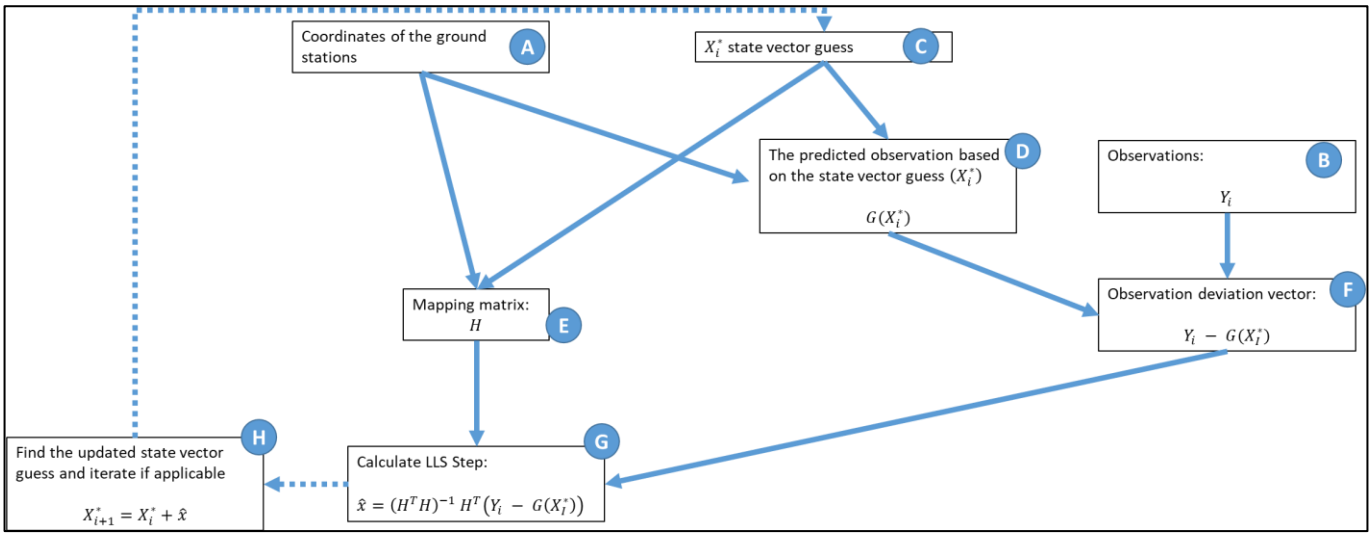

Figure 65: schematic representation of the LLS algorithm, each element is indicated with a letter to facilitate the written explanation

Blocks (A), (B) and (C) are effectively unchanged, note however that the state vector guess is now implicitly associated with a certain (start) time. But one should note that block (D) has become more complex. We must generate predicted observations for the initial state vector as before, but we must take into account that the

target satellite is moving while being observed. This means we must propagate the state vector guess forward in time to each time step where the satellite transmits a message. One potential solution is to add the transmission times to the state vector guess. Then the LLS solver will not only estimate the target satellite orbital parameters but also the times at which it transmits.
Next up is block (E) which is a single block in Figure 65 whereas it has been split in three in Figure 66 below. The observation state matrix could previous be established in one go but has now become more involved. In (E1) the observation-state matrix is established which relates how a change in the initial state vector will affect the (predicted) observations. In (E2) the state transition matrix is calculated (see section 8.2). This is matrix is used to propagate the observation-state matrix forward in time. The two matrices are then combined in (E3) into the mapping matrix H.
Blocks (F) remain unchanged, so does block (G) except for the addition of the weight matrix to the formula. In block (H) the weighting matrix is added. This diagonal matrix has on its diagonal the weights to be assigned to each observation. This can be especially useful when different quality sensors are being used, one can give more weight to the measurements made by high performance sensors. It is recommended to include the weight matrix from the start, if one does not want to use the weight matrix it can be set to be the identity matrix and will have no effect on the results.
In block (I) the state vector guess is updated, note that as previous it is useful to use tolerance and a limit to the number of iterations allowed to the algorithm. The algorithm may be interated or may proceed to the next batch. The word batch is usually used to indicate a group of observations spread in time.

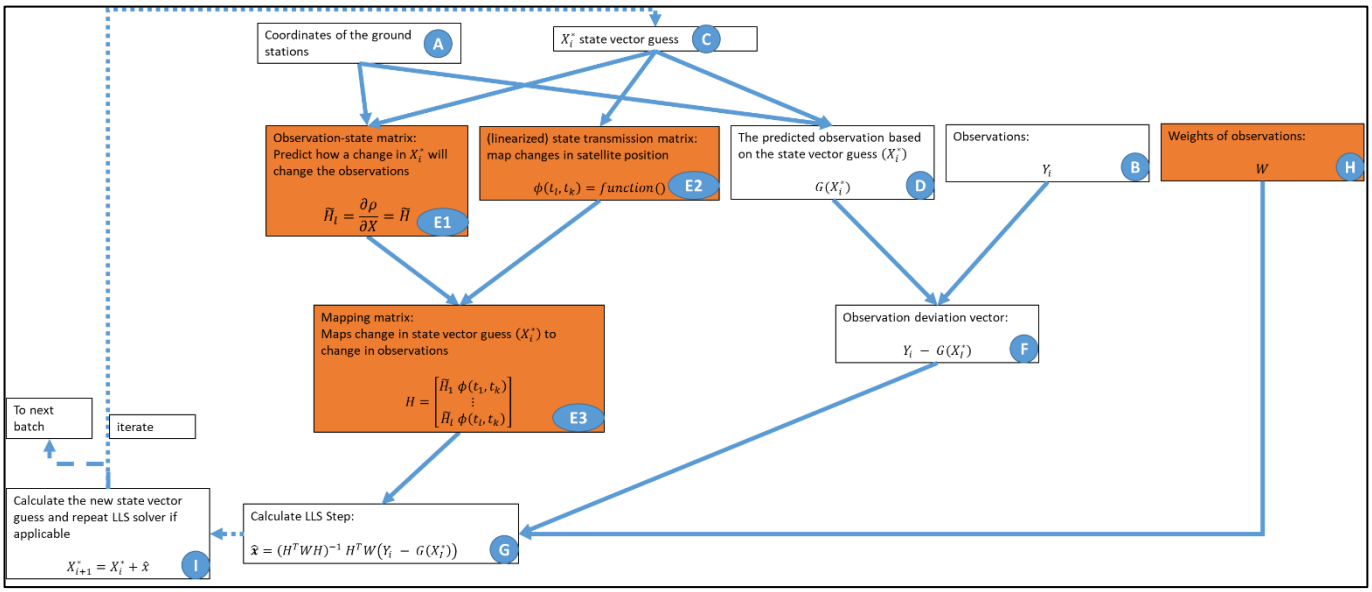

Figure 66: schematic representation of the 4D TDOA LLS algorithm, each element is indicated with a letter to facilitate the written explanation.

Conceptually the procedure operates as follows. The state vector guess and knowledge of the coordinates of the ground stations are used to predict the expected observations (D) which are then compared with the actual observation in block (F) to find the observation deviation vector (or cost function). This is what the algorithm wants to minimize (once multiplied with the weights vector), if the expected and actual observations are exactly the same then the state vector guess is correct. In reality this will not happen due to the presence of noise and measurement (and model and state transition matrix) errors there will always be some difference between the actual and predicted observations.
In order to minimize the observation deviation vector, the 4D TDOA LLS algorithm will make changes to the initial state vector guess. However, it has information on how a change in the state vector guess will affect the predicted observations: the mapping matrix. The mapping matrix is the product of the $\tilde{H}$ matrix and the state transitions matrix. The state transition matrix is used propagate the state vector guess into the future, whereas the $\tilde{H}$ matrix predicts the effect of a change in the state vector guess on the predicted observations.

Note that the orbit propagation used to generate the predicted observations can be complex and involve integration, it can for example be an SGP4 propagator. But the state transition matrix is a square matrix of size equal to the state vector guess. The means that usually the state transition matrix is less accurate since it is by nature linearized. See also section 8.2**.**

In the diagram presented above the only information being passed between two batches is the state vector guess. A further improvement to the algorithm is to pass additional information from batch to batch. This gives additional information to better estimate the target satellite trajectory. We have explored this approach in a test environment. However, the implementation proved challenging.
A number of challenges were overcome, for instance: utilizing Cholesky decomposition (already implemented in 3D TDOA simulation tool) and establishing the state transition matrix (see below). However, it proved difficult to fully consolidate the information in the diagrams with the text description in [46].
This is a topic requiring further study. It may prove valuable to compare with additional sources or existing implementation not specific to TDOA.

8.2 State Transition Matrices

State transition matrices or STMs are the linchpin of the algorithm presented above and are also used in Kalman and extended Kalman filters.

An STM is used to propagate a state vector froward in time and symbolically written as $\phi(t_l, t_k)$ or the STM from the time t_k to the time t_l. As an example, if we have an object in rectilinear motion in 2D its state vector may be written as:

$$X_i^* = \begin{bmatrix} x \\ y \\ \dot{x} \\ \dot{y} \end{bmatrix} \tag{8-1}$$

And an STM may be used to propagate this state vector forward in time:

$$\phi(t_l, t_k) * X_i^* = \begin{bmatrix} 1 & 0 & 1 & 0 \\ 0 & 1 & 0 & 1 \\ 0 & 0 & 1 & 0 \\ 0 & 0 & 0 & 1 \end{bmatrix} \times \begin{bmatrix} x \\ y \\ \dot{x} \\ \dot{y} \end{bmatrix} = \begin{bmatrix} x_k \\ y_k \\ \dot{x}_k \\ \dot{y}_k \end{bmatrix} \tag{8-2}$$

For example, for $t_k - t_l = 1\ sec$

$$(t_l, t_k) * X_i^* = \begin{bmatrix} 1 & 0 & 1 & 0 \\ 0 & 1 & 0 & 1 \\ 0 & 0 & 1 & 0 \\ 0 & 0 & 0 & 1 \end{bmatrix} \times \begin{bmatrix} 5 \\ 10 \\ 2 \\ 3 \end{bmatrix} = \begin{bmatrix} 7 \\ 13 \\ 2 \\ 3 \end{bmatrix} \tag{8-3}$$

In the example above the state vector captures the full motion since the system is linear.

Note that STM's can be multiplied: $\phi(t_2, t_0) = \phi(t_1, t_0) \times \phi(t_2, t_1)$

Conceptually the STM is used to provide information to the LLS algorithm on how a change in the initial state vector guess will lead to a change in state vector at a future time. This can then be combined with the $\widetilde{H}$ matrix which predicts how a change in state vector will change the (predicted) observations.
As such the $\widetilde{H}$ matrix is dependent on the measurements being made (e.g. TDOA or other measurements), whereas the STM depends on the dynamics of the target being tracked, which in our case is a satellite in orbit around the earth. Because the motion of a satellite around the earth is nonlinear the STM we derive will not perfectly predict the future state, there will be some errors. Hence it may also be called linearized state transition matrix.

As a preparation for the 4D TDOA simulation tool several methods to generate a satellite STM were investigated, as explained below.

In [45] the difference quotient approximation is mentioned, which is conceptually simple. Take the initial state vector and propagate it to the time t_k through an orbit propagator of choice. Then we in turn apply a small change to each element of the initial state vector and this modified vector is then propagated to the time t_k through the same orbit propagator. By calculating the difference between the results of the propagated modified and unmodified initial state vectors the STM matrix can be derived. Note that this takes a significant amount of orbit propagation, which will introduce integration errors and require computational resources.
Alternatively, if we utilize orbital elements (rather than ECEF) then we can assume that the orbit is unperturbed, meaning only the mean motion varies in time. Then the transition matrix is the identity matrix except for one element describing the change in mean motion [45]. See Figure 67 below. Note that this also necessitates that the $\widetilde{H}$ matrix be expressed in orbital elements.

$$\boldsymbol{\Phi}_{\alpha}(t, t_0) = \begin{pmatrix} 1 & 0 & 0 & 0 & 0 & 0 \\ 0 & 1 & 0 & 0 & 0 & 0 \\ 0 & 0 & 1 & 0 & 0 & 0 \\ 0 & 0 & 0 & 1 & 0 & 0 \\ 0 & 0 & 0 & 0 & 1 & 0 \\ \frac{\partial M(t)}{\partial a(t_0)} & 0 & 0 & 0 & 0 & 1 \end{pmatrix},$$

where the only non-vanishing off-diagonal element is given by the term

$$\frac{\partial M(t)}{\partial a(t_0)} = -\frac{3}{2}\frac{n}{a}(t - t_0)$$

Figure 67: orbital-elements state transition matrix from time t to time t_0, reproduced from [45]*. Where a is the semi-major axis and n is the mean motion.*

The STM can also be calculated through derivation of the equation of motion, this was done in the 1965 paper by Goodyear [53] and the 1966 report by the same author [54]. This approach is much more conceptually complex.

A simpler version is used in [55] and a modified version is listed below:

$$\phi(k, k-t) = \begin{bmatrix} 1 & 0 & 0 & t & 0 & 0 \\ 0 & 1 & 0 & 0 & t & 0 \\ 0 & 0 & 1 & 0 & 0 & t \\ t*(3\mu x^2 r^{-5} - \mu r^{-3}) & t*3\mu xyr^{-5} & t*3\mu xzr^{-5} & 1 & 0 & 0 \\ t*3\mu yxr^{-5} & t*(3\mu y^2 r^{-5} - \mu r^{-3}) & t*3\mu yzr^{-5} & 0 & 1 & 0 \\ t*3\mu zxr^{-5} & t*3\mu zyr^{-5} & t*(3\mu z^2 r^{-5} - \mu r^{-3}) & 0 & 0 & 1 \end{bmatrix} \quad 8\text{-}4$$

Where:

k	End time
$k-t$	Start time
μ	Standard gravitational parameter
x, y, z	Target earth centred earth fixed coordinates x, y and z at time $k-t$
r	Norm of the target satellite earth centred earth fixed coordinates: $r = \sqrt{x^2+y^2+z^2}$
t	The time step of the STM. Or the time span it is propagating the state vector over. Note that a larger time span can be split into multiple shorter STM's: $\phi(t_2, t_0) = \phi(t_1, t_0) \times \phi(t_2, t_1)$

Note the STM is rewritten for clarity and two changes are made with respect to [55]. Firstly, part of the STM is explicitly multiplied with the time step (t). Furthermore in [55] submatrix shown below is transposed. This is assumed to be erroneous.

$$\begin{bmatrix} 3\mu x^2 r^{-5} - \mu r^{-3} & 3\mu xyr^{-5} & 3\mu xzr^{-5} \\ 3\mu yxr^{-5} & 3\mu y^2 r^{-5} - \mu r^{-3} & 3\mu yzr^{-5} \\ 3\mu zxr^{-5} & 3\mu zyr^{-5} & 3\mu z^2 r^{-5} - \mu r^{-3} \end{bmatrix}$$

As can be observed from the methods presented above there are many ways to generate STM's. It is highly recommended to analyze the impact of the batch size and the STM on the 4D TDOA simulation tool. Note that the ability to specify which STM method to use could be valuable feature of the 4D TDOA simulation tool. If we want to track a satellite to communicate with it, we need an STM generation method that is fast enough to ensure we can get an orbit estimate while the satellite is in view (so probably in a matter of minutes). But if we are analysis satellite orbits to, for example, try to measure the earth's atmosphere, we may be willing to have a slower but more accurate STM method.

8.3 Possible Features, Considerations and Additions to 4D TDOA

This section contains a large number of potential addition and features of the 4D TDOA code. This is not meant as an exhaustive "feature list". Rather it is intended to bring to the attention of the reader to a number of useful features and possible additions which may be pertinent to include in either the operational TDOA code or in the more advanced 4D TDOA simulation tool.

Add additional unknowns to the state vector

As explained in section 8.1 the 4D TDOA can solve for an initial state vector $(x, y, z, \dot{x}, \dot{y}, \dot{z})$. However, this state vector does not need to be limited to the target position and velocity but can also include aspects such as the target satellite ballistic coefficient. This coefficient is also know and B* and can be used to predict the effects of atmospheric drag on the target satellite [56]. The addition of this term would improve the capability of a SGP4 propagator to predict future satellite positions. Note that adding terms to the state-vector will require associated changes to the $\widetilde{H}$ and state transition matrices.

Another potential variable to add would be TEC (see section 6.1), this would allow the algorithm to estimate the TEC content from the measurement data. The TEC predicted could then be compared with publicly available TEC measurements.

Other potential additions to the state vector could be the ground station coordinates, should their positions be unknown. One potential complication of the TDOA system is dealing with a target satellite which is transmitting intermittently or who's onboard clock has drifted. We must be able to predict the observations that are generated for a certain initial state vector $(G(X_i^*))$ for this we must know the times at which the satellite transmits. This can be assumed to be known and implicitly included in the code. But this can also be treated as an unknown either by adding the transmission rate and start time to the state vector or by having each transmission time as an element in the state vector.

Sensor fusion

The approach presented in section 8.1 is not specific to TDOA, it can be applied to other tracking/detection techniques such as ranging, doppler, etc. In this case the $\widetilde{H}$ matrix would be calculated in a different manner as well as the predicted observations $(G(X_i^*))$, but the overall approach would remain the same.

And crucial it can be applied to different tracking techniques simultaneously. This opens the door to a sensor fusion approach, where many different types of measurements are used to track the satellite.

It is expected that adding doppler and differential doppler tracking capabilities to the ground stations would be relatively straightforward. Afterall each ground station is already receiving and recording each incoming

message. If we have 9 ground stations, we will then have 36 TDOA, 36 Differential doppler and 9 doppler measurements for a total of 81. For the rest of this chapter, we will continue to refer to the TDOA system, but may of the topic discussed could be applied to an alternate tracking/detection technique or sensor fusion approach.
Note that adding sensors to the TDOA system may also introduce additional unknowns in the state vector. For instance, when applying doppler knowing the initial transmission frequency is important. However, this can drift in time due to the target satellite clock drifting. But this can be corrected for by adding the transmission frequency (and it rate of change) as an unknown in the state vector.

Total electron content mitigation through doppler
The final system could mitigate for total electron content by utilizing doppler and/or differential doppler to generate a coarse estimate of the target satellite position. From this coarse position the signal delay due to TEC can be corrected for enabling TDOA or time of arrival tracking to be more accurate.
In this case the final system will have 4 stages:

1) The doppler and/or differential doppler quickly generate a rough state vector for the satellite (system error at this time may be +-1 km).
2) The TDOA and other systems refine the state vector using the rough state vector to correct for TEC (system error at the point of hand over $\leq$ 83 meters).
3) The optical system searches and finds the satellite (system error could be as low as mm level).
4) Identification/communication.
5) Data gathered in previous steps is used to improve the target satellite predicted orbit to make future acquisition and tracking easier.

Kalman filter and extended Kalman filter
The method proposed in section 8.1 is the so called “batch” method. It Is called this because it analyses a large “batch” of measurements simultaneously to predict the state vector. However, this method has some similarities with the so called Kalman filter or extended Kalman filter. Such as state transition matrices, prediction of observation, etc. It may be interesting to compare the performance of these algorithms.
In addition, there may be other advantages such as faster computation times or better synergy with the overall system.

Radio message analysis and simulation
One of the main factors in the performance of a TDOA system is the noise and measurement errors inherent in the interaction between the target satellite and the ground stations. As such it may be valuable to simulate the message transmission, propagation through space and the atmosphere, reception at the ground station and message detection. From this signal simulation the measurement errors could then be calculated. Note that this would make the measurement errors unique for each ground station and vary them in time as well as the signal path changes. This could also be used to generate the weight matrix, since we could predict the relative performance of each ground station.
And it could be used to better understand the interaction between the space and ground communication segments and the satellite orbit and how these affect the TDOA system accuracy.

Optical segment simulation
The optical segment is critical to the proposed overall tracking, identification (and communication) system. However, it was not the focus of this thesis. In future work it would be valuable to include the optical segment directly in the TDOA system simulation.
For example in [57] deals with the different methods to search a given volume by telescope (e.g. spiral method). But there are many other factors such as the observation time needed to detect the satellite, laser divergence, the field of view of the optical telescope, telescope slew rate, etc.
This can then be used to answer questions such as: when we should start searching with the telescope. If we give little time to the TDOA system before we start the optical search, we will have a less certain track on the target satellite but more time to search optically. In the opposite case we may spend so much time refining the

track through TDOA means that little time is left for identification and/or communication with the target satellite. These considerations are also related to the time required for identification and/or communication and the length of the orbital pass of the satellite. This case is of course simplified in reality we can refine the target satellite track through TDOA while searching for it with optically means. The question that then rises is how to integrate an optical search with a continually refining TDOA search.
Another consideration is that if this system proliferates, we may have situations where multiple target satellites are visible simultaneously and we have multiple optical ground stations. In this case the questions above become even more complex and important.

The influence of time
The main feature of the 4D TDOA system is that it has adds the element of time. This allows us to estimate the target satellite position in the future. But it also complicates matters.
Say we have a 4D TDOA system we can estimate the initial state vector this must then be propagated forward in time which induces inevitable errors.
Effectively we are always using "old" information to predict a future state, since the satellite messages must reach the ground stations, be processed, transmitted to a central location to generate TDOA measurements and run the chosen algorithm all these steps take and time. This is also why the computation time of the chosen algorithm matters, at some point refinements in the state vector will be negated by additional propagation errors.

Communication between the ground stations
This relates to the previous topic, the communication network between the ground stations will also play a role. Assuming we utilize the internet to connect the ground stations question such as the maximum data rate and upload and download pings will play a role in system performance and cost.

Improved clock accuracy
As explained in chapter 6) one of the important sources of measurement errors in TDOA system may be the clock accuracy of the ground stations. Should this be the case then timing synchronisation up to 2 nano seconds is possible [58] by detecting aircraft beacons, which contain the aircraft altitude and position and utilizing this information to synchronization the clocks of the ground stations. Other methods also exist including the publicly available White Rabbit project, which claims sub-nano second synchronization [59].

Cholesky
It is highly recommended to utilize Cholesky decomposition as described in section 7.2.2.1. Otherwise, it is probable that problems will occur such as a lack of convergence.

Prepare for implementation
The 4D TDOA simulation tool may be a very multifaceted program. But it will most probably closely match the final code to be used by the 4D TDOA tracking system. It is recommended to ensure that (part of) the 4D TDOA simulation tool can be reused as the 4D TDOA tracking system code. In this way the code can be tested and validated in the simulation tool and the development of the 4D TDOA tracking system should go faster.

Coordinate system
Broadly speaking one may use either Keplerian orbital elements (semi-major axis, eccentric, etc.) or ECEF or some other Cartesian coordinates. This choice will affect the implementation of the algorithm since it will affect the $\tilde{H}$ and STM matrices. It is highly recommended to carefully consider which coordinate system is most suited to the system under consideration.

In summary there are many features which are valuable to include in the future 4D TDOA simulation tool and 4D TDOA system. In this chapter an overview was given of some of these features to facilitate the future development of the code.

9) Conclusions

Satellite tracking is an ever more important aspect of space operations to enable (optical) communication, prevent collisions, etc. This thesis investigates two possible radio-based satellite tracking systems for implementation on the next TU Delft satellite. The main requirements of the tracking system are to achieve sufficient accuracy for communication, tracking and/or identification by a ground based optical system, by utilizing the inherent radio communications system of the target satellite. The ground segment of the proposed tracking system should be compatible with TU Delft resources.

The first research question is given below, the sub questions will be answered first:

1) Is phase interferometry, a radio-based tracking technology, applied to a cooperating spacecraft in low-earth orbit, a suitable technique to be used by TU Delft for the DelfiSpace program to improve the tracking accuracy?
   - 1A) What are the consequences with respect to the target satellite?
   - 1B) What are the consequences with respect to the ground station(s)?
   - 1C) What are the consequences with respect to the entire tracking system?

1A) What are the consequences with respect to the target satellite?
As elaborated in section 4.3.1 the design space is highly restricted and may require a high signal to noise ratio to be achieved by the satellite's communications system to meet the required tracking accuracy.

1B) What are the consequences with respect to the ground station(s)?
As covered in section 4.3.2 a phase interferometry ground station would not meet the requirements placed on the ground station(s).

1C) What are the consequences with respect to the entire tracking system?
A phase interferometry system implementation is not a practical solution for implementation by TU Delft. This is due to the correlation being performed in the radio frequency domain necessitating high frequency measurements and consequently high-volume data transfers between the ground stations.

In summary for the first research question, phase interferometry is not a suitable technique for the TU Delft DELFI-X program.

The second research question is given below, the sub questions will be answered first:

2) Is Time Difference Of Arrival (TDOA), a radio-based tracking technologies applied to cooperating spacecraft in low-earth orbit a suitable technique to be used by TU Delft for the DelfiSpace program?
   - 2A) What are the consequences of TDOA with respect to the target satellite?
   - 2B) What are the consequences of TDOA with respect to the ground station(s)?
   - 2C) What are the consequences of TDOA with respect to the entire tracking system?

2A) What are the consequences of TDOA with respect to the target satellite?
No obstacles were identified in integrating the satellite communications systems with a TDOA tracking system (see sections 5.3.2 and 7.4.3).

2B) What are the consequences of TDOA with respect to the ground station(s)?
The ground stations geometric configuration can be the dominant factor in the TDOA system performance. The baseline (distance between the ground stations) is another critical aspect of the TDOA system

performance, as is the number of ground stations (minimum four ground stations are required to position a point in 3D space). The ground stations also play a role in the noise levels of the TDOA measurements. As such the successful implementation of a TDOA tracking system will be heavily dependent on the ground stations. See section 5.3.2 for a more detailed discussion.

2C) What are the consequences of TDOA with respect to the entire tracking system?
The system performance is mostly dependent on the ground stations, not the satellite. Note that the satellite communications system does play a role in the noise levels of the TDOA measurements. In other words, the characteristics of the satellite communication system and the ground stations must conform to one another. See chapter 6) and section 7.4.4.
It was furthermore found that by utilizing 25 ground stations in a 1000-km baseline square configuration, Delfi-PQ can be tracked with the required accuracy in 18% of the coverage area.

In summary for the second research question, TDOA is considered a promising system for further research and development by TU Delft as part of the DelfiSpace program. We have determined that the accuracy, satellite, and ground station requirements can be met using certain combinations of ground stations number, geometry, noise level, and baseline size.

As future work it is recommended to develop a 4D TDOA simulation tool (see chapter 8). The primary feature of this tool is the ability to utilize measurements taken at different times to better estimate the target satellite position and velocity. Recommended additional features are the ability to synergize measurements taken by different types of sensors (sensor fusion), as well as the estimation of the satellite ballistic (drag) coefficient to predict the satellite orbit more accurately. Features such as a full simulation of the radio message propagation and the optical segment can also be added. For an extensive elaboration, see chapter 8).

Bibliography

[1] R. Wang, J. Liu, and Q. M. Zhang, “Propagation errors analysis of TLE data,” *Adv. Sp. Res.*, vol. 43, no. 7, pp. 1065–1069, 2009, doi: 10.1016/j.asr.2008.11.017.

[2] T. Nachtergaele, “Situational Awareness An overview of surveillance and tracking systems,” Huldenberg, 2021.

[3] TNO, “SATELLITE COMMUNICATION,” 2020. https://www.tno.nl/en/focus-areas/industry/roadmaps/space-scientific-instrumentation/satellite-communication/ (accessed Jan. 11, 2022).

[4] NA, “Spacecraft tracking implications on operations and the design of small satellites,” 2018. Accessed: Jan. 25, 2021. [Online]. Available: https://nebula.esa.int/content/spacecraft-tracking-implications-operations-and-design-small-satellites-0.

[5] J. McGarry, “An Overview of Satellite Laser Ranging (SLR),” 2012. [Online]. Available: http://space-geodesy.nasa.gov/docs/2012/OverviewSLR_mcgarry_120606.pdf.

[6] L. Boldt-Christmas and esa, “Low Earth orbit,” 2020. https://www.esa.int/ESA_Multimedia/Images/2020/03/Low_Earth_orbit (accessed Dec. 10, 2021).

[7] “GRAVES, the 1st European space surveillance system.” https://www.onera.fr/en/news/graves-the-1st-european-space-surveillance-system (accessed Mar. 22, 2021).

[8] Lockheed Martin Corporation, “Space Fence.” https://www.lockheedmartin.com/en-us/products/space-fence.html (accessed Mar. 22, 2021).

[9] TU Delft, “Facilities.” https://www.tudelft.nl/lr/organisatie/afdelingen/space-engineering/space-systems-engineering/facilities (accessed Jan. 16, 2021).

[10] “SPACE SITUATIONAL AWARENESS (SSA).” https://www.satcen.europa.eu/page/ssa (accessed Mar. 30, 2021).

[11] “New ESA-UNOOSA debris infographics and podcast,” 2021. https://www.esa.int/Safety_Security/Space_Debris/New_ESA-UNOOSA_debris_infographics_and_podcast (accessed Mar. 30, 2021).

[12] T. S. Kelso, “Analysis of the Iridium 33-Cosmos 2251 collision,” [Online]. Available: https://celestrak.com/publications/AAS/09-368/AAS-09-368.pdf.

[13] A. Abraham, “GPS TRANSPONDERS FOR SPACE TRAFFIC MANAGEMENT CENTER FOR SPACE POLICY AND STRATEGY,” 2018. Accessed: Feb. 05, 2021. [Online]. Available: www.aerospace.org/policy.

[14] E. Gregersen, “Kinetic energy.” https://www.britannica.com/science/kinetic-energy (accessed Apr. 20, 2021).

[15] “The cost of avoiding collision.” p. 1, 2020, [Online]. Available: https://www.esa.int/ESA_Multimedia/Images/2021/02/The_cost_of_avoiding_collision.

[16] “ESA ’ s Annual Space Environment Report,” 2020. [Online]. Available: https://www.sdo.esoc.esa.int/environment_report/Space_Environment_Report_latest.pdf.

[17] M. Y. Huang, B. Hunt, and D. Mosher, “What Elon Musk’s 42,000 Starlink satellites could do for — and to — planet Earth,” *Insider*, Mar. 04, 2021.

[18] A. BOYLE, “Critics take aim at SpaceX’s Starlink, Amazon’s Project Kuiper and other satellite constellations,” *GeekWire*, Mar. 11, 2021.

[19] S. Clark, “SpaceX smashes record with launch of 143 small satellites,” *Spaceflight now*, Jan. .

[20] I. Ploom, “Analysis of variations in orbital parameters of CubeSats,” UNIVERSITY OF TARTU, 2014.

[21] “Measuring the Economic Impact of the Space Sector: Key Indicators and Options to Improve Data,” RIYADH, 2020. [Online]. Available: http://www.oecd.org/sti/inno/space-forum/measuring-economic-impact-space-sector.pdf.

[22] S. Merkowitz, “SGP: Space Geodesy Project, What is DORIS?” https://space-geodesy.nasa.gov/techniques/DORIS.html (accessed Mar. 23, 2021).
[23] H. J. Kramer, “DORIS Tracking System.” https://directory.eoportal.org/web/eoportal/satellite-missions/d/doris (accessed Mar. 23, 2021).
[24] G. Cohen *et al.*, “Event-based Sensing for Space Situational Awareness,” *J. Astronaut. Sci.*, vol. 66, no. 2, pp. 125–141, 2019, doi: 10.1007/s40295-018-00140-5.
[25] S. Kawase, *Radio Interferometry and Satellite Tracking*. Norwood: Artech House, 2012.
[26] “9.0 Communications,” 2021. https://www.nasa.gov/smallsat-institute/sst-soa/communications (accessed Nov. 10, 2021).
[27] S. Speretta, “DPQ-TUD-BU-04 [1.2] Delfi-PQ Link Budget,” 2020.
[28] ASTRON, “LOFAR,” 2021. https://www.astron.nl/telescopes/lofar/ (accessed Dec. 28, 2021).
[29] D. Bartlett, *Essentials of Positioning and Location Technology*, 2013th ed. Cambridge: Cambridge University Press, 2013.
[30] G. Iraci, C. Gnam, and D. J. Crassidis, “SSC18- PII - 19 An Open Source Radio for Low Cost Small Satellite Ranging,” in *32nd Annual AIAA/USU Conference on Small Satellites*, 2018, p. 8, [Online]. Available: https://digitalcommons.usu.edu/cgi/viewcontent.cgi?article=4211&context=smallsat.
[31] “TOTAL ELECTRON CONTENT,” *SPACE WEATHER PREDICTION CENTER NATIONAL OCEANIC AND ATMOSPHERIC ADMINISTRATION*, 2021. https://www.swpc.noaa.gov/phenomena/total-electron-content (accessed Nov. 23, 2021).
[32] R. Acharya, “Chapter 5 - Ionospheric impairments: Measurement and mitigation,” in *Satellite Signal Propagation, Impairments and Mitigation*, 2017th ed., C. Bolger, Ed. London: Elsevier Ltd., 2017, pp. 127–157.
[33] “CTIPE TOTAL ELECTRON CONTENT FORECAST,” *SPACE WEATHER PREDICTION CENTER NATIONAL OCEANIC AND ATMOSPHERIC ADMINISTRATION*, 2021. https://www.swpc.noaa.gov/products/ctipe-total-electron-content-forecast (accessed Nov. 23, 2021).
[34] European Space Agency, “Transionospheric Radio Link - Near-real-time TEC maps,” 2021. https://swe.ssa.esa.int/tio_tcr (accessed Dec. 29, 2021).
[35] “Ionospheric Correction Algorithm for Galileo Single Frequency Users,” 2016. [Online]. Available: https://galileognss.eu/wp-content/uploads/2020/08/Galileo_Ionospheric_Model_v1.2.pdf.
[36] C. Wolff, “Radars Accuracy.” https://www.radartutorial.eu/01.basics/Radars Accuracy.en.html (accessed Nov. 13, 2021).
[37] K. Andrews, J. Hamkins, S. Shambayati, and V. Vilnrotter, “Telemetry-based ranging,” *IEEE Aerosp. Conf. Proc.*, p. 16, 2010, doi: 10.1109/AERO.2010.5446926.
[38] J. R. Wertz, H. F. Meissinger, L. K. Newman, and G. N. Smit, *Orbit & Constellation Design & Management*, 2009th-secon ed. Hawtorne: Microcosm, Inc., 2009.
[39] National Coordination Office for Space-Based Positioning, Navigation, and Timing, “GPS Accuracy,” *GPS.GOV Official U.S. government information about the Global Positioning System (GPS) and related topics*, 2021. https://www.gps.gov/systems/gps/performance/accuracy/ (accessed Nov. 23, 2021).
[40] M. Brodie, “The Empirical Rule for Normal Distributions,” 2014. https://demonstrations.wolfram.com/TheEmpiricalRuleForNormalDistributions/ (accessed Nov. 23, 2021).
[41] F. M. Dekking, C. Kraaikamp, H. P. Lopuhaä, and L. E. Meester, “11.2 Sums of continous random variables,” in *A Modern Introduction to Probability and Statistics, Understanding Why and How*, 2005th, firs ed., Delft: Springer, London, 2005, pp. 154–166.
[42] H. C. So, “Chapter 2: SOURCE LOCALIZATION: ALGORITHMS AND ANALYSIS,” in *HANDBOOK OF POSITION LOCATION Theory, Practice, and Advances*, 2012th ed., S. A. (REZA) ZEKAVAT and R. M. BUEHRER, Eds. Singapore: IEEE PRESS, WILEY, JOHN WILEY & SONS, INC., PUBLICATION, 2012, pp. 25–65.

[43] MathWorks, “elevation,” 2021. https://nl.mathworks.com/help/comm/ref/txsite.elevation.html (accessed Dec. 29, 2021).
[44] G. Timár and G. Molnár, *MAP GRIDS AND DATUMS*. Budapest, 2013.
[45] O. Montenbruck and E. Gill, *Satellite Orbits: Models, Methods, and Applications*, Kindle ed. Heidelberg, Springer Berlin, 2012.
[46] B. D. Tapley, B. E. Schutz, and G. H. Born., *Statistical Orbit Determination*, 2004th ed. Burlington: Elsevier Academic Press, 2004.
[47] U. Tamer, “TDOA simulation.” 2021, [Online]. Available: https://www.mathworks.com/matlabcentral/fileexchange/70146-tdoa-simulation.
[48] Benoit and Cholesky, “Note Sur Une Méthode de Résolution des équations Normales Provenant de L’Application de la Méthode des Moindres Carrés a un Système D’équations Linéaires en Nombre Inférieur a Celui des Inconnues. — Application de la Méthode a la Résolution D’un Système D,” *Bull. Géodésique*, vol. 2, no. 1, pp. 67–77, 1924, [Online]. Available: https://link.springer.com/article/10.1007%2FBF03031308.
[49] D. Q. Nykamp, “‘Distance from point to plane.,’” *From Math Insight.* http://mathinsight.org/distance_point_plane (accessed Dec. 07, 2021).
[50] MathWorks, “pca Principal component analysis of raw data,” *MathWorks Accelerating the pace of engineering and science*. https://nl.mathworks.com/help/stats/pca.html (accessed Dec. 09, 2021).
[51] E. W. Weisstein, “Rotation Matrix,” *From MathWorld--A Wolfram Web Resource.* https://mathworld.wolfram.com/RotationMatrix.html (accessed Dec. 09, 2021).
[52] Reinaldo Perez, “Chapter 1 - Introduction to Satellite Systems and Personal Wireless Communications,” in *Wireless Communications Design Handbook*, R. Perez, Ed. San Diego: Elsevier, 1998, pp. 1–30.
[53] W. H. Goodyear, “Completely general closed-form solution for coordinates and partial derivative of the two-body problem,” *Astron. J.*, vol. 70, pp. 189–192, 1965, doi: 10.1086/109713.
[54] W. H. Goodyear, “A GENERAL METHOD FOR THE COMPUTATION OF CARTESIAN COORDINATES AND PARTIAL DERIVATIVES OF THE TWO-BODY PROBLEM,” Greenbelt, 1966. [Online]. Available: https://ntrs.nasa.gov/api/citations/19660027556/downloads/19660027556.pdf.
[55] S. A. G. Sandip Tukaram Aghav, “SIMPLIFIED ORBIT DETERMINATION ALGORITHM FOR LOW EARTH ORBIT SATELLITES USING SPACEBORNE GPS NAVIGATION SENSOR,” *Artif. Satell.*, vol. vol.49, no, pp. 81–99, 2014, doi: https://doi.org/10.2478/arsa-2014-0007.
[56] D. T. S. Kelso, “Frequently Asked Questions: Two-Line Element Set Format,” 2019. https://celestrak.com/columns/v04n03/ (accessed Jan. 04, 2021).
[57] H. Kaushal, V. K. Jain, and S. Kar, *Free Space Optical Communication*, 2017th ed. New Delhi: Springer (India) Pvt. Ltd., 2017.
[58] A. Aab and et. al., “Nanosecond-level time synchronization of autonomous radio detector stations for extensive air showers,” *J. Instrum.*, vol. 11, 2016, doi: https://doi.org/10.1088/1748-0221/11/01/P01018.
[59] M. Lipinski, “White Rabbit,” 2021. https://ohwr.org/project/white-rabbit/wikis/home.

Appendix A

Identifiying information	batch_name [-]	"V&V and	"V&V and	"V&V and	"V&V and	"V&V and	"V&V and	"V&V and	"V&V and	"V&V and	"V&V and	"V&V and	"V&V and	"V&V and	"V&V and	"V&V and	"V&V and	"V&V and	"V&V and	"V&V and	"V&V and	"V&V and	"V&V and	"V&V and	"V&V and	"V&V and	"V&V and	"V&V and re
	run_name [-]	"baseline "	"lat step 5 to 10"	"long step 5 to 10"	"alitude 250km"	"alitude 1000km"	"noise matrtix length"	"noise matrtix length"	"noise time"	"noise time"	"noise time"	"noise time"	"referenc e area"	"rng seed"	"max steps"	"max step size"	"tolleran ce"	"optical grnd location"	"optical grnd location"	"optical grnd altitude"	"optical grnd view"	"optical grnd view"	"9 grnds, 10-km"	"9 grnds, 1000-km"	"9 grnds, 100-km, 0 DEG"	"4 GRNDS"	"16 GRNDS"	"noise time"
	date [dd/mm/yyyy]	#########	########	########	########	########	########	########	########	########	########	########	########	########	########	########	########	########	########	########	########	########	########	########	########	########	########	15/12/2021
Location of the results	filename of excel with results [-]	"C:\Users\	"C:\Users	"C:\Users	"C:\Users	"C:\Users	"C:\Users	"C:\Users	"C:\Users	"C:\Users	"C:\Users	"C:\Users	"C:\Users	"C:\Users	"C:\Users	"C:\Users	"C:\Users	"C:\Users	"C:\Users	"C:\Users	"C:\Users	"C:\Users	"C:\Users	"C:\Users	"C:\Users	"C:\Users	"C:\Users	"C:\Users\ti
	tab of the excel sheet containing the results [-]	1	2	3	4	5	6	7	8	9	10	11	12	13	14	15	16	17	18	19	20	21	22	23	24	25	26	27
Targets population	latitude_step_size [deg]	5	10	5	5	5	5	5	5	5	5	5	5	5	5	5	5	5	5	5	5	5	5	5	5	5	5	5
	longitude_step_size [deg]	5	5	10	5	5	5	5	5	5	5	5	5	5	5	5	5	5	5	5	5	5	5	5	5	5	5	5
	altitude [m]	500000	500000	500000	250000	1000000	500000	500000	500000	500000	500000	500000	500000	500000	500000	500000	500000	500000	500000	500000	500000	500000	500000	500000	500000	500000	500000	500000
noise matrix	noise_matrix_length [rows]	1000	1000	1000	1000	1000	500	2000	1000	1000	1000	1000	1000	1000	1000	1000	1000	1000	1000	1000	1000	1000	1000	1000	1000	1000	1000	1000
	noise_time [sec]	2.8E-08	2.8E-08	2.8E-08	2.8E-08	2.8E-08	2.8E-08	2.8E-08	2.36E-06	2.36E-07	2.8E-08	1.52E-08	2.8E-08	2.8E-08	2.8E-08	2.8E-08	2.8E-08	2.8E-08	2.8E-08	2.8E-08	2.8E-08	2.8E-08	2.8E-08	2.8E-08	2.8E-08	2.8E-08	2.8E-08	0
	reference_area [m^2]	21642	21642.43	21642.43	21642.43	21642.43	21642.43	21642.43	21642.43	21642.43	21642.43	21642.43	2164.243	21642.43	21642.43	21642.43	21642.43	21642.43	21642.43	21642.43	21642.43	21642.43	21642.43	21642.43	21642.43	21642.43	21642.43	21642.4318
	rng seed	1	1	1	1	1	1	1	1	1	1	1	1	2	1	1	1	1	1	1	1	1	1	1	1	1	1	1
LLS solver inputs	max_steps [-]	100	100	100	100	100	100	100	100	100	100	100	100	100	50	50	50	100	50	50	50	50	50	50	50	50	50	50
	max_step_size [m]	5000	5000	5000	5000	5000	5000	5000	5000	5000	5000	5000	5000	5000	5000	500	5000	5000	5000	500	5000	5000	5000	5000	5000	5000	5000	5000
	tolerance [m]	0.01	0.01	0.01	0.01	0.01	0.01	0.01	0.01	0.01	0.01	0.01	0.01	0.01	0.01	0.01	1	0.01	0.01	0.01	0.01	0.01	0.01	0.01	0.01	0.01	0.01	0.01
Accuracy_groundstation_lla	lat [deg]	50	50	50	50	50	50	50	50	50	50	50	50	50	50	50	50	-50	50	50	50	50	50	50	50	50	50	50
	long [deg]	5	5	5	5	5	5	5	5	5	5	5	5	5	5	5	5	5	10	5	5	5	5	5	5	5	5	5
	alt [m]	0	0	0	0	0	0	0	0	0	0	0	0	0	0	0	0	0	0	10000	0	0	0	0	0	0	0	0
	Accuracy Groundstations min elevation [deg]	-90	-90	-90	-90	-90	-90	-90	-90	-90	-90	-90	-90	-90	-90	-90	-90	-90	-90	-90	10	89	-90	-90	-90	-90	-90	-90
	Number of groundstations [-]	9	9	9	9	9	9	9	9	9	9	9	9	9	9	9	9	9	9	9	9	9	9	9	9	4	16	9
Groundstations_lla	lat [deg]	50	50	50	50	50	50	50	50	50	50	50	50	50	50	50	50	50	50	50	50	50	50	50	50	50.44966	50.22483	50.2248304
	long [deg]	5	5	5	5	5	5	5	5	5	5	5	5	5	5	5	5	5	5	5	5	5	5	5	5	5.449661	5.22483	5.2248304
	alt [m]	20	20	20	20	20	20	20	20	20	20	20	20	20	20	20	20	20	20	20	20	20	20	20	20	20	20	20
	min elevation angle [deg]	15	15	15	15	15	15	15	15	15	15	15	15	15	15	15	15	15	15	15	15	15	15	15	0	15	15	15
	lat [deg]	50.449661	50.44966	50.44966	50.44966	50.44966	50.44966	50.44966	50.44966	50.44966	50.44966	50.44966	50.44966	50.44966	50.44966	50.44966	50.44966	50.44966	50.44966	50.44966	50.44966	50.44966	50.04497	54.49661	50.44966	49.55034	49.77517	49.7751696
	long [deg]	5.4496608	5.449661	5.449661	5.449661	5.449661	5.449661	5.449661	5.449661	5.449661	5.449661	5.449661	5.449661	5.449661	5.449661	5.449661	5.449661	5.449661	5.449661	5.449661	5.449661	5.449661	5.044966	9.496608	5.449661	5.449661	5.22483	5.2248304
	alt [m]	20	20	20	20	20	20	20	20	20	20	20	20	20	20	20	20	20	20	20	20	20	20	20	20	20	20	20
	min elevation angle [deg]	15	15	15	15	15	15	15	15	15	15	15	15	15	15	15	15	15	15	15	15	15	15	15	0	15	15	15
	lat [deg]	49.550339	49.55034	49.55034	49.55034	49.55034	49.55034	49.55034	49.55034	49.55034	49.55034	49.55034	49.55034	49.55034	49.55034	49.55034	49.55034	49.55034	49.55034	49.55034	49.55034	49.55034	49.95503	45.50339	49.55034	50.44966	50.22483	50.2248304
	long [deg]	5.4496608	5.449661	5.449661	5.449661	5.449661	5.449661	5.449661	5.449661	5.449661	5.449661	5.449661	5.449661	5.449661	5.449661	5.449661	5.449661	5.449661	5.449661	5.449661	5.449661	5.449661	5.044966	9.496608	5.449661	4.550339	4.77517	4.7751696
	alt [m]	20	20	20	20	20	20	20	20	20	20	20	20	20	20	20	20	20	20	20	20	20	20	20	20	20	20	20
	min elevation angle [deg]	15	15	15	15	15	15	15	15	15	15	15	15	15	15	15	15	15	15	15	15	15	15	15	0	15	15	15
	lat [deg]	50.449661	50.44966	50.44966	50.44966	50.44966	50.44966	50.44966	50.44966	50.44966	50.44966	50.44966	50.44966	50.44966	50.44966	50.44966	50.44966	50.44966	50.44966	50.44966	50.44966	50.44966	50.04497	54.49661	50.44966	49.55034	49.77517	49.7751696
	long [deg]	4.5503392	4.550339	4.550339	4.550339	4.550339	4.550339	4.550339	4.550339	4.550339	4.550339	4.550339	4.550339	4.550339	4.550339	4.550339	4.550339	4.550339	4.550339	4.550339	4.550339	4.550339	4.955034	0.503392	4.550339	4.550339	4.77517	4.7751696
	alt [m]	20	20	20	20	20	20	20	20	20	20	20	20	20	20	20	20	20	20	20	20	20	20	20	20	20	20	20
	min elevation angle [deg]	15	15	15	15	15	15	15	15	15	15	15	15	15	15	15	15	15	15	15	15	15	15	15	0	15	15	15
	lat [deg]	49.550339	49.55034	49.55034	49.55034	49.55034	49.55034	49.55034	49.55034	49.55034	49.55034	49.55034	49.55034	49.55034	49.55034	49.55034	49.55034	49.55034	49.55034	49.55034	49.55034	49.55034	49.95503	45.50339	49.55034		50.44966	50.4496608
	long [deg]	4.5503392	4.550339	4.550339	4.550339	4.550339	4.550339	4.550339	4.550339	4.550339	4.550339	4.550339	4.550339	4.550339	4.550339	4.550339	4.550339	4.550339	4.550339	4.550339	4.550339	4.550339	4.955034	0.503392	4.550339		5.22483	5.2248304
	alt [m]	20	20	20	20	20	20	20	20	20	20	20	20	20	20	20	20	20	20	20	20	20	20	20	20		20	20
	min elevation angle [deg]	15	15	15	15	15	15	15	15	15	15	15	15	15	15	15	15	15	15	15	15	15	15	15	0		15	15
	lat [deg]	50	50	50	50	50	50	50	50	50	50	50	50	50	50	50	50	50	50	50	50	50	50	50	50		50.44966	50.4496608
	long [deg]	5.4496608	5.449661	5.449661	5.449661	5.449661	5.449661	5.449661	5.449661	5.449661	5.449661	5.449661	5.449661	5.449661	5.449661	5.449661	5.449661	5.449661	5.449661	5.449661	5.449661	5.449661	5.044966	9.496608	5.449661		4.77517	4.7751696
	alt [m]	20	20	20	20	20	20	20	20	20	20	20	20	20	20	20	20	20	20	20	20	20	20	20	20		20	20
	min elevation angle [deg]	15	15	15	15	15	15	15	15	15	15	15	15	15	15	15	15	15	15	15	15	15	15	15	0		15	15
	lat [deg]	50	50	50	50	50	50	50	50	50	50	50	50	50	50	50	50	50	50	50	50	50	50	50	50		49.55034	49.5503392
	long [deg]	4.5503392	4.550339	4.550339	4.550339	4.550339	4.550339	4.550339	4.550339	4.550339	4.550339	4.550339	4.550339	4.550339	4.550339	4.550339	4.550339	4.550339	4.550339	4.550339	4.550339	4.550339	4.955034	0.503392	4.550339		5.22483	5.2248304
	alt [m]	20	20	20	20	20	20	20	20	20	20	20	20	20	20	20	20	20	20	20	20	20	20	20	20		20	20
	min elevation angle [deg]	15	15	15	15	15	15	15	15	15	15	15	15	15	15	15	15	15	15	15	15	15	15	15	45		15	15
	lat [deg]	50.449661	50.44966	50.44966	50.44966	50.44966	50.44966	50.44966	50.44966	50.44966	50.44966	50.44966	50.44966	50.44966	50.44966	50.44966	50.44966	50.44966	50.44966	50.44966	50.44966	50.44966	50.04497	54.49661	50.44966		49.55034	49.5503392
	long [deg]	5	5	5	5	5	5	5	5	5	5	5	5	5	5	5	5	5	5	5	5	5	5	5	5		4.77517	4.7751696
	alt [m]	20	20	20	20	20	20	20	20	20	20	20	20	20	20	20	20	20	20	20	20	20	20	20	20		20	20
	min elevation angle [deg]	15	15	15	15	15	15	15	15	15	15	15	15	15	15	15	15	15	15	15	15	15	15	15	0		15	15
	lat [deg]	49.550339	49.55034	49.55034	49.55034	49.55034	49.55034	49.55034	49.55034	49.55034	49.55034	49.55034	49.55034	49.55034	49.55034	49.55034	49.55034	49.55034	49.55034	49.55034	49.55034	49.55034	49.95503	45.50339	49.55034		50.22483	50.2248304
	long [deg]	5	5	5	5	5	5	5	5	5	5	5	5	5	5	5	5	5	5	5	5	5	5	5	5		5.449661	5.4496608
	alt [m]	20	20	20	20	20	20	20	20	20	20	20	20	20	20	20	20	20	20	20	20	20	20	20	20		20	20
	min elevation angle [deg]	15	15	15	15	15	15	15	15	15	15	15	15	15	15	15	15	15	15	15	15	15	15	15	0		15	15
																											49.77517	
																											5.449661	
																											20	
																											15	
																											50.22483	
																											4.550339	
																											20	
																											15	
																											49.77517	
																											4.550339	
																											20	
																											15	
																											50.44966	
																											5.449661	
																											20	
																											15	
																											49.55034	
																											5.449661	
																											20	
																											15	
																											50.44966	
																											4.550339	
																											20	
																											15	
																											49.55034	
																											4.550339	
																											20	
																											15	

Appendix B

batch_name [-]	full VS partial	full VS partial
run_name [-]	full equations 9-grnds 1000km	partial equations 9-grnds 1000km
date [dd/mm/yyyy]	########	########
filename of excel with results [-]	C:\Users\timna\OneDrive\Desktop\thesis\thesis writing and final code\code thesis writing\Matlab excel sheets OUTPUTS\OUTPUTS_5.xlsx	C:\Users\timna\OneDrive\Desktop\thesis\thesis writing and final code\code thesis writing\Matlab excel sheets OUTPUTS\OUTPUTS_5.xlsx
tab of the excel sheet containing the results [-]	1	2
latitude_step_size [deg]	5	5
longitude_step_size [deg]	5	5
altitude [m]	500000	500000
noise_matrix_length [rows]	1000	1000
noise_time [sec]	2.8E-08	2.8E-08
reference_area [m^2]	21642.43	21642.43
rng seed	1	1
max_steps [-]	100	100
max_step_size [m]	5000	5000
tolerance [m]	0.01	0.01
lat [deg]	50	50
long [deg]	5	5
alt [m]	0	0
Accuracy Groundstations min elevation [deg]	-90	-90
Number of groundstations [-]	9	9
lat [deg]	50	50
long [deg]	5	5
alt [m]	20	20
min elevation angle [deg]	15	15
etc.	54.49661	54.49661
	9.496608	9.496608
	20	20
	15	15
	45.50339	45.50339
	9.496608	9.496608
	20	20
	15	15

	54.49661	54.49661
	0.503392	0.503392
	20	20
	15	15
	45.50339	45.50339
	0.503392	0.503392
	20	20
	15	15
	50	50
	9.496608	9.496608
	20	20
	15	15
	50	50
	0.503392	0.503392
	20	20
	15	15
	54.49661	54.49661
	5	5
	20	20
	15	15
	45.50339	45.50339
	5	5
	20	20
	15	15

batch_name [-]	**"full VS partial**	**"full VS partial**	**"full VS partial**	**"full VS partial**	**"full VS partial**	**"full VS partial**
run_name [-]	"full, baseline, delft centered 100 km - 4 grnds"	"full, baseline, delft centered 100 km - 25 grnds"	"partial, baseline, delft centered 100 km - 4 grnds"	"partial, baseline, delft centered 100 km - 25 grnds"	"full, baseline, delft centered 100 km - 9grnds"	"partial, baseline, delft centered 100 km -9grnds"
date [dd/mm/yyyy]	**30/12/2021**	**30/12/2021**	**30/12/2021**	**30/12/2021**	**30/12/2021**	**30/12/2021**
filename of excel with results [-]	C:\Users\timna\OneDrive\Desktop\thesis\thesis writing and final code\code thesis writing\Matla	**C:\Users\timna\OneDrive\Desktop\thesis\thesis writing and final code\code thesis writing\Matl**	**C:\Users\timna\OneDrive\Desktop\thesis\thesis writing and final code\code thesis writing\Matl**	**C:\Users\timna\OneDrive\Desktop\thesis\thesis writing and final code\code thesis writing\Matl**	**C:\Users\timna\OneDrive\Desktop\thesis\thesis writing and final code\code thesis writing\Matl**	**C:\Users\timna\OneDrive\Desktop\thesis\thesis writing and final code\code thesis writing\Matl**

	b excel sheets OUTPUTS\OUTPUTS_7.xlsx	**ab excel sheets OUTPUTS\OUTPUTS_7.xlsx**	**ab excel sheets OUTPUTS\OUTPUTS_7.xlsx**	**ab excel sheets OUTPUTS\OUTPUTS_7.xlsx**	**ab excel sheets OUTPUTS\OUTPUTS_7.xlsx**	**ab excel sheets OUTPUTS\OUTPUTS_7.xlsx**
tab of the excel sheet containing the results [-]	**1**	**2**	**3**	**4**	**6**	**7**
latitude_step_size [deg]	**5**	**5**	**5**	**5**	**5**	**5**
longitude_step_size [deg]	**5**	**5**	**5**	**5**	**5**	**5**
altitude [m]	**500000**	**500000**	**500000**	**500000**	**500000**	**500000**
noise_matrix_length [rows]	**1000**	**1000**	**1000**	**1000**	**1000**	**1000**
noise_time [sec]	2.8E-08	2.8E-08	2.8E-08	2.8E-08	2.8E-08	2.8E-08
reference_area [m^2]	**21642.4318**	**21642.4318**	**21642.4318**	**21642.4318**	**21642.4318**	**21642.4318**
rng seed	**1**	**1**	**1**	**1**	**1**	**1**
max_steps [-]	100	100	100	100	100	100
max_step_size [m]	5000	5000	5000	5000	5000	5000

tolerance [m]	**0.01**	**0.01**	**0.01**	**0.01**	**0.01**	**0.01**
lat [deg]	**51.9900937**	**51.9900937**	**51.9900937**	**51.9900937**	**51.9900937**	**51.9900937**
long [deg]	**4.37515161**	**4.37515161**	**4.37515161**	**4.37515161**	**4.37515161**	**4.37515161**
alt [m]	**20**	**20**	**20**	**20**	**20**	**20**
Accuracy Groundstations min elevation [deg]	**-90**	**-90**	**-90**	**-90**	**-90**	**-90**
Number of groundstations [-]	4	25	4	25	9	9
lat [deg]	52.4397545	51.5404329	52.4397545	51.5404329	51.9900937	51.9900937
long [deg]	4.82481241	3.92549081	4.82481241	3.92549081	4.37515161	4.37515161
alt [m]	20	20	20	20	20	20
min elevation angle [deg]	15	15	15	15	15	15
etc.	51.5404329	51.7652633	51.5404329	51.7652633	52.4397545	52.4397545
	4.82481241	3.92549081	4.82481241	3.92549081	4.82481241	4.82481241
	20	20	20	20	20	20
	15	15	15	15	15	15
	52.4397545	51.9900937	52.4397545	51.9900937	51.5404329	51.5404329
	3.92549081	3.92549081	3.92549081	3.92549081	4.82481241	4.82481241
	20	20	20	20	20	20
	15	15	15	15	15	15
	51.5404329	52.2149241	51.5404329	52.2149241	52.4397545	52.4397545
	3.92549081	3.92549081	3.92549081	3.92549081	3.92549081	3.92549081
	20	20	20	20	20	20
	15	15	15	15	15	15
		52.4397545		52.4397545	51.5404329	51.5404329
		3.92549081		3.92549081	3.92549081	3.92549081
		20		20	20	20

		15		15	15	15
		51.5404329		51.5404329	51.9900937	51.9900937
		4.15032121		4.15032121	4.82481241	4.82481241
		20		20	20	20
		15		15	15	15
		51.7652633		51.7652633	51.9900937	51.9900937
		4.15032121		4.15032121	3.92549081	3.92549081
		20		20	20	20
		15		15	15	15
		51.9900937		51.9900937	52.4397545	52.4397545
		4.15032121		4.15032121	4.37515161	4.37515161
		20		20	20	20
		15		15	15	15
		52.2149241		52.2149241	51.5404329	51.5404329
		4.15032121		4.15032121	4.37515161	4.37515161
		20		20	20	20
		15		15	15	15
		52.4397545		52.4397545		
		4.15032121		4.15032121		
		20		20		
		15		15		
		51.5404329		51.5404329		
		4.37515161		4.37515161		
		20		20		
		15		15		
		51.7652633		51.7652633		
		4.37515161		4.37515161		
		20		20		
		15		15		
		51.9900937		51.9900937		
		4.37515161		4.37515161		
		20		20		
		15		15		
		52.2149241		52.2149241		
		4.37515161		4.37515161		
		20		20		
		15		15		
		52.4397545		52.4397545		
		4.37515161		4.37515161		
		20		20		
		15		15		
		51.5404329		51.5404329		
		4.59998201		4.59998201		
		20		20		
		15		15		
		51.7652633		51.7652633		

		4.59998201		4.59998201		
		20		20		
		15		15		
		51.9900937		51.9900937		
		4.59998201		4.59998201		
		20		20		
		15		15		
		52.2149241		52.2149241		
		4.59998201		4.59998201		
		20		20		
		15		15		
		52.4397545		52.4397545		
		4.59998201		4.59998201		
		20		20		
		15		15		
		51.5404329		51.5404329		
		4.82481241		4.82481241		
		20		20		
		15		15		
		51.7652633		51.7652633		
		4.82481241		4.82481241		
		20		20		
		15		15		
		51.9900937		51.9900937		
		4.82481241		4.82481241		
		20		20		
		15		15		
		52.2149241		52.2149241		
		4.82481241		4.82481241		
		20		20		
		15		15		
		52.4397545		52.4397545		
		4.82481241		4.82481241		
		20		20		
		15		15		

Note there is no seeming difference between the two cases presented in the tables above since to use only the non-redundant equations a change must be made in the code itself. Specifically, just prior to the use of the Cholesky function the redundant equations are removed from the H, G etc. matrices.

Appendix C

batch_name [-]	"results"	"results"	"results"	"results"	"results"	"results"	"results"	"results"	"results"	"results"	"results"	"results"	"results"	"results"	"results"	"results"	"results"	"results"	"results"	"results"	"results"	"results"	"results"
run_name [-]	Noise 2358.	Noise 236.3	Noise 27.95	Noise 15.18	Noise 1518.	Noise 151.8	Noise 15.18	Noise 1.518	"baseline, delft centered 100 km - 4 grnds"	"baseline, delft centered 100 km - 8 grnds"	"baseline, delft centered 100 km - 9 grnds"	"baseline, delft centered 100 km - 16 grnds"	"baseline, delft centered 100 km - 25 grnds"	baseline, delft centered 50 km - 9 grnds	baseline, delft centered 100 km - 9 grnds	baseline, delft centered 200 km - 9 grnds	baseline, delft centered 400 km - 9 grnds	baseline, delft centered 100 km - 9 grnds	delft centered 100 km - 9 grnds - circle	delft centered 100 km - 9 grnds - cross	delft centered 100 km - 9 grnds - line	delft centered 100 km - 9 grnds - clustered
date [dd/mm/yyyy]	19/12/2021	19/12/2021	19/12/2021	19/12/2021	19/12/2021	19/12/2021	19/12/2021	19/12/2021	19/12/2021	19/12/2021	19/12/2021	19/12/2021	19/12/2021	21/12/2021	22/12/2021	23/12/2021	24/12/2021	22/12/2021	22/12/2021	22/12/2021	22/12/2021	22/12/2021	
filename of excel with results [-]	"C:\Users\t	"C:\Users\t	"C:\Users\t	"C:\Users\t	"C:\Users\t	"C:\Users\t	"C:\Users\t	"C:\Users\t	"C:\Users\t	"C:\Users\t	"C:\Users\t	"C:\Users\t	"C:\Users\t	"C:\Users\t	"C:\Users\t	"C:\Users\t	"C:\Users\t	"C:\Users\t	"C:\Users\t	"C:\Users\t	"C:\Users\t	"C:\Users\t	"C:\Users\t
tab of the excel sheet containing the results [-]	2	3	4	5	6	7	8	9	10	11	12	13	14	15	16	17	18	19	20	21	22	23	
latitude_step_size [deg]	5	5	5	5	5	5	5	5	5	5	5	5	5	5	5	5	5	5	5	5	5	5	
longitude_step_size [deg]	5	5	5	5	5	5	5	5	5	5	5	5	5	5	5	5	5	5	5	5	5	5	
altitude [m]	500000	500000	500000	500000	500000	500000	500000	500000	500000	500000	500000	500000	500000	500000	500000	500000	500000	500000	500000	500000	500000	500000	
noise_matrix_length [rows]	1000	1000	1000	1000	1000	1000	1000	1000	1000	1000	1000	1000	1000	1000	1000	1000	1000	1000	1000	1000	1000	1000	
noise_time [sec]	2.3587E-06	2.3634E-07	2.7952E-08	1.5184E-08	1.5184E-06	1.5184E-07	1.5184E-08	1.5184E-09	1.5184E-08	1.5184E-08	1.5184E-08	1.5184E-08	1.5184E-08	1.5184E-08	1.5184E-08	1.5184E-08	1.5184E-08	1.518E-08	1.518E-08	1.518E-08	1.518E-08	1.518E-08	
reference_area [m^2]	21642	21642.4318	21642.4318	21642.4318	21642.4318	21642.4318	21642.4318	21642.4318	21642.4318	21642.4318	21642.4318	21642.4318	21642.4318	21642.4318	21642.4318	21642.4318	21642.4318	21642.432	21642.432	21642.432	21642.432	21642.432	
rng seed	1	1	1	1	1	1	1	1	1	1	1	1	1	1	1	1	1	1	1	1	1	1	
max_steps [-]	250	250	250	250	250	250	250	250	100	100	100	100	100	100	100	100	100	250	250	250	250	250	
max_step_size [m]	10000	10000	10000	10000	10000	10000	10000	10000	500	500	500	500	500	500	500	500	500	10000	10000	10000	10000	10000	
tolerance [m]	0.01	0.01	0.01	0.01	0.01	0.01	0.01	0.01	0.01	0.01	0.01	0.01	0.01	0.01	0.01	0.01	0.01	0.01	0.01	0.01	0.01	0.01	
lat [deg]	51.9900937	51.9900937	51.9900937	51.9900937	51.9900937	51.9900937	51.9900937	51.9900937	51.9900937	51.9900937	51.9900937	51.9900937	51.9900937	51.9900937	51.9900937	51.9900937	51.9900937	51.990094	51.990094	51.990094	51.990094	51.990094	
long [deg]	4.37515161	4.37515161	4.37515161	4.37515161	4.37515161	4.37515161	4.37515161	4.37515161	4.37515161	4.37515161	4.37515161	4.37515161	4.37515161	4.37515161	4.37515161	4.37515161	4.37515161	4.3751516	4.3751516	4.3751516	4.3751516	4.3751516	
alt [m]	20	20	20	20	20	20	20	20	20	20	20	20	20	20	20	20	20	20	20	20	20	20	
Accuracy Groundstations min elevation [deg]	-90	-90	-90	-90	-90	-90	-90	-90	-90	-90	-90	-90	-90	-90	-90	-90	-90	-90	-90	-90	-90	-90	
Number of groundstations [-]	9	9	9	9	9	9	9	9	4	8	9	16	25	9	9	9	9	9	9	9	9	9	
lat [deg]	51.9900937	51.9900937	51.9900937	51.9900937	51.9900937	51.9900937	51.9900937	51.9900937	52.4397545	52.4397545	51.9900937	52.4397545	51.5404329	51.9900937	51.9900937	51.9900937	51.9900937	51.990094	52.439755	51.990094	51.990094	51.540433	
long [deg]	4.37515161	4.37515161	4.37515161	4.37515161	4.37515161	4.37515161	4.37515161	4.37515161	4.82481241	4.82481241	4.37515161	4.82481241	3.92549081	4.37515161	4.37515161	4.37515161	4.37515161	4.3751516	4.3751516	4.8248124	4.8248124	4.8248124	
alt [m]	20	20	20	20	20	20	20	20	20	20	20	20	20	20	20	20	20	20	20	20	20	20	
min elevation angle [deg]	15	15	15	15	15	15	15	15	15	15	15	15	15	15	15	15	15	15	15	15	15	15	
etc.	52.4397545	52.4397545	52.4397545	52.4397545	52.4397545	52.4397545	52.4397545	52.4397545	51.5404329	51.5404329	52.4397545	51.5404329	51.7652633	52.2149241	52.4397545	52.8894154	53.788737	52.439755	51.540433	51.540433	51.990094	51.540433	
	4.82481241	4.82481241	4.82481241	4.82481241	4.82481241	4.82481241	4.82481241	4.82481241	4.82481241	4.82481241	4.82481241	4.82481241	3.92549081	4.59998201	4.82481241	5.2747321	6.1737982	4.8248124	4.3751516	4.3751516	4.7123972	4.7798463	
	20	20	20	20	20	20	20	20	20	20	20	20	20	20	20	20	20	20	20	20	20	20	
	15	15	15	15	15	15	15	15	15	15	15	15	15	15	15	15	15	15	15	15	15	15	
	51.5404329	51.5404329	51.5404329	51.5404329	51.5404329	51.5404329	51.5404329	51.5404329	52.4397545	52.4397545	51.5404329	52.4397545	51.9900937	51.7652633	51.5404329	51.0907721	50.1914505	51.540433	51.990094	51.990094	51.990094	51.585399	
	4.82481241	4.82481241	4.82481241	4.82481241	4.82481241	4.82481241	4.82481241	4.82481241	3.92549081	3.92549081	4.82481241	3.92549081	3.92549081	4.59998201	4.82481241	5.2747321	6.1737982	4.8248124	4.8248124	3.9254908	4.599982	4.8248124	
	20	20	20	20	20	20	20	20	20	20	20	20	20	20	20	20	20	20	20	20	20	20	
	15	15	15	15	15	15	15	15	15	15	15	15	15	15	15	15	15	15	15	15	15	15	
	52.4397545	52.4397545	52.4397545	52.4397545	52.4397545	52.4397545	52.4397545	52.4397545	51.5404329	51.5404329	52.4397545	51.5404329	52.2149241	52.2149241	52.4397545	52.8894154	53.788737	52.439755	51.990094	52.439755	51.990094	51.585399	
	3.92549081	3.92549081	3.92549081	3.92549081	3.92549081	3.92549081	3.92549081	3.92549081	3.92549081	3.92549081	3.92549081	3.92549081	3.92549081	4.15032121	3.92549081	3.47583	2.5765084	3.9254908	3.9254908	4.3751516	4.4875668	4.7798463	
	20	20	20	20	20	20	20	20	20	20	20	20	20	20	20	20	20	20	20	20	20	20	
	15	15	15	15	15	15	15	15	15	15	15	15	15	15	15	15	15	15	15	15	15	15	
	51.5404329	51.5404329	51.5404329	51.5404329	51.5404329	51.5404329	51.5404329	51.5404329		51.9900937	51.5404329	52.1399807	52.4397545	51.7652633	51.5404329	51.0907721	50.1914505	51.540433	52.308052	51.990094	51.990094	52.439755	
	3.92549081	3.92549081	3.92549081	3.92549081	3.92549081	3.92549081	3.92549081	3.92549081		4.82481241	3.92549081	4.52503854	3.92549081	4.15032121	3.92549081	3.47583	2.5765084	3.9254908	4.6931098	4.3751516	4.3751516	3.9254908	
	20	20	20	20	20	20	20	20		20	20	20	20	20	20	20	20	20	20	20	20	20	
	15	15	15	15	15	15	15	15		15	15	15	15	15	15	15	15	15	15	15	15	15	
	51.9900937	51.9900937	51.9900937	51.9900937	51.9900937	51.9900937	51.9900937	51.9900937		51.9900937	51.9900937	51.8402068	51.5404329	51.9900937	51.9900937	51.9900937	51.9900937	51.990094	52.308052	51.990094	51.990094	52.439755	
	4.82481241	4.82481241	4.82481241	4.82481241	4.82481241	4.82481241	4.82481241	4.82481241		3.92549081	4.82481241	4.52503854	4.15032121	4.59998201	4.82481241	5.2747321	6.1737982	4.8248124	4.0571934	4.599982	4.037906	3.9704569	
	20	20	20	20	20	20	20	20		20	20	20	20	20	20	20	20	20	20	20	20	20	
	15	15	15	15	15	15	15	15		15	15	15	15	15	15	15	15	15	15	15	15	15	
	51.9900937	51.9900937	51.9900937	51.9900937	51.9900937	51.9900937	51.9900937	51.9900937		52.4397545	51.9900937	52.1399807	51.7652633	51.9900937	51.9900937	51.9900937	51.9900937	51.990094	51.672136	51.765263	51.990094	52.394788	
	3.92549081	3.92549081	3.92549081	3.92549081	3.92549081	3.92549081	3.92549081	3.92549081		4.37515161	3.92549081	4.22526467	4.15032121	4.15032121	3.92549081	3.47583	2.5765084	3.9254908	4.6931098	4.3751516	4.1503212	3.9254908	
	20	20	20	20	20	20	20	20		20	20	20	20	20	20	20	20	20	20	20	20	20	
	15	15	15	15	15	15	15	15		15	15	15	15	15	15	15	15	15	15	15	15	15	
	52.4397545	52.4397545	52.4397545	52.4397545	52.4397545	52.4397545	52.4397545	52.4397545		51.5404329	52.4397545	51.8402068	51.9900937	52.2149241	52.4397545	52.8894154	53.788737	52.439755	51.672136	51.990094	51.990094	52.394788	
	4.37515161	4.37515161	4.37515161	4.37515161	4.37515161	4.37515161	4.37515161	4.37515161		4.37515161	4.37515161	4.22526467	4.15032121	4.37515161	4.37515161	4.37515161	4.37515161	4.3751516	4.0571934	4.1503212	4.2627364	3.9704569	
	20	20	20	20	20	20	20	20		20	20	20	20	20	20	20	20	20	20	20	20	20	
	15	15	15	15	15	15	15	15		15	15	15	15	15	15	15	15	15	15	15	15	15	
	51.5404329	51.5404329	51.5404329	51.5404329	51.5404329	51.5404329	51.5404329	51.5404329			51.5404329	52.1399807	52.2149241	51.7652633	51.5404329	51.0907721	50.1914505	51.540433	51.990094	52.214924	51.990094	51.990094	
	4.37515161	4.37515161	4.37515161	4.37515161	4.37515161	4.37515161	4.37515161	4.37515161			4.37515161	4.82481241	4.15032121	4.37515161	4.37515161	4.37515161	4.37515161	4.3751516	4.3751516	4.3751516	3.9254908	4.3751516	
	20	20	20	20	20	20	20	20			20	20	20	20	20	20	20	20	20	20	20	20	
	15	15	15	15	15	15	15	15			15	15	15	15	15	15	15	15	15	15	15	15	
												51.8402068	52.4397545										
												4.82481241	4.15032121										
												20	20										
												15	15										
												52.1399807	51.5404329										
												3.92549081	4.37515161										
												20	20										
												15	15										
												51.8402068	51.7652633										
												3.92549081	4.37515161										
												20	20										
												15	15										
												52.4397545	51.9900937										
												4.52503854	4.37515161										
												20	20										
												15	15										
												52.4397545	52.2149241										
												4.22526467	4.37515161										
												20	20										
												15	15										
												51.5404329	52.4397545										
												4.52503854	4.37515161										
												20	20										
												15	15										
												51.5404329	51.5404329										
												4.22526467	4.59998201										
												20	20										
												15	15										
													51.7652633										
													4.59998201										
													20										
													15										
													51.9900937										
													4.59998201										
													20										
													15										
													52.2149241										
													4.59998201										
													20										
													15										
													52.4397545										
													4.59998201										
													20										
													15										
													51.5404329										
													4.82481241										
													20										
													15										
													51.7652633										
													4.82481241										
													20										
													15										
													51.9900937										
													4.82481241										
													20										
													15										
													52.2149241										
													4.82481241										
													20										
													15										
													52.4397545										
													4.82481241										
													20										
													15										

batch_name [-]	"results"	"results"	**"results"**	**"results"**	"results"	**"results"**	**"results"**	**"results"**	**"results"**	**"results"**	**"results"**	**"results"**	**"results"**	**"results"**	**"results"**	**"results"**	**"results"**	**"results"**	**"results"**	**"results"**	**"results"**	**"results"**
run_name [-]	Noise 2358.70203295543 ns	Noise 236.341919266729 ns	Noise 27.9521918286708 ns	Noise 15.1843093448556 ns	Noise 1518.43093448556 ns	Noise 151.843093448556 ns	Noise 15.1843093448556 ns	Noise 1.51843093448556 ns	"baseline, delft centered 100 km - 4 grnds"	"baseline, delft centered 100 km - 8 grnds"	"baseline, delft centered 100 km - 9 grnds"	"baseline, delft centered 100 km - 16 grnds"	"baseline, delft centered 100 km - 25 grnds"	baseline, delft centered 50 km - 9 grnds	baseline, delft centered 100 km - 9 grnds	baseline, delft centered 200 km - 9 grnds	baseline, delft centered 400 km - 9 grnds	baseline, delft centered 100 km - 9 grnds	delft centered 100 km - 9 grnds - circle	delft centered 100 km - 9 grnds - cross	delft centered 100 km - 9 grnds - line	delft centered 100 km - 9 grnds - clustered
date [dd/mm/yyyy]	19/12/2021	**19/12/2021**	**19/12/2021**	**19/12/2021**	**19/12/2021**	**19/12/2021**	**19/12/2021**	**19/12/2021**	**19/12/2021**	**19/12/2021**	**19/12/2021**	**19/12/2021**	**19/12/2021**	21/12/2021	22/12/2021	23/12/2021	24/12/2021	22/12/2021	22/12/2021	22/12/2021	22/12/2021	22/12/2021
filename of excel with results [-]	"C:\Users\timna\OneDrive\Desktop\thesis\thesis writing and final code\code thesis writing\Matlab excel sheets OUTPUTS\OUTPUTS_6.xlsx"	**"C:\Users\timna\OneDrive\Desktop\thesis\thesis writing and final code\code thesis writing\Matlab excel sheets OUTPUTS\OUTPUTS_6.xlsx"**	**"C:\Users\timna\OneDrive\Desktop\thesis\thesis writing and final code\code thesis writing\Matlab excel sheets OUTPUTS\OUTPUTS_6.xlsx"**	**"C:\Users\timna\OneDrive\Desktop\thesis\thesis writing and final code\code thesis writing\Matlab excel sheets OUTPUTS\OUTPUTS_6.xlsx"**	**"C:\Users\timna\OneDrive\Desktop\thesis\thesis writing and final code\code thesis writing\Matlab excel sheets OUTPUTS\OUTPUTS_6.xlsx"**	**"C:\Users\timna\OneDrive\Desktop\thesis\thesis writing and final code\code thesis writing\Matlab excel sheets OUTPUTS\OUTPUTS_6.xlsx"**	**"C:\Users\timna\OneDrive\Desktop\thesis\thesis writing and final code\code thesis writing\Matlab excel sheets OUTPUTS\OUTPUTS_6.xlsx"**	**"C:\Users\timna\OneDrive\Desktop\thesis\thesis writing and final code\code thesis writing\Matlab excel sheets OUTPUTS\OUTPUTS_6.xlsx"**	**"C:\Users\timna\OneDrive\Desktop\thesis\thesis writing and final code\code thesis writing\Matlab excel sheets OUTPUTS\OUTPUTS_6.xlsx"**	**"C:\Users\timna\OneDrive\Desktop\thesis\thesis writing and final code\code thesis writing\Matlab excel sheets OUTPUTS\OUTPUTS_6.xlsx"**	**"C:\Users\timna\OneDrive\Desktop\thesis\thesis writing and final code\code thesis writing\Matlab excel sheets OUTPUTS\OUTPUTS_6.xlsx"**	**"C:\Users\timna\OneDrive\Desktop\thesis\thesis writing and final code\code thesis writing\Matlab excel sheets OUTPUTS\OUTPUTS_6.xlsx"**	**"C:\Users\timna\OneDrive\Desktop\thesis\thesis writing and final code\code thesis writing\Matlab excel sheets OUTPUTS\OUTPUTS_6.xlsx"**	**"C:\Users\timna\OneDrive\Desktop\thesis\thesis writing and final code\code thesis writing\Matlab excel sheets OUTPUTS\OUTPUTS_6.xlsx"**	**"C:\Users\timna\OneDrive\Desktop\thesis\thesis writing and final code\code thesis writing\Matlab excel sheets OUTPUTS\OUTPUTS_6.xlsx"**	**"C:\Users\timna\OneDrive\Desktop\thesis\thesis writing and final code\code thesis writing\Matlab excel sheets OUTPUTS\OUTPUTS_6.xlsx"**	**"C:\Users\timna\OneDrive\Desktop\thesis\thesis writing and final code\code thesis writing\Matlab excel sheets OUTPUTS\OUTPUTS_6.xlsx"**	**"C:\Users\timna\OneDrive\Desktop\thesis\thesis writing and final code\code thesis writing\Matlab excel sheets OUTPUTS\OUTPUTS_6.xlsx"**	**"C:\Users\timna\OneDrive\Desktop\thesis\thesis writing and final code\code thesis writing\Matlab excel sheets OUTPUTS\OUTPUTS_6.xlsx"**	**"C:\Users\timna\OneDrive\Desktop\thesis\thesis writing and final code\code thesis writing\Matlab excel sheets OUTPUTS\OUTPUTS_6.xlsx"**	**"C:\Users\timna\OneDrive\Desktop\thesis\thesis writing and final code\code thesis writing\Matlab excel sheets OUTPUTS\OUTPUTS_6.xlsx"**	**"C:\Users\timna\OneDrive\Desktop\thesis\thesis writing and final code\code thesis writing\Matlab excel sheets OUTPUTS\OUTPUTS_6.xlsx"**
tab of the excel sheet containing the results [-]	2	**3**	**4**	**5**	**6**	**7**	**8**	**9**	**10**	**11**	**12**	**13**	**14**	**15**	**16**	**17**	**18**	**19**	**20**	**21**	**22**	**23**
latitude_step_size [deg]	5	**5**	**5**	**5**	**5**	**5**	**5**	**5**	**5**	**5**	**5**	**5**	**5**	**5**	**5**	**5**	**5**	**5**	**5**	**5**	**5**	**5**
longitude_step_size [deg]	5	**5**	**5**	**5**	**5**	**5**	**5**	**5**	**5**	**5**	**5**	**5**	**5**	**5**	**5**	**5**	**5**	**5**	**5**	**5**	**5**	**5**
altitude [m]	500000	**500000**	**500000**	**500000**	**500000**	**500000**	**500000**	**500000**	**500000**	**500000**	**500000**	**500000**	**500000**	**500000**	**500000**	**500000**	**500000**	**500000**	**500000**	**500000**	**500000**	**500000**
noise_matrix_length [rows]	1000	**1000**	**1000**	**1000**	**1000**	**1000**	**1000**	**1000**	**1000**	**1000**	**1000**	**1000**	**1000**	**1000**	**1000**	**1000**	**1000**	**1000**	**1000**	**1000**	**1000**	**1000**
noise_time [sec]	2.3587E-06	2.3634E-07	2.7952E-08	1.5184E-08	1.5184E-06	1.5184E-07	1.5184E-08	1.5184E-09	1.5184E-08	1.5184E-08	1.5184E-08	1.5184E-08	1.5184E-08	1.5184E-08	1.5184E-08	1.5184E-08	1.5184E-08	1.518E-08	1.518E-08	1.518E-08	1.518E-08	1.518E-08
reference_area [m^2]	21642	**21642.4318**	**21642.4318**	**21642.4318**	**21642.4318**	**21642.4318**	**21642.4318**	**21642.4318**	**21642.4318**	**21642.4318**	**21642.4318**	**21642.4318**	**21642.4318**	**21642.4318**	**21642.4318**	**21642.4318**	**21642.4318**	**21642.432**	**21642.432**	**21642.432**	**21642.432**	**21642.432**
rng seed	1	**1**	**1**	**1**	**1**	**1**	**1**	**1**	**1**	**1**	**1**	**1**	**1**	**1**	**1**	**1**	**1**	**1**	**1**	**1**	**1**	**1**
max_steps [-]	250	**250**	**250**	**250**	**250**	**250**	**250**	**250**	100	100	100	100	100	100	100	100	100	**250**	**250**	**250**	**250**	**250**
max_step_size [m]	10000	**10000**	**10000**	**10000**	**10000**	**10000**	**10000**	**10000**	500	500	500	500	500	500	500	500	500	**10000**	**10000**	**10000**	**10000**	**10000**
tolerance [m]	0.01	**0.01**	**0.01**	**0.01**	**0.01**	**0.01**	**0.01**	**0.01**	**0.01**	**0.01**	**0.01**	**0.01**	**0.01**	**0.01**	**0.01**	**0.01**	**0.01**	**0.01**	**0.01**	**0.01**	**0.01**	**0.01**
lat [deg]	51.9900937	**51.9900937**	**51.9900937**	**51.9900937**	**51.9900937**	**51.9900937**	**51.9900937**	**51.9900937**	**51.9900937**	**51.9900937**	**51.9900937**	**51.9900937**	**51.9900937**	**51.9900937**	**51.9900937**	**51.9900937**	**51.9900937**	**51.990094**	**51.990094**	**51.990094**	**51.990094**	**51.990094**
long [deg]	4.37515161	**4.37515161**	**4.37515161**	**4.37515161**	**4.37515161**	**4.37515161**	**4.37515161**	**4.37515161**	**4.37515161**	**4.37515161**	**4.37515161**	**4.37515161**	**4.37515161**	**4.37515161**	**4.37515161**	**4.37515161**	**4.37515161**	**4.3751516**	**4.3751516**	**4.3751516**	**4.3751516**	**4.3751516**
alt [m]	20	**20**	**20**	**20**	**20**	**20**	**20**	**20**	**20**	**20**	**20**	**20**	**20**	**20**	**20**	**20**	**20**	**20**	**20**	**20**	**20**	**20**
Accuracy Groundstations min elevation [deg]	-90	**-90**	**-90**	**-90**	**-90**	**-90**	**-90**	**-90**	**-90**	**-90**	**-90**	**-90**	**-90**	**-90**	**-90**	**-90**	**-90**	**-90**	**-90**	**-90**	**-90**	**-90**
Number of groundstati	9	**9**	**9**	**9**	**9**	**9**	**9**	**9**	4	8	9	16	25	9	9	9	9	9	9	9	9	9

ons [-]																						
lat [deg]	51.990093	**51.990093**	**51.990093**	**51.990093**	**51.990093**	**51.990093**	**51.990093**	**51.990093**	52.439754	52.439754	51.990093	52.439754	51.540429	51.990093	51.990093	51.990093	51.990093	51.990094	52.439755	51.990094	51.990094	51.540433
long [deg]	4.3751561	**4.3751561**	**4.3751561**	**4.3751561**	**4.3751561**	**4.3751561**	**4.3751561**	**4.3751561**	4.8248121	4.8248121	4.3751561	4.8248121	3.9254081	4.3751561	4.3751561	4.3751561	4.3751561	4.3751561	4.3751561	4.8248124	4.8248124	4.8248124
alt [m]	20	**20**	**20**	**20**	**20**	**20**	**20**	**20**	20	20	20	20	20	20	20	20	20	20	20	20	20	20
min elevation angle [deg]	15	**15**	**15**	**15**	**15**	**15**	**15**	**15**	15	15	15	15	15	15	15	15	15	15	15	15	15	15
etc.	52.439754	**52.439754**	**52.439754**	**52.439754**	**52.439754**	**52.439754**	**52.439754**	**52.439754**	51.540429	51.540429	52.439754	51.540429	51.765263	52.214924	52.439754	52.889415	53.788737	52.439755	51.540433	51.540433	51.990094	51.540433
	4.8248121	**4.8248121**	**4.8248121**	**4.8248121**	**4.8248121**	**4.8248121**	**4.8248121**	**4.8248121**	4.8248121	4.8248121	4.8248121	4.8248121	3.9254081	4.599982	4.8248121	5.274732	6.173794	4.8248124	4.3751516	4.3751516	4.712397	4.779846
	20	**20**	**20**	**20**	**20**	**20**	**20**	**20**	20	20	20	20	20	20	20	20	20	20	20	20	20	20
	15	**15**	**15**	**15**	**15**	**15**	**15**	**15**	15	15	15	15	15	15	15	15	15	15	15	15	15	15
	51.540429	**51.540429**	**51.540429**	**51.540429**	**51.540429**	**51.540429**	**51.540429**	**51.540429**	52.439754	52.439754	51.540429	52.439754	51.990093	51.765263	51.540429	51.090772	50.191455	51.540433	51.990094	51.990094	51.990094	51.585399
	4.8248121	**4.8248121**	**4.8248121**	**4.8248121**	**4.8248121**	**4.8248121**	**4.8248121**	**4.8248121**	3.9254081	3.9254081	4.8248121	3.9254081	3.9254081	4.599982	4.8248121	5.274732	6.173794	4.8248124	4.8248124	3.9254908	4.599982	4.8248124
	20	**20**	**20**	**20**	**20**	**20**	**20**	**20**	20	20	20	20	20	20	20	20	20	20	20	20	20	20
	15	**15**	**15**	**15**	**15**	**15**	**15**	**15**	15	15	15	15	15	15	15	15	15	15	15	15	15	15
	52.439754	**52.439754**	**52.439754**	**52.439754**	**52.439754**	**52.439754**	**52.439754**	**52.439754**	51.540429	51.540429	52.439754	51.540429	52.214924	52.214924	52.439754	52.889415	53.788737	52.439755	51.990094	52.439755	51.990094	51.585399
	3.9254081	**3.9254081**	**3.9254081**	**3.9254081**	**3.9254081**	**3.9254081**	**3.9254081**	**3.9254081**	3.9254081	3.9254081	3.9254081	3.9254081	3.9254081	4.150321	3.9254081	3.47583	2.576508	3.9254908	3.9254908	4.3751516	4.487566	4.779846
	20	**20**	**20**	**20**	**20**	**20**	**20**	**20**	20	20	20	20	20	20	20	20	20	20	20	20	20	20
	15	**15**	**15**	**15**	**15**	**15**	**15**	**15**	15	15	15	15	15	15	15	15	15	15	15	15	15	15
	51.540429	**51.540429**	**51.540429**	**51.540429**	**51.540429**	**51.540429**	**51.540429**	**51.540429**		51.990093	51.540429	52.139980	52.439754	51.765263	51.540429	51.090772	50.191455	51.540433	52.308052	51.990094	51.990094	52.439755
	3.9254081	**3.9254081**	**3.9254081**	**3.9254081**	**3.9254081**	**3.9254081**	**3.9254081**	**3.9254081**		4.8248121	3.9254081	4.525038	3.9254081	4.150321	3.9254081	3.47583	2.576508	3.9254908	4.6931098	4.3751516	4.3751516	3.9254908
	20	**20**	**20**	**20**	**20**	**20**	**20**	**20**		20	20	20	20	20	20	20	20	20	20	20	20	20
	15	**15**	**15**	**15**	**15**	**15**	**15**	**15**		15	15	15	15	15	15	15	15	15	15	15	15	15
	51.990093	**51.990093**	**51.990093**	**51.990093**	**51.990093**	**51.990093**	**51.990093**	**51.990093**		51.990093	51.990093	51.840206	51.540429	51.990093	51.990093	51.990093	51.990093	51.990094	52.308052	51.990094	51.990094	52.439755
	4.8248121	**4.8248121**	**4.8248121**	**4.8248121**	**4.8248121**	**4.8248121**	**4.8248121**	**4.8248121**		3.9254081	4.8248121	4.525038	4.150321	4.599982	4.8248121	5.274732	6.173794	4.8248124	4.0571934	4.599982	4.037906	3.9704569
	20	**20**	**20**	**20**	**20**	**20**	**20**	**20**		20	20	20	20	20	20	20	20	20	20	20	20	20
	15	**15**	**15**	**15**	**15**	**15**	**15**	**15**		15	15	15	15	15	15	15	15	15	15	15	15	15
	51.990093	**51.990093**	**51.990093**	**51.990093**	**51.990093**	**51.990093**	**51.990093**	**51.990093**		52.439754	51.990093	52.139980	51.765263	51.990093	51.990093	51.990093	51.990093	51.990094	51.672136	51.765263	51.990094	52.394788
	3.9254081	**3.9254081**	**3.9254081**	**3.9254081**	**3.9254081**	**3.9254081**	**3.9254081**	**3.9254081**		4.3751516	3.9254081	4.225264	4.150321	4.150321	3.9254081	3.47583	2.576508	3.9254908	4.6931098	4.3751516	4.150321	3.9254908
	20	**20**	**20**	**20**	**20**	**20**	**20**	**20**		20	20	20	20	20	20	20	20	20	20	20	20	20
	15	**15**	**15**	**15**	**15**	**15**	**15**	**15**		15	15	15	15	15	15	15	15	15	15	15	15	15
	52.439754	**52.439754**	**52.439754**	**52.439754**	**52.439754**	**52.439754**	**52.439754**	**52.439754**		51.540429	52.439754	51.840206	51.990093	52.214924	52.439754	52.889415	53.788737	52.439755	51.672136	51.990094	51.990094	52.394788
	4.3751516	**4.3751516**	**4.3751516**	**4.3751516**	**4.3751516**	**4.3751516**	**4.3751516**	**4.3751516**		4.3751516	4.3751516	4.225264	4.150321	4.3751516	4.3751516	4.3751516	4.3751516	4.3751516	4.0571934	4.1503212	4.262736	3.9704569
	20	**20**	**20**	**20**	**20**	**20**	**20**	**20**		20	20	20	20	20	20	20	20	20	20	20	20	20
	15	**15**	**15**	**15**	**15**	**15**	**15**	**15**		15	15	15	15	15	15	15	15	15	15	15	15	15
	51.540429	**51.540429**	**51.540429**	**51.540429**	**51.540429**	**51.540429**	**51.540429**	**51.540429**			51.540429	52.139980	52.214924	51.765263	51.540429	51.090772	50.191455	51.540433	51.990094	52.214924	51.990094	51.990094
	4.3751516	**4.3751516**	**4.3751516**	**4.3751516**	**4.3751516**	**4.3751516**	**4.3751516**	**4.3751516**			4.3751516	4.8248121	4.150321	4.3751516	4.3751516	4.3751516	4.3751516	4.3751516	4.3751516	4.3751516	3.9254908	4.3751516
	20	**20**	**20**	**20**	**20**	**20**	**20**	**20**			20	20	20	20	20	20	20	20	20	20	20	20
	15	**15**	**15**	**15**	**15**	**15**	**15**	**15**			15	15	15	15	15	15	15	15	15	15	15	15
												51.840206	52.439754									
												4.8248121	4.150321									
												20	20									
												15	15									
												52.139980	51.540429									

												3.9254908 1	4.3751516 1									
												20	20									
												15	15									
												51.840206 8	51.765263 3									
												3.9254908 1	4.3751516 1									
												20	20									
												15	15									
												52.439754 5	51.990093 7									
												4.5250385 4	4.3751516 1									
												20	20									
												15	15									
												52.439754 5	52.214924 1									
												4.2252646 7	4.3751516 1									
												20	20									
												15	15									
												51.540432 9	52.439754 5									
												4.5250385 4	4.3751516 1									
												20	20									
												15	15									
												51.540432 9	51.540432 9									
												4.2252646 7	4.5999820 1									
												20	20									
												15	15									
													51.765263 3									
													4.5999820 1									
													20									
													15									
													51.990093 7									
													4.5999820 1									
													20									
													15									
													52.214924 1									
													4.5999820 1									
													20									
													15									
													52.439754 5									
													4.5999820 1									
													20									
													15									
													51.540432 9									
													4.8248124 1									
													20									
													15									

													51.765263									
													4.8248124									
													20									
													15									
													51.990093									
													4.8248124									
													20									
													15									
													52.214924									
													4.8248124									
													20									
													15									
													52.439754									
													4.8248124									
													20									
													15									

Appendix D

batch_name [-]	delfi PQ case
run_name [-]	236 ns, 25 grnds, 1000-km, square
date [dd/mm/yyyy]	28/01/2022 00:00
filename of excel with results [-]	C:\Users\timna\OneDrive\Desktop\thesis\thesis writing and final code\code thesis writing\Matlab excel sheets OUTPUTS\OUTPUTS_8_V2.xlsx
tab of the excel sheet containing the results [-]	8
latitude_step_size [deg]	5
longitude_step_size [deg]	5
altitude [m]	500000
noise_matrix_length [rows]	1000
noise_time [sec]	0.000000236
reference_area [m^2]	21642.43179
rng seed	1
max_steps [-]	100
max_step_size [m]	5000
tolerance [m]	1
lat [deg]	51.99009375
long [deg]	4.375151609
alt [m]	20
Accuracy Groundstations min elevation [deg]	-90
Number of groundstations [-]	25
lat [deg]	47.49348572
long [deg]	-0.121456421
alt [m]	20
min elevation angle [deg]	15
etc.	49.74178973
	-0.121456421
	20
	15
	51.99009375
	-0.121456421
	20
	15
	54.23839776
	-0.121456421
	20
	15
	56.48670178
	-0.121456421
	20
	15

	47.49348572
	2.126847594
	20
	15
	49.74178973
	2.126847594
	20
	15
	51.99009375
	2.126847594
	20
	15
	54.23839776
	2.126847594
	20
	15
	56.48670178
	2.126847594
	20
	15
	47.49348572
	4.375151609
	20
	15
	49.74178973
	4.375151609
	20
	15
	51.99009375
	4.375151609
	20
	15
	54.23839776
	4.375151609
	20
	15
	56.48670178
	4.375151609
	20
	15
	47.49348572
	6.623455623
	20
	15
	49.74178973
	6.623455623

	20
	15
	51.99009375
	6.623455623
	20
	15
	54.23839776
	6.623455623
	20
	15
	56.48670178
	6.623455623
	20
	15
	47.49348572
	8.871759638
	20
	15
	49.74178973
	8.871759638
	20
	15
	51.99009375
	8.871759638
	20
	15
	54.23839776
	8.871759638
	20
	15
	56.48670178
	8.871759638
	20
	15

Appendix E

batch_name [-]	full VS partial
run_name [-]	full, baseline, delft centered 100 km -9grnds
date [dd/mm/yyyy]	16/01/2022 00:00
filename of excel with results [-]	C:\Users\timna\OneDrive\Desktop\thesis\thesis writing and final code\code thesis writing\Matlab excel sheets OUTPUTS\OUTPUTS_7 mod coverage area.xlsx
tab of the excel sheet containing the results [-]	1
latitude_step_size [deg]	1
longitude_step_size [deg]	1
altitude [m]	500000
noise_matrix_length [rows]	1000
noise_time [sec]	0.000000028
reference_area [m^2]	21642.43179
rng seed	1
max_steps [-]	100
max_step_size [m]	5000
tolerance [m]	0.01
lat [deg]	51.99009375
long [deg]	4.375151609
alt [m]	20
Accuracy Groundstations min elevation [deg]	-90
Number of groundstations [-]	9
lat [deg]	51.99009375
long [deg]	4.375151609
alt [m]	20
min elevation angle [deg]	15
etc.	52.43975455
	4.824812412
	20
	15
	51.54043294
	4.824812412
	20
	15
	52.43975455
	3.925490806
	20
	15
	51.54043294

	3.925490806
	20
	15
	51.99009375
	4.824812412
	20
	15
	51.99009375
	3.925490806
	20
	15
	52.43975455
	4.375151609
	20
	15
	51.54043294
	4.375151609
	20
	15